

# Dehumidification of Greenhouses

Jouke Berend Campen

Thesis committee

*Thesis supervisor:*

Prof.Dr.Ir. G.P.A. Bot  
Emeritus Professor of Applied Physics  
Wageningen University

*Other members:*

Prof.Dr. O. van Kooten  
Wageningen University

Prof.Dr.Ir. Th. van der Meer  
University of Twente

Dr.Ir. J.J.W. Westra  
Priva B.V., De Lier

Dr. J.I. Montero  
IRTA, Centre de Cabrils, Spain

# Dehumidification of Greenhouses

Jouke Berend Campen

Thesis

submitted in partial fulfilment of the requirements for the degree of doctor  
at Wageningen University

by the authority of the Rector Magnificus

Prof. dr. M.J. Kropff,

in the presence of the

Thesis Committee appointed by the Doctorate Board

to be defended in public

on Friday 23 October 2009

at 4 PM in the Aula

J.B. Campen

Dehumidification of Greenhouses, 117 pages.

Thesis, Wageningen University, Wageningen, NL (2009)

With summaries in English and Dutch.

ISBN: 978-90-8585-429-6



## **Abstract**

Dehumidification is an essential part of greenhouse climate control. High humidity is a cause of diseases which ultimately reduce the quantity and quality of production. The risk of diseases affecting the crop increases when crops are wet. The humidity surrounding the crop differs since the air temperature in the greenhouse is not homogenous. This heterogeneity should be minimised for this reason by a proper greenhouse climate management. Part of it cannot be resolved as a result of physical laws. Therefore, humidity control is needed. Humidity control increases energy consumption during heating periods. The work presented describes energy-saving measures to dehumidify a greenhouse where also the practical and economical feasibility are considered.

Three methods of dehumidification can be applied in greenhouses: ventilation with outside air, condensation on a cold surface, and absorption by a hygroscopic material. Ventilation with outside air is the current method to dehumidify greenhouses.

The method of condensation on a cold surface was evaluated with and without heat recovery. Without heat recovery, it was found that less than half of the total heat transfer is related to the heat released during condensation. The rest is sensible heat removed from the greenhouse air that needs to be returned through heating. This energy transfer, performed by a heat pump, therefore consumes more energy than necessary for the dehumidification only. Using a hygroscopic material to dehumidify a greenhouse was concluded to be not practical and economically feasible. The various methods of dehumidification were evaluated from an economical, practical, and energetic point of view. It was concluded that the ventilation with outside air with heat recovery is the most economical, practical, and energy-saving method. Ventilation driven by buoyancy and wind cannot be controlled accurately though and gives rise to a heterogenic greenhouse climate. Therefore, the dehumidifying ventilation has to be mechanically controlled and the incoming air has to be distributed evenly over the greenhouse. Heat recovery can be included to save energy. Using this system the humidity can be controlled accurately in an energy-friendly way and the climate is more homogenous. This already holds for nowadays greenhouses. For more sustainable greenhouses with lower heat demand realisable in the future this method will be indispensable.



## Voorwoord

Ongeveer twee jaar na mijn aanstelling bij IMAG-DLO werd de vraag aan mij gesteld of ik zou willen promoveren. Dit zou een promotie worden op basis van het werk dat gevormd wordt door projecten. Nico van de Braak, die vreemd genoeg zelf nooit wat in een promotie heeft gezien, raadde mij aan dit zeker te doen. Ook Sjaak Bakker en Gerard Bot zeiden dat het een verrijking zou zijn. De overige collegae Peter Knies, Jo Breuer, Gert-Jan Swinkels, Silke Hemming, Cecilia Stanghellini, Jan Bontsema, Feije de Zwart en Theo Gieling bleven over de jaren ook positief ten aanzien van een promotie van mij, mogelijk omdat er dan ook een feest in het verschiet lag. Frank Kempkes wist mij over de jaren te stimuleren met het feit dat hij het dankwoord voor het proefschrift al klaar had. Dit was natuurlijk een enorme stimulans maar meer nog zijn enorme inzet in de projecten die ik samen met hem heb mogen doen. De kwaliteit van dit proefschrift heb ik mede te danken aan voor mij anonieme reviewers van de verschillende papers die zijn gepubliceerd. Verbetering van het engels was een belangrijk onderdeel van dit werk wat voor de laatste hoofdstukken door Tom Dueck is uitgevoerd.

Het feit dat de afronding van het proefschrift nog zo lang heeft geduurd is niet te wijten aan het geforceerde job-hoppen van de afgelopen jaren. Deze carrière begon bij IMAG-DLO om vervolgens naar Agrotechnology and Food Innovations te gaan. Dit onderdeel van Wageningen UR zou worden opgeheven wat later bleek toch niet helemaal waar te zijn maar onze groep van Greenhouse Technology werd ondergebracht bij Plant Research International onder de vleugels van Agro. Begin 2006 werd een nieuwe business unit binnen de Plant Sciences Group opgericht die WUR Glastuinbouw heette waarvan wij logischerwijs deel gingen uitmaken. Mijn vrouw en overige familieleden blijven tot op de dag van vandaag zeggen dat ik bij het IMAG in Wageningen werk en ik corrigeer ze daar niet in aangezien de groep mensen om mij heen van Greenhouse Technology voor een groot deel nog hetzelfde is.

Het onderwerp van dit proefschrift is lang niet duidelijk geweest. Pas in het laatste jaar na een gesprek met Gerard Bot, op aandringen van Silke Hemming, werd duidelijk wat het hoofdonderwerp van dit proefschrift moest worden. Vochtafvoeren uit kassen was het onderwerp waarop ik in 1997 werd aangenomen bij IMAG-DLO en zou uiteindelijk ook het onderwerp worden van het proefschrift.

Ik wil iedereen danken voor de feedback die ik in de loop der jaren heb gehad op de verschillende artikels, rapporten en presentaties die ik heb gemaakt. Naast het commentaar van de vele collegae wil ik hier ook de opdrachtgevers van het ministerie van LNV in de persoon van Leo Oprel en het productschap tuinbouw in de persoon van Anja Jolman danken. Dit proefschrift is het resultaat van de vele projecten die ik in

opdracht van deze organisaties heb kunnen uitvoeren. Specifiek wil ik ten slotte Gerard Bot bedanken die vanaf het begin van dit promotie traject zeer betrokken is geweest en op een relaxte manier mij naar de eindstreep heeft weten te brengen.

# Contents

Abstract	v
Voorwoord	vii
1 Introduction	1
1.1 General	2
1.2 Definition of humidity	3
1.3 Dehumidifying methods	4
1.4 Computational fluid dynamics	5
1.5 Setup of the thesis	6
2 Dehumidification in greenhouses by condensation on finned pipes	7
2.1 Introduction	9
2.2 Theoretical considerations	10
2.2.1 Film condensation from a vapour-air mixture to a cold surface.	11
2.2.2 The computational fluid dynamics calculations	13
2.3 Experiments	15
2.3.1 The dehumidifying system	15
2.3.2 Data	16
2.4 Results	17
2.4.1 The computational fluid dynamics results	17
2.4.2 The experimental results	18
2.5 Conclusions	21
3 Design of a Low Energy Dehumidifying System for Greenhouses	23
3.1 Introduction	25
3.2 Theoretical considerations	26
3.2.1 Dehumidification	26
3.2.2 Flow phenomena	28
3.3 Results and discussion	31
3.3.1 First layout of the dehumidifier	32
3.3.2 Second layout of the dehumidifier	36
3.3.3 Condensation based on computational fluid dynamics calculations	37
3.3.4 Experiment using a prototype	42
3.3.5 Comparison between experiments and calculations	43
3.4 Conclusions	43
4 Determination of greenhouse-specific aspects of ventilation using three-dimensional computational fluid dynamics	45
4.1 Introduction	47

4.2	Theoretical considerations	48
4.2.1	Theory on ventilation	48
4.2.2	Theory on computational fluid dynamics	50
4.3	Experiments	50
4.3.1	Measurements of the natural ventilation of "parral" greenhouses	51
4.3.2	The CFD model	52
4.4	Results	53
4.4.1	Flap windows	53
4.4.2	Rollup windows	56
4.5	Discussion	57
4.6	Conclusions	58
5	Dehumidification of Greenhouses at Northern Latitudes	61
5.1	Introduction	62
5.2	Dehumidifying methods	63
5.2.1	Dehumidification by natural ventilation	63
5.2.2	Condensation on a cold surface	63
5.2.3	Forced ventilation in conjunction with a heat exchanger	64
5.2.4	Hygroscopic dehumidification	65
5.3	Methodology	66
5.4	Results and discussion	68
5.4.1	Dehumidification needed	68
5.4.2	Dehumidification by natural ventilation	70
5.4.3	Condensation on a cold surface	71
5.4.4	Forced ventilation using a heat exchanger	72
5.4.5	Hygroscopic dehumidification	73
5.5	Conclusions	74
6	Mechanically controlled moisture removal from greenhouses	75
6.1	Introduction	76
6.2	Materials and methods	78
6.2.1	Theoretical calculations	78
6.2.2	Experimental setup	83
6.3	Results and discussion	86
6.3.1	Theoretical analysis	87
6.3.2	Experimental results	90
6.3.3	Practical implications	93
6.4	Conclusions	93
7	Conclusions	95
7.1	Humidity control	96
7.2	Dehumidifying methods	97

7.3	Future perspectives	99
7.4	Computational fluid dynamics	100
7.5	Overall conclusion	101
	References	103
	Summary	109
	Samenvatting	113
	Curriculum Vitae	117





---

# 1

Introduction

---

## 1.1 General

In this thesis the physical methods to control humidity, an important aspect of greenhouse climate conditioning, are investigated. This is even crucial for current greenhouse production, while optimal crop production demands the humidity to be within a specific range. Low humidity increases evaporation to the extent which may cause stress to the crop (Bakker, 1991). Crops exposed to high humidity levels have a higher risk of developing fungal diseases and physiological disorders (Hand, 1988; Bakker *et al.*, 1995). Bakker (1991) concluded that the major effect of high humidity on yield is mediated through its impact on light interception resulting from either the enlargement (through number of leaves and leaf expansion) or the decrease (through calcium deficiency) of the leave area index and the (marginal) effect on photosynthesis as such. Another problem linked to humidity is that some fungal diseases like *Botrytis cinerea* grow on wounds of the plant caused by picking of leafs and fruits. The healing of these wounds is dependent on the temperature and humidity surrounding the plant (Köhl *et al.*, 2007). The humidity problem is partly due to the non-uniform temperature distribution in practical greenhouses while a high local humidity is linked to low local air temperatures. To prevent a high local relative humidity the grower will set his maximum relative humidity to a lower level than required in a uniform climate. Thus humidity has to be controlled within a close optimal range, and depends on the crop in combination with a uniform of greenhouse climate.

The level of humidity results from the balance between the sources and sinks of water vapor within the greenhouse environment. The main source of water vapor in greenhouses is the crop transpiration. Transpiration depends on solar radiation, CO<sub>2</sub> concentration, temperature of the greenhouse air and relative humidity in the greenhouse (Stanghellini, 1987). Another source of water vapor is the evaporation of water from surfaces within the greenhouse like the soil surface. The main sink of water vapor is active removal by ventilation. The humidity level outside the greenhouse is always lower than indoors, so ventilation causes the humidity to decrease. Furthermore condensation on cold surfaces within the greenhouse like the cover extracts moisture from the greenhouse air. In the heating period, ventilation with cold outdoor air necessary for dehumidification is directly related to an increase of energy consumption. In Table 1.1 the annual transpiration for a common crop is presented for two maximum humidity levels set in the control system, together with the dehumidification in the heating season and the energy consumption.

*Table 1.1 Annual transpiration of a tomato crop, dehumidification during heating periods, and the energy consumption needed per square meter of greenhouse under Dutch climate conditions grown under standard conditions (Vermeulen, 2008) as calculated by KASPRO (De Zwart, 1996)*

<i>Conditions</i>	<i>Transpiration, <math>l m^{-2} y^{-1}</math></i>	<i>Dehumidification <math>l m^{-2} y^{-1}</math></i>	<i>Energy consumption, <math>MJ m^{-2} y^{-1}</math></i>
Maximum RH 80%	662	158	1459
Maximum RH 85%	640	102	1322

Increasing the maximum humidity level from 80% to 85%, decreases the necessity for dehumidification by more than 30% during periods of heating. As a result the energy consumption decreases by almost 10%. As stated earlier, the humidity in greenhouses can only be increased when the temperature distribution is homogeneous. Thus for current greenhouse practice, more energy friendly dehumidification methods may already contribute to energy saving.

For the energy saving greenhouses in the future the dehumidification problem is even more striking. Due to improved insulation of the greenhouse cover the total energy consumption will be reduced. (Swinkels *et al.*, 2001). However, the better cover insulation is linked to reduced condensation on the cover, making additional dehumidification necessary will be needed to prevent an excessively high air humidity. With the conventional method of dehumidification by ventilation the benefits of the better insulation are reduced. So for the greenhouses of the future more energy friendly dehumidification methods will be indispensable.

## **1.2 Definition of humidity**

In horticultural practice humidity is expressed in several notations:

- *Absolute humidity*: defined as the quantity of water vapor per unit volume ( $kg m^{-3}$ ) or per unit mass ( $kg kg^{-1}$ ) of air.
- *Relative humidity*: defined as the ratio of the actual partial water vapor pressure of water vapor in a gaseous mixture of air and water vapor to the saturated water vapor pressure at the actual air temperature. For judging the absolute humidity the temperature level has to be considered when using this notation since air of for example 10°C and relative humidity of 80% contains 7.5  $gr m^{-3}$  of water vapour while saturated air of 10°C contains 9.5  $gr m^{-3}$  whereas air of 20°C with a relative humidity of 80% contains 14.0  $gr m^{-3}$  while saturated air of 20 °C

contains  $17.6 \text{ gr m}^{-3}$ . So almost double the amount of moisture can be added to air at a temperature of  $20^\circ\text{C}$  before this is saturated compared to the colder air at  $10^\circ\text{C}$ .

- *Vapour deficit*: defined as the difference between the absolute humidity of the greenhouse air and the absolute humidity of saturated air at the same temperature. The vapor deficit indicates how much water vapor can be added to the air before it is saturated.

The common method to determine humidity in commercial greenhouses is with a wet and dry bulb psychrometer. The humidity can be determined with a psychrometric chart based on these two measured temperatures. Humidity can also be measured by other methods but these are usually not resistant to the greenhouse environmental conditions.

Humid air is less dense than dry air because a mole of water weighs less than the moles of nitrogen and oxygen. Air consists of around 78% of nitrogen with a molecular weight of  $28 \text{ kg kmol}^{-1}$  and oxygen makes up 21%, with a molecular weight of 32. The resulting molar weight of air is about 29. In humid air water vapour molecules, with a molecular weight of  $18 \text{ kg kmol}^{-1}$  replace the diatomic nitrogen or oxygen molecules in this fixed isobaric volume resulting in decreased mass of the volume of the air and hence the density decreases. Saturated air of  $20^\circ\text{C}$  is for this reason 0.9% lighter than dry air of this temperature.

### 1.3 Dehumidifying methods

In this study several dehumidifying methods have been designed and tested. Important considerations when dealing with dehumidification are:

- Humid air is lighter than dry air
- Evaporation of moisture consumes a great deal of energy
- The saturated moisture content of air depends on the air temperature

There are several methods to dehumidify air. As discussed before the common method to dehumidify greenhouse air is by replacing the greenhouse air with outside air (ventilation). When ventilation is applied for cooling the greenhouse, there is no extra energy consumption but while heating, ventilation will increase energy costs (Section 1.1). Therefore, the quantification and control of the minimal ventilation air exchange required to control humidity during the heating season has been studied. To decrease heat losses by this controlled ventilation, heat recovery has also been studied by applying a heat exchanger between outgoing and incoming air.

An alternative dehumidification method under study is controlled condensation on a surface with temperature below dew point temperature of the greenhouse air, with and without heat recovery. Another is the application of a hygroscopic material taking into

account the effect of regeneration of this material. For the various dehumidification methods, uniformity of greenhouse temperature is an important aspect.

Energy saving is the leading principle in studying and testing these methods in connection to practical application in current and future greenhouses aiming at low energy consuming greenhouse systems.

#### 1.4 Computational fluid dynamics

As previously stated in Section 1.1, the humidity problems are linked to the temperature distribution in the greenhouse. This means that we have to deal with distributed flow phenomena, temperatures and vapour pressures. Moreover, in the various dehumidifying methods, local transport phenomena play an important role. Therefore computational fluid dynamics (CFD) has been applied for several cases described in this thesis.

CFD has become a widely used tool to determine flow field, temperature and concentration distributions in and around geometries. As computers become faster and cheaper and the CFD software becomes more user-friendly, more comprehensive cases can be studied using this technique. The number of publications on CFD applied to the ventilation of greenhouses has rapidly increased over the years (Norton *et al.*, 2007).

The physical aspects of any fluid flow are governed by the fundamental principle of conservation of mass (total as well as mass of a specific component like water vapour, carbon dioxide, *etc.*, of momentum (3 components) and of energy.

A general description of the application of CFD on greenhouses is given by Mistriotis *et al.* (1997a). In a CFD programme a system is modelled by discretising the considered space (finite volume method) and time (transient solutions) and by solving the conservation equations (balances) for the discretised parts for the relevant quantities considered. The conservation equation reads:

$$\frac{\partial \varphi}{\partial t} + \vec{\nabla} \cdot \varphi \vec{v} = \vec{\nabla} \cdot (\Gamma_{\varphi} \vec{\nabla} \varphi) + S_{\varphi} \quad (1.1)$$

where  $\vec{v}$  is the velocity vector in  $\text{m s}^{-1}$ ,  $\Gamma_{\varphi}$  is the diffusion coefficient in  $\text{m}^2 \text{s}^{-1}$  and  $S_{\varphi}$  is the source term. The symbol  $\varphi$  represents the concentration of the quantity (total mass, mass of a specific component, momentum, energy,) considered. Solving the resulting set of equations provides the spatial distribution of momentum, pressure, temperature and mass concentration(s), and thus the transport of momentum, heat and mass between the parts of the model can be determined. Separate models describing the contribution of the fluctuating part account for turbulence. The k- $\epsilon$  model is widely used as a turbulence model (Launder *et al.*, 1974).

The CFD calculations described in this thesis are performed using a commercial software FLUENT (Fluent, 1998). More studies on CFD concerning dehumidification

of greenhouses have been recently reported since humidity is a crucial factor for climate control (Kittas *et al.*, 2007).

## 1.5 Setup of the thesis

The principle of dehumidification by condensation is put into practice in the first chapter following the introduction. In this system consisting of finned pipes fixed under the gutter, condensation on the pipes cooled below the dew point temperature of the greenhouse air dehumidifies the greenhouse. This system was also designed using computational fluid dynamics. Following the results of this system, the design process of a low-energy dehumidifying system for greenhouses based on condensation in combination with heat recovery, is described in the third chapter. The air circulation in the system is realised by natural convection. Computational fluid dynamics is used for studying the natural convection air circulation. A prototype was built and tested and the design has been patented. Ventilation is the conventional method for dehumidification. Ventilation of greenhouses is caused by the buoyancy effect and by wind. The wind effect dominates the ventilation when the wind speed exceeds 3 m/s. Ventilation can be described by general characteristics, however as described in chapter 4, greenhouse characteristics always have to be included. In this chapter the ventilation of a Spanish ‘parral’ greenhouse is calculated from three-dimensional computational fluid dynamics simulations. The results are compared to experimental data. In chapter 5 the various dehumidification techniques, controlled ventilation with heat recovery, condensation and the application of a hygroscopic material, are compared to the conventional method of ventilation for four different crops under Dutch climate conditions. The evaluation is based on annual energy consumption and economic impact using a dynamic simulation model. Chapter 6 describes a system which was concluded to be the most promising in the previous chapter: controlled ventilation with outside air. In this chapter the design process of this technique and the practical implementation at a commercial grower are described. Conclusions are drawn in the final chapter.

---

# 2

## Dehumidification in greenhouses by condensation on finned pipes

---

This chapter was published before as:  
J.B. Campen and G.P.A. Bot (2002). Dehumidification in  
greenhouses by condensation on finned pipes. *Biosystems  
Engineering* 82(2) pp 177-185  
Doi:10.1006/bioe.2002.0058

### Abstract

In this study, an experimental dehumidifying system for greenhouses is tested. The system uses finned pipes fixed under the gutter of the greenhouse. The pipes are cooled below the dew point of the greenhouse air by cold water. The humid air passes the pipe and fins by natural convection and condensation occurs reducing the humidity in the greenhouse. The performance of the system in relation to its location and dimensions are studied by computational fluid dynamics calculations. The total heat transferred and condense removed are monitored as a function of the greenhouse conditions.

The system removes 40 grams of condensate per hour per square metre of greenhouse floor from the humid air sufficient during periods when heating is applied and ventilation is minimised. The heat transferred at the cold surface by condensation is less than one third of the total heat removed by the system at a relative humidity of 80%.

### Notation

$A$	surface area per metre length of apparatus, $\text{m}^2 \text{m}^{-1}$
$a$	factor defined in Eqn (2.6)
$B$	gain factor
$b$	factor defined in Eqn (2.6)
$C_p$	specific heat, $\text{J kg}^{-1} \text{K}^{-1}$
$c$	mass fraction of water vapour in air, $\text{kg kg}^{-1}$
$D$	fin distance, m
$d_{\text{pipe}}$	diameter of pipe, m
$g$	acceleration due to gravity, $\text{m s}^{-2}$
Gr	Grashof number
$H_R$	relative humidity, %
$h_{\text{fin}}$	height of fin, m
$k$	mass transfer coefficient, $\text{m s}^{-1}$
$L$	length, m
$L_v$	latent heat of vaporisation, $\text{J kg}^{-1}$
Le	Lewis number
Nu	Nusselt number
Pr	Prandtl number
$\dot{q}$	heat transfer, W
$T$	temperature, K
$u$	velocity, $\text{m s}^{-1}$
$w$	width, m



$z$	distance, m
$\alpha$	heat transfer coefficient, $\text{W m}^{-2} \text{K}^{-1}$
$\beta$	gas expansion coefficient, $\text{K}^{-1}$
$\Delta x$	moisture deficit, $\text{kg kg}^{-1}$
$\delta$	diffusion coefficient, $\text{m}^2 \text{s}^{-1}$
$\varepsilon$	absorption coefficient
$\varepsilon_{eff}$	effective absorption coefficient on the considered surface
$\varepsilon_{solar}$	absorption coefficient for solar radiation
$\phi$	mass flow, $\text{kg s}^{-1}$
$\lambda$	thermal conductivity, $\text{W m}^{-1} \text{K}^{-1}$
$\eta$	dynamic viscosity, $\text{kg m}^{-1} \text{s}^{-1}$
$\nu$	kinematic viscosity, $\text{m}^2 \text{s}^{-1}$
$\rho$	density, $\text{kg m}^{-3}$
$\sigma$	Stefan-Boltzmann constant, $\text{W m}^{-2} \text{K}^{-4}$
Subscripts	
<i>air</i>	air
<i>conv</i>	convective
<i>lat</i>	latent part
<i>pipe</i>	pipe
<i>rad</i>	radiation
<i>setpoint</i>	setpoint
<i>surr</i>	surroundings
<i>tot</i>	total
<i>vapour</i>	vapour
<i>wall</i>	wall
<i>wet bulb</i>	wet bulb

## 2.1 Introduction

In greenhouse technology, energy saving is one of the main topics. Lowering energy demand by improved insulation has large impact on greenhouse climate. Especially air humidity will rise due to less condensation on the cover. Active humidity control will be necessary for optimal plant production (Bakker, 1991). Dehumidification by ventilation, absorption or condensation implies not only the transport of water vapour and thereby latent heat but also the transport of sensible heat. In energy friendly dehumidification, the ratio of latent to sensible heat has to be high. In greenhouse climate models, sensible and latent heat fluxes by condensation to the cold cover and by ventilation in

conventional greenhouses are calculated (De Zwart *et al.*, 1997). So dehumidifying strategies can be developed by simulation. However experimental results must be used to calibrate the models and to check their validity. In the study presented here experiments were designed for a simple dehumidifying system in a well-insulated greenhouse. In this system, water vapour is removed by condensation on cooled finned pipes. This will be the basis for the development of practical systems for greenhouse dehumidification.

First the theory on heat transfer between a cold surface and greenhouse air, including condensation is given. For the specific geometry used in this study, i.e. a finned pipe, computational fluid dynamics calculations are performed. Experimental results are followed by the overall conclusions.

## **2.2 Theoretical considerations**

The dehumidifying system considered in this study consists of finned pipes fixed under the gutter of the greenhouse. This location is preferred for three reasons. Firstly, the flow is enhanced by natural convection, the cold surface is best placed high in the system. Secondly, the system is in the shadow of the gutter reducing the light interception; however, approximately 3% of the light is still intercepted by the system calculated by TNO using the IDT-method (TNO, 1996). The pipes are finned to increase the heat exchanging area without increasing the overall dimensions of the system. Thirdly, the air tends to flow downwards under the cold cover thus pre-cooling the air passing the finned pipes.

## 2.2.1 Film condensation from a vapour-air mixture to a cold surface.

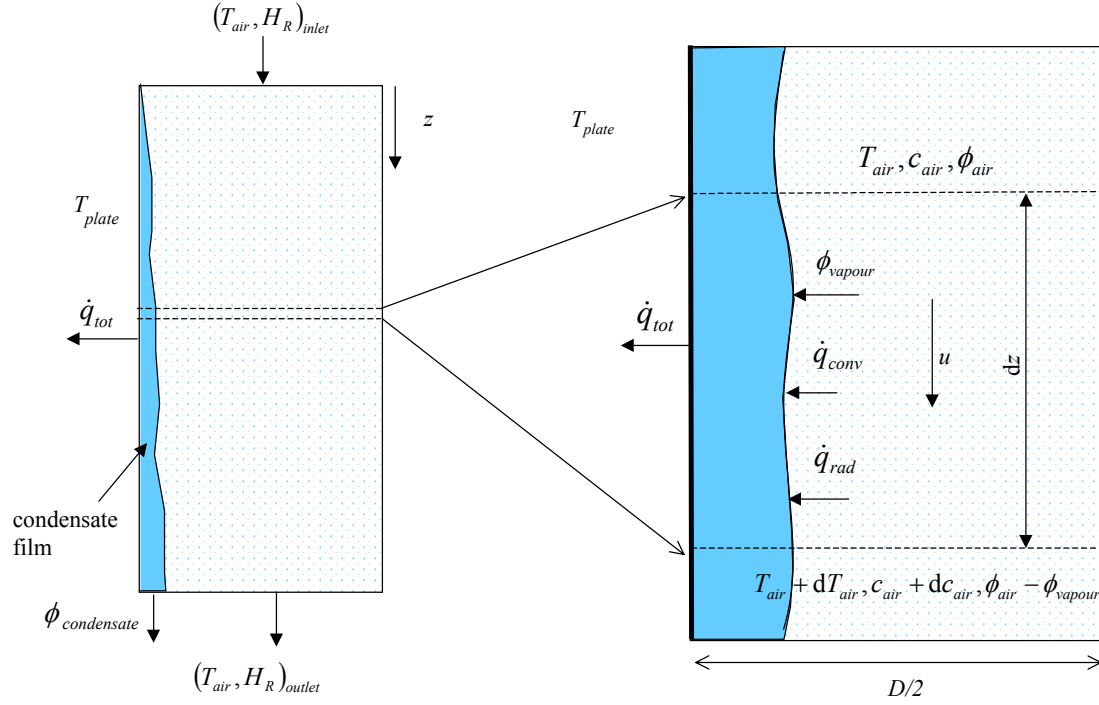


Figure 2.1 A gas mixture of air and vapour passing a plate with the condensed film on it (left) and a section of the geometry used for the iterative calculations (right);  $T_{air}$ ,  $T_{plate}$ , temperature of air and plate;  $\dot{q}_{tot}$ ,  $\dot{q}_{conv}$ ,  $\dot{q}_{rad}$ , the total heat transfer and by convection and radiation;  $z$ , distance in the flow direction;  $H_R$ , relative humidity;  $\phi_{condensate}$ ,  $\phi_{air}$ ,  $\phi_{vapour}$ , mass flow of condensate, air and vapour;  $c_{air}$ , mass fraction of water vapour in air

Condensation on a cold plate from a humid airflow involves coupled heat and mass transfer. Condensation occurs when the vapour concentration in the air is higher than the vapour concentration very near the cold surface. The local steady state balance for the sensible heat can be read from Figure. 2.1:

$$-\frac{d}{dz}(\phi_{air} C_p T_{air}) - \alpha w (T_{air} - T_{wall}) = 0 \quad (2.1)$$

where:  $z$  is the distance in the flow direction in m;  $\phi_{air}$  is the mass flow of humid air in  $\text{kg s}^{-1}$ ;  $C_p$  is the specific heat of the humid air in  $\text{J kg}^{-1} \text{K}^{-1}$ ;  $T_{air}$  and  $T_{wall}$  are the temperatures of the air and wall respectively in K;  $\alpha$  is the heat transfer coefficient by convection in  $\text{W m}^{-2} \text{K}^{-1}$ ; and  $w$  is the width of the plate in m.

Assuming constant mass flow (*i.e.* condensing mass is very small related to the total mass flow which is true in a greenhouse environment) and constant specific heat (so the

change in vapour content does not affect specific heat which is also true for the greenhouse air), Eqn (2.1) can be simplified to:

$$-u \frac{D}{2} \rho C_p \frac{dT_{air}}{dz} - \alpha (T_{air} - T_{wall}) = 0 \quad (2.2)$$

where:  $u$  is the flow velocity in  $\text{m s}^{-1}$ ;  $D$  is the distance between two fins in  $\text{m}$ ; and  $\rho$  is the density of the humid air in  $\text{kg m}^{-3}$ .

The steady state mass balance for the water vapour in the small section is given analogously by

$$-u \frac{D}{2} \frac{dc_{air}}{dz} - k(c_{air} - c_{wall}) = 0 \quad (2.3)$$

where:  $k$  is the mass transfer coefficient in  $\text{m s}^{-1}$ ;  $c_{air}$  is the mass fraction of vapour in the air in  $\text{kg kg}^{-1}$  and  $c_{wall}$  is the mass fraction of vapour at the surface of the wall.

The Lewis relation can determine the relation between the coefficients for heat and mass transfer in a phase changing flow:

$$\frac{\alpha}{k} = \rho C_p Le^{2/3} \quad (2.4)$$

with the Lewis number  $Le$  given by:

$$Le = \frac{\lambda}{\rho C_p \delta} \quad (2.5)$$

where:  $\lambda$  is thermal conductivity of air in  $\text{W m}^{-1} \text{K}^{-1}$ ; and  $\delta$  is the diffusion coefficient of water vapour in air in  $\text{m}^2 \text{s}^{-1}$ .

The heat transfer coefficient  $\alpha$  for natural convection at the finned tube can be found from relations between the Nusselt  $Nu$ , Grashof  $Gr$  and Prandtl  $Pr$  numbers:

$$\begin{aligned} Nu &= a (Gr Pr)^{1/4} & 10^4 < Gr Pr < 10^8 \\ Nu &= b (Gr Pr)^{1/3} & Gr Pr > 10^8 \end{aligned} \quad (2.6)$$

where:  $a$  and  $b$  are factors given by the geometry of the system and the Grashof  $Gr$  number is:

$$Gr = \frac{L^3 g \beta (T_{air} - T_{wall})}{\nu^2} \quad (2.7)$$

where:  $L$  is the length in the flow direction in  $\text{m}$ ;  $g$  is the gravitational acceleration in  $\text{m s}^{-2}$ ;  $\beta$  is the gas expansion coefficient in  $\text{K}^{-1}$ ;  $\nu$  is the kinematic viscosity in  $\text{m}^2 \text{s}^{-1}$ .

The Prandtl number is

$$Pr = \frac{\eta C_p}{\lambda} \quad (2.8)$$

where  $\eta$  is the dynamic viscosity in  $\text{kg m}^{-1} \text{s}^{-1}$ .

For a vertical plate the factors  $a$  and  $b$  are found to be 0.50 and 0.10, for a cylinder  $a$  is 0.53 and  $b$  is 0.13 (Becker, 1986). The factors  $a$  and  $b$  for a finned pipe are a combination of the factors of the two geometries.

The latent heat transfer at the fin  $\dot{q}_{lat}$  (W) is given by:

$$\dot{q}_{lat} = \phi_{vapour} L_v \quad (2.9)$$

where:  $\phi_{vapour}$  is the condensing mass flow in  $\text{kg s}^{-1}$ ; and  $L_v$  is the latent heat of vaporisation in  $\text{J kg}^{-1}$ .

The condensing mass flow  $\phi_{vapour}$  is given by:

$$\phi_{vapour} = k A \rho (c_{air} - c_{wall}) \quad (2.10)$$

where  $A$  is the surface area per metre length of apparatus in  $\text{m}^2 \text{m}^{-1}$ .

For the finned tube in the greenhouse environment, the radiative heat transfer  $\dot{q}_{rad}$  in W has to be considered. This is described by the Stefan Boltzmann equation:

$$\dot{q}_{rad} = \varepsilon_{eff} \sigma A_{rad} (T_{surr}^4 - T_{wall}^4) \quad (2.11)$$

where:  $\varepsilon_{eff}$  is the effective absorption coefficient of the surface considered;  $A_{rad}$  is the outside surface of the finned tube system which is in interaction with the surroundings in  $\text{m}^2$ ; and  $\sigma$  is the Stefan-Boltzmann constant in  $\text{W m}^{-2} \text{K}^{-4}$ . For a finned tube with small distance between the fins compared to the height of the fins, the radiation area  $A_{rad}$  can be taken to be the circumference of the finned pipe times the length of the pipe. The effective absorption coefficient  $\varepsilon_{eff}$  is higher than that of the material because the radiation is ‘trapped’ between the fins. The finned pipe considered in this experiment is painted white with an absorption coefficient  $\varepsilon$  of 0.95 (Weast, 1981). This absorption coefficient being so high, the effective absorption coefficient  $\varepsilon_{eff}$  is set to 1. The finned pipes located above the crop also absorb solar radiation. The absorption coefficient  $\varepsilon_{solar}$  for solar radiation differs from that for the thermal wavelength band. For white paint  $\varepsilon_{solar}$  is 0.35 (Weast, 1981). The surface area absorbing this radiation is approximately the diameter of the finned pipe times its length.

### **2.2.2 The computational fluid dynamics calculations**

A crucial element in the analysis of Section 2.2.1 is the determination of the coefficient for heat and mass transfer. From the literature (Becker, 1986) the convective heat transfer coefficient for basic geometries such as plate, cylinder and sphere can be deduced. A finned pipe is not a standard geometry and the heat transfer is more difficult to determine. To overcome this difficulty, computational fluid dynamics (CFD) is used for analysis. A commercial programme FLUENT 5.2 (Fluent, 1998) is used. Several commercially available finned pipes are studied by means of CFD. The parameters

considered are the spacing between the fins, the height of the fins and the diameter of the pipe. The selection is based on light interception, heat removal, and condensate removal.

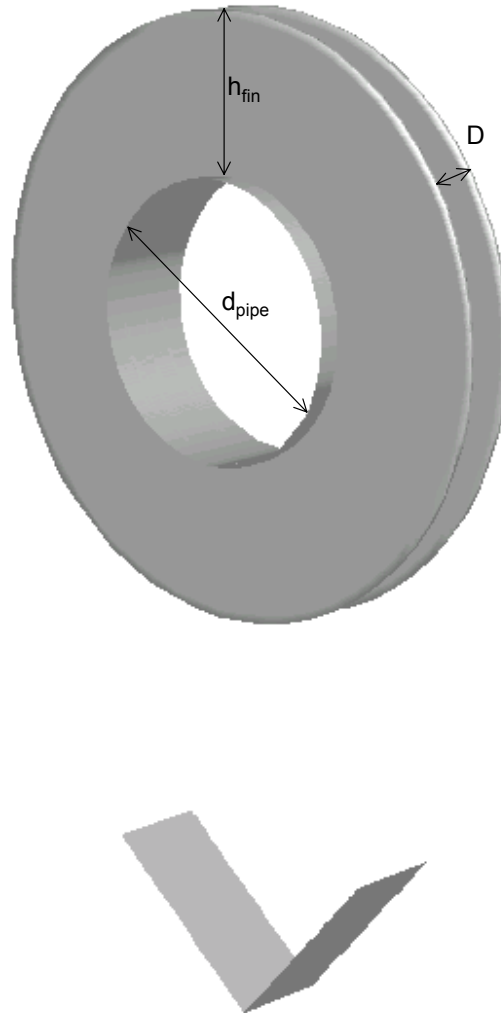


*Figure 2.2 The computational fluid dynamics model of the finned pipe with gutter for condensate removal;  $d_{pipe}$ , diameter of pipe;  $D$ , distance between fins;  $h_{fin}$ , height of fin*

The model used for the CFD calculations of sensible heat and vapour transfer is depicted in Figure 2.2. The extra gutter placed under the finned pipe to remove condensate is also included in the model because it is an obstruction to the flow. The temperature and the mass fraction of vapour in the air are the boundary conditions for the ambient air. The boundary conditions for the finned pipe are the temperature and the mass fraction at the surface, the latter being the mass fraction of saturated air at a temperature equal to the plate temperature. The absorption coefficient  $\varepsilon$  at the surface is set to 0.95.

The flow is initiated by natural convection. The physical properties of air together with the diffusion coefficient  $\delta$  for vapour through air are taken from Weast (1981). The latent heat flow by condensation is not taken into account for the CFD calculations. The latent heat flow can be determined from the mass flow using Eqn (2.9). The solar radiation is not included in the CFD model.

## **2.3 Experiments**

The experiment is conducted in a two span Venlo-type double glazed greenhouse compartment with a ground surface area of 6.4 m by 25 m, with a cucumber crop cultivated in a traditional way. Both day and night temperature are set at 20.5°C and ventilation is controlled to prevent temperature excess only.

### **2.3.1 The dehumidifying system**



*Figure 2.3 Photograph of the greenhouse where finned tubes are placed under the gutter and an enlargement of a finned tube with condensation on the surface.*

The cooled pipes made of steel, which are finned for extended surface area, are placed below the gutter (Figure. 2.3). The total length of the finned pipes in the greenhouse compartment under consideration is four pipes of 25 m. The outer diameter of the fin is 103 mm, that of the pipe is 48 mm and there are 110 fins per metre of pipe. The fin thickness is 1 mm. Condensation occurs when the temperature of the finned pipes is below the dew point temperature of the air passing the pipes.

The temperature of the cooling water pumped into the system is controlled depending on the moisture deficit  $\Delta x$ . The moisture deficit is the amount of vapour that can be added to the air before saturation. The installation is switched on when moisture deficit is less than the setpoint  $\Delta x_{setpoint}$ . Then the temperature of the cooling water  $T_{pipe}$  is determined using,

$$T_{pipe} = B (\Delta x_{air} - \Delta x_{setpoint}) + T_{wet\ bulb} \quad (2.12)$$

where:  $B$  is a gain factor in K; and  $T_{wet\ bulb}$  is the wet bulb temperature in K. The wet bulb temperature is used because it is measured by the climate computer and varies with the dew point temperature, thus condensation can be ensured. The setpoint deficit  $\Delta x_{setpoint}$  is set to  $4 \text{ g kg}^{-1}$ , equal to the value when in greenhouse practice ventilation is applied for dehumidification. The gain factor  $B$  is set to a value of 10 to give a temperature difference of 10 K with  $T_{wet\ bulb}$  for a difference of  $1 \text{ g kg}^{-1}$  between  $\Delta x_{air}$  and  $\Delta x_{setpoint}$ . This will give a reasonable dehumidification in relation to the transpiration of the crop. The temperature difference between the greenhouse air and the finned pipe is kept almost constant for the whole system (temperature drop between inlet and outlet  $< 1^\circ\text{C}$ ) by pumping a large mass flow of cooling water through the system ( $8 \text{ m}^3 \text{ h}^{-1}$ ).

### 2.3.2 Data

The climate in the greenhouse is monitored at four positions at different heights near the centre of the greenhouse using wet and dry Pt-100 thermometers. The climate control computer measures the solar radiation, the outside temperature, the window opening and the temperature of the heating system. The total heat removed by the dehumidifying system is calculated from the temperature difference between inlet and outlet of the finned pipes (accuracy  $\pm 0.05 \text{ K}$ ) and the mass flow through the system. The error in the determination of the heat transfer increases as a result of this large water flow, the maximum error based on the minimum heat transfer is 12%. The latent heat removed is calculated from the collected condense monitored by a rain gauge (ARG100\EC) producing a pulse for each  $11.0 \pm 1\% \text{ ml}$  collected. The measuring frequency is once per minute.



## 2.4 Results

### 2.4.1 The computational fluid dynamics results

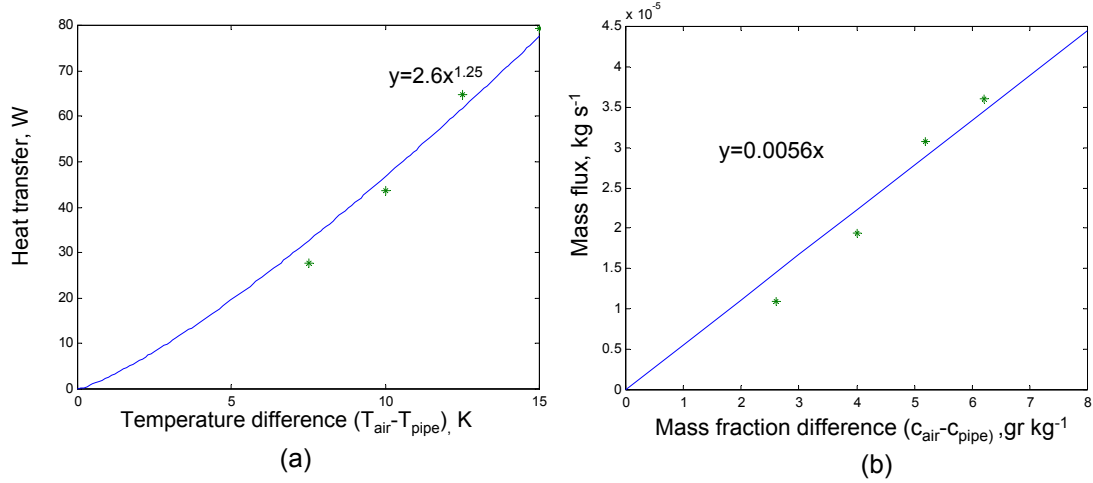


Figure 2.4 (a) The heat transfer by convection as a function of the temperature difference between the air  $T_{air}$  and the pipe  $T_{pipe}$  for a metre of finned pipe; (b) the mass flux of condensate as a function of the difference between the mass fraction of vapour in the air and at the surface of the finned pipe for a metre of finned pipe

In Figure 2.4, the results of CFD calculations are depicted. All results are for one metre of pipe. Figure 2.4(a) shows the heat transfer by convection  $\dot{q}_{conv}$  as a function of the temperature difference between the pipe and the air. Figure 2.4 (b) shows the mass flux  $\phi$  in  $\text{kg s}^{-1}$  as a function of the concentration difference between the air near the pipe and the air. The relative humidity  $H_R$  of the surrounding air is set to 80% in the calculation. The calculation showed no turbulence as expected based on  $\text{Gr Pr}$  is  $1.2 \cdot 10^6$ , causing the vapour transport to be mainly due to diffusion. The factor  $a$  in Eqn (2.6) is 0.23 calculated from the fit shown in Figure 2.4 (a). The slope in Figure 2.4 (b) indicates using Eqn (2.10) that the mass transfer coefficient  $k$  is  $3.1 \cdot 10^{-3} \text{ m s}^{-1}$ . Based on this number the heat transfer coefficient  $\alpha$  equals  $3.1 \text{ W m}^{-2} \text{ K}^{-1}$  according to Eqn (2.4). The heat transfer coefficient by convection from Figure 2.4 (a) equals  $3.0 \text{ W m}^{-2} \text{ K}^{-1}$  for a temperature difference of  $10^\circ\text{C}$ . So the transfer of water vapour through the air predicted by CFD corresponds with the Lewis relation.

2.4.2 The experimental results

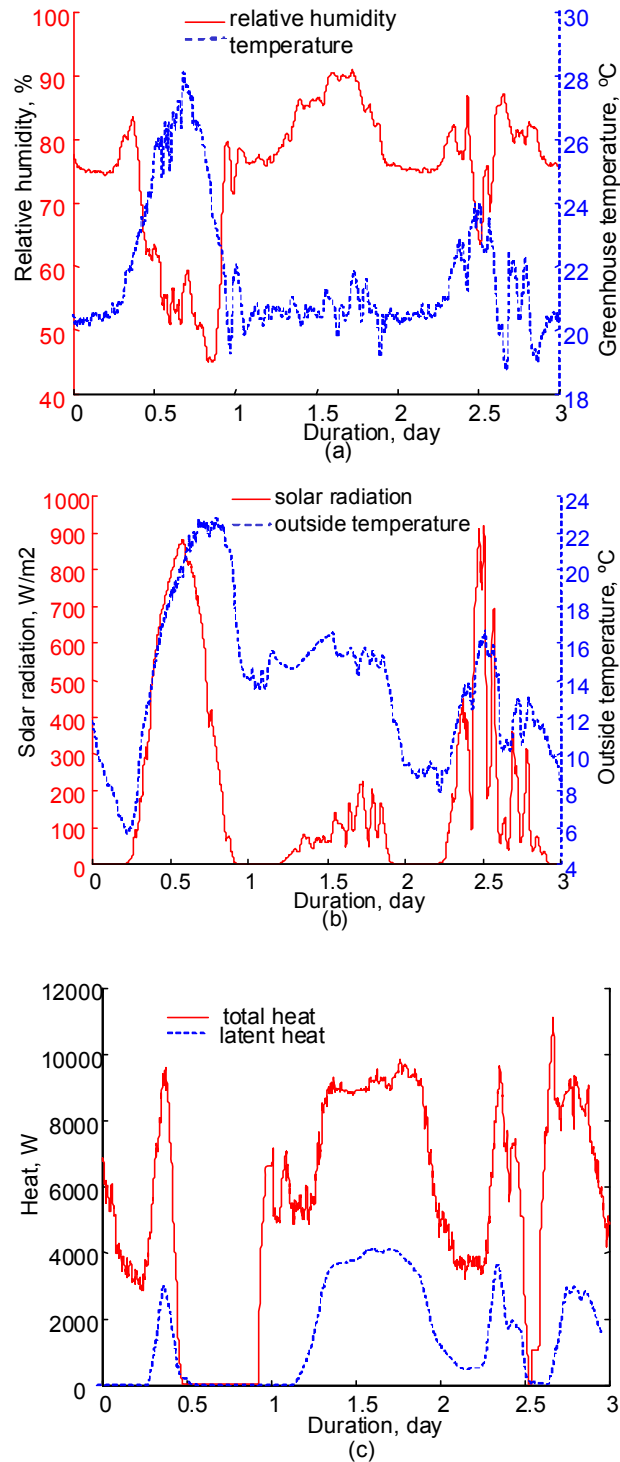
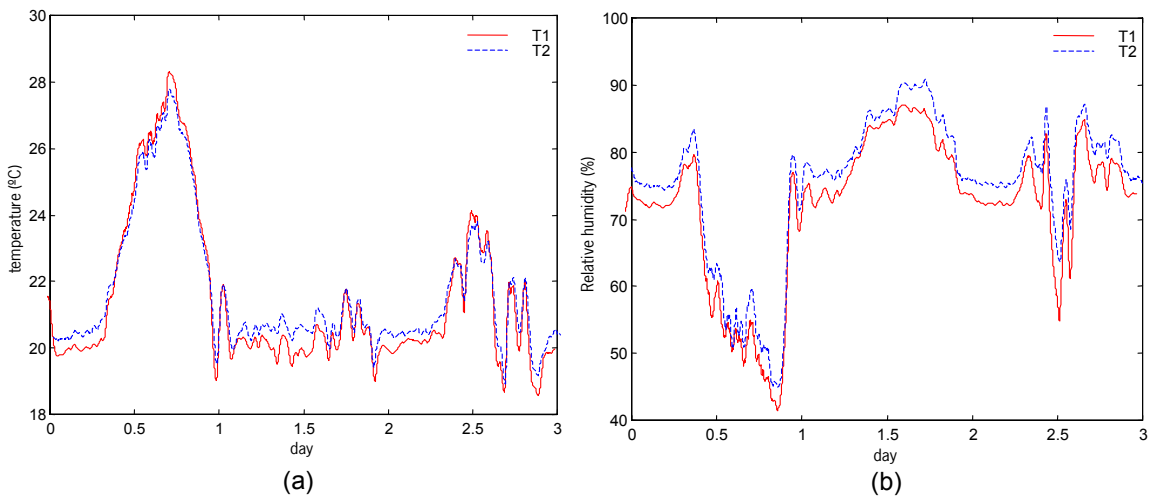


Figure 2.5 (a) The relative humidity and temperature in the greenhouse; (b) the solar radiation and the temperature outside the greenhouse; (c) the total heat and latent heat removed from the greenhouse

The graphs in Figure 2.5 show data collected over a three-day period, starting at midnight. During the first day the solar radiation is high, resulting in a high greenhouse temperature. During this period the relative humidity in the greenhouse is low due to a high ventilation rate with the relatively cold and dry outside air. Consequently the dehumidifying system is switched off during this period. The greenhouse temperature decreases as solar radiation diminishes, causing an increase in relative humidity. At about 0.9 day the dehumidifying system is switched on. Latent heat removal can only be measured from 1.1 day on because the system (fins, gutters, pipes) first has to be filled with condense before it runs off and can be measured by the rain gauge. During the night the relative humidity remains below 80%. At sunrise (after 1.2 day) the relative humidity starts to increase due to crop transpiration. Because the outside temperature is about 15°C and solar radiation is low, ventilation is not necessary. Condensation on the double glazed roof is minimal during these conditions. No ventilation and a relatively high outside temperature cause the relative humidity in the greenhouse to reach 90%. During this period the rate of heat removed by the dehumidifying system is approximately 9000 W of which almost 4000 W is latent heat. This is around 6 litres of condensate per hour, which is  $40 \text{ g m}^{-2} \text{ h}^{-1}$ . The total heat removal is influenced by the solar radiation during the day mainly because of the extra transpiration by the crop.



*Figure 2.6 (a) The temperature at two locations in the greenhouse; (b) the relative humidity at two locations in the greenhouse;—position T1 in the centre of the greenhouse 40 cm under the gutter; - - - position T2 under the ridge of one of the two spans at the same height*

During the same period, for two positions in the greenhouse, temperature and relative humidity as indicated in Figure 2.5, are shown in Figure 2.6. Location T1 is in the centre of the greenhouse 40 cm under the gutter and location T2 is under the ridge of one of the two spans at the same height. The temperature at location T1 is only half a

degree lower than at location T2 when the dehumidifying system is on. The relative humidity is less than 5% lower directly under the cold finned tubes. So no large temperature or humidity gradients occur when the installation is in operation.

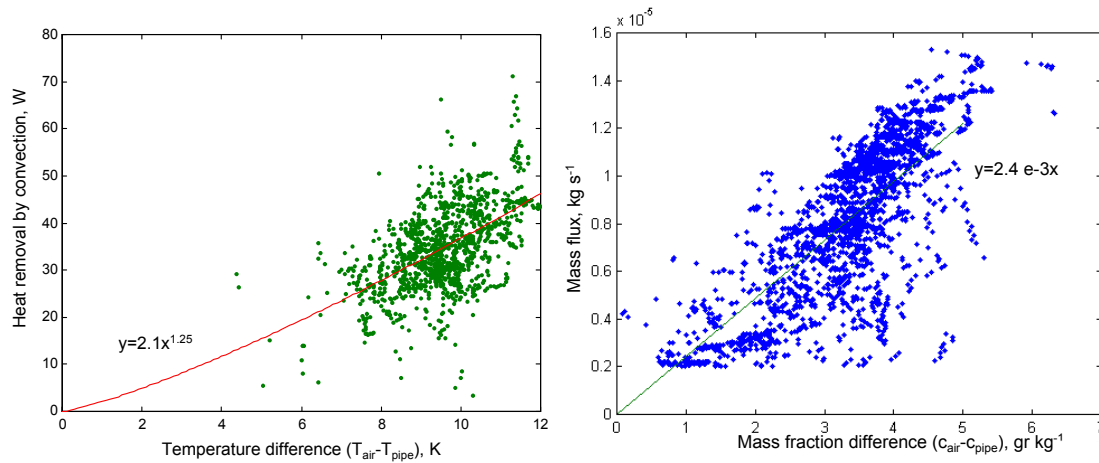


Figure 2.7 (a) Instantaneous measurements of the heat transfer by convection as a function of the temperature difference between the air and the finned pipe for a metre of finned pipe; (b) The mass flux of condensate as a function of the difference between the mass fraction of vapour in the air and at the surface of the finned pipe for a metre of finned pipe

Instantaneous measurements of the heat transfer by convection and condensation per metre of pipe as a function of the temperature and the concentration difference between the greenhouse and the finned pipe for a month are shown in Figure 2.7(a) and (b) respectively. The heat removal by convection is calculated from the total heat removal minus the latent heat, the solar radiation and the radiation calculated by Eqns (2.9 and 2.11). The relation based on theory (Section 2.2.1) is fitted through the data points using the method of least squares. The heat transfer by convection in the experiment as given in Figure 2.7(a) is less than that in the CFD calculations as given in Figure 2.4(a). This can be explained by the fact that the temperature difference is based on the greenhouse temperature not the temperature of the air passing the finned pipe. Air first passes the cold roof of the greenhouse where it is cooled and dehumidified before passing the cold surface. This effect was not taken into account in the CFD calculations.

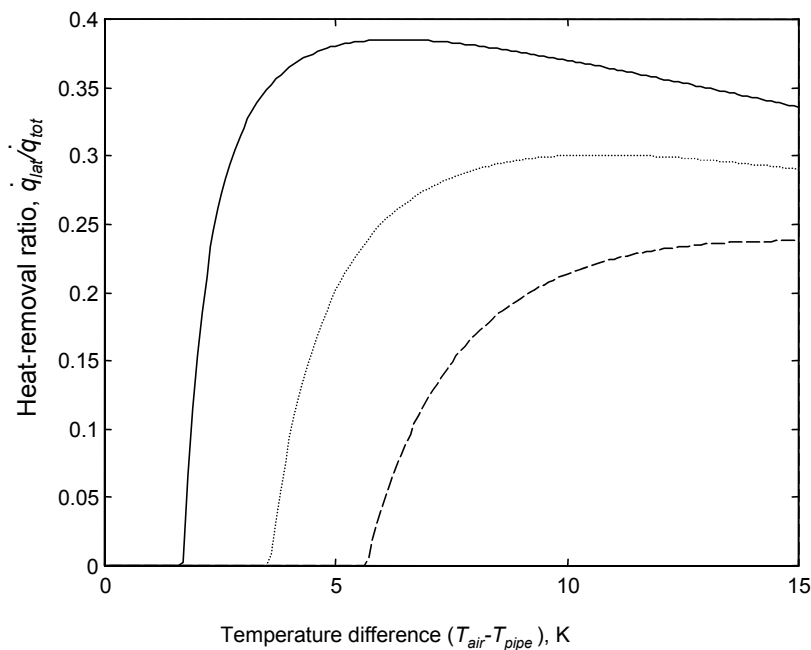


Figure 2.8 The latent heat removal over the total (convection, radiation and condensation) heat removal as a function of the temperature difference between the air and the pipe for a relative humidity of 70 (---), 80 (···) and 90 (—) %.

Based on the experimental results the ratio between the latent heat removal over the total heat removal (heat transferred by convection, radiation, solar radiation and condensation) as a function of the temperature difference for air with a different relative humidity  $H_R$  is in Figure 2.8. The fraction of latent heat removal is less than 40%. For greenhouse conditions with a relative humidity around 80% the ratio is only one-third.

## 2.5 Conclusions

A dehumidifying system based on condensing water vapour from the greenhouse air is tested. As the heat and mass transfer coefficients are not known a priori, the system is first investigated by means of computational fluid dynamics. The system is then tested in a greenhouse. One metre of finned pipe used in this experiment at a temperature of 5°C, can remove 54 grams of vapour per hour from air at a temperature of 20°C and 80% relative humidity.

The 3% light interception of the construction used in this experiment is not acceptable in a commercial greenhouse. By implementing the system directly in the construction of the greenhouse part of this problem can be solved.

It can be concluded from the results that the fraction of latent heat removal over the total heat removal is less than 40%. For air with a relative humidity of 80 % only one third of the heat removed is latent heat.

A year round simulation based on this experiment would show if the presented system is more energy efficient compared with ventilation.

**Acknowledgements**

This research was financed by the E.E.T. (Ecology, Economy and Technology) research programme funded by the Dutch Ministries of EZ (Economic Affairs), of OCW (Education) and of VROM (Environmental Affairs).

---

# 3

## Design of a Low Energy Dehumidifying System for Greenhouses

---

This chapter was published before as:  
J.B. Campen and G.P.A. Bot (2001). Design of a Low Energy  
Dehumidifying System for Greenhouses. Journal of Agricultural  
Engineering Research 78(1) pp 65-73  
Doi:10.1006/jear.2000.0633

### Abstract

A concept for a greenhouse dehumidifier has been designed. Important constraints for the design are low energy consumption and homogeneous greenhouse climate. From a survey of dehumidifying methods, condensation to a cooled surface was selected as most promising. Low energy demand is achieved by natural air circulation through the system and by recovering sensible heat. A homogeneous climate can be realised by decentralised local dehumidification in the greenhouse. Applying a computational fluid dynamics (CFD) program to simulate fluid flow and heat exchange enabled great improvements in the design. A vertical geometry was chosen first in a double chimney approach to exploit the vertical distance between inlet and cold surface and that between cold and hot surface for natural convection air circulation. However, CFD calculations indicated stagnating flow in this vertically oriented system. Orienting the system horizontally greatly enhanced the systems performance.

A separate model for condensation has been created to complement the CFD program that did not include condensation. A prototype of the designed dehumidifier was built and tested. Calculations and experiments were in fair agreement and demonstrated the potential for practical application.

### Notation

$A^*$	total heat exchanging surface area per meter length of apparatus, $\text{m}^2 \text{m}^{-1}$
$a$	proportionality factor, $\text{K}^{-1} \text{m}^{-1} \text{s}^{-1}$
$b$	proportionality factor, $\text{W m}^{5/2} \text{K}^{3/2}$
$c$	concentration, $\text{kg kg}^{-1}$
$C_p$	specific heat, $\text{J kg}^{-1} \text{K}^{-1}$
$D$	plate distance, m
$D_h$	hydraulic diameter, m
$f$	Fanning factor
$g$	gravity, $\text{m s}^{-2}$
$k$	mass transfer coefficient, $\text{m s}^{-1}$
$K_w$	friction loss factor, $\text{J s}^2 \text{kg}^{-1} \text{m}^{-2}$
$L$	length, m
$L_v$	latent heat of vaporisation, $\text{J kg}^{-1}$
Le	Lewis number
Nu	Nusselt number
$P$	heat, W



$p$	pressure, Pa
Re	Reynolds number
$H_R$	relative humidity, %
$S_\varphi$	source term for $\varphi$
$T$	temperature, °C
$t$	time, s
$u$	velocity, m s <sup>-1</sup>
$v$	velocity vector, m s <sup>-1</sup>
$W$	width, m
$\Gamma_\varphi$	diffusion coefficient for $\varphi$ , m <sup>2</sup> s <sup>-1</sup>
$\alpha$	heat transfer coefficient, W m <sup>-2</sup> K <sup>-1</sup>
$\beta$	gas expansion coefficient, K <sup>-1</sup>
$\delta$	diffusion coefficient, m <sup>2</sup> s <sup>-1</sup>
$\varphi$	concentration of transported quantity
$\phi_{cond}$	dehumidification per hour, ml h <sup>-1</sup>
$\phi_m$	mass flow, kg s <sup>-1</sup>
$\lambda$	thermal conductivity, W m <sup>-1</sup> K <sup>-1</sup>
$\nu$	kinematic viscosity, m <sup>2</sup> s <sup>-1</sup>
$\rho$	density, kg m <sup>-3</sup>
Subscripts	
<i>air</i>	air
<i>cold</i>	cold section
<i>warm</i>	warm section
<i>g</i>	greenhouse or ambient
<i>he</i>	heat recovery unit
<i>incoming</i>	coming into a section
<i>lat</i>	latent part
<i>out</i>	going out a section
<i>removed</i>	removed by a section
<i>sens</i>	sensible part
<i>plate</i>	plate

### 3.1 Introduction

Humidity is one of the key factors in greenhouse climate. It usually tends to be high due to crop transpiration. Crops exposed to high humidity levels have a higher risk of developing fungal diseases and physiological disorders (Hand, 1988; Bakker, 1991;

Bakker *et al.*, 1995). In conventional greenhouses with a single cover, humidity level is limited by condensation on the relatively cold cover and by ventilation through air leaks. Moreover, ventilators can be opened for water vapour removal. If this is combined with heating, extra energy is consumed which is about 20% of the greenhouse energy demand (De Zwart, 1996). Nowadays, low energy demand greenhouses with high insulating covers are developed aiming at sustainable crop production (Sonneveld, 1999). However, this induces higher humidity levels. Opening the ventilators and simultaneous heating reduces high cover insulation so has to be prevented. Therefore, active dehumidification with low energy consumption is essential in low energy demand greenhouses. This low energy demand not only concerns the power to drive the dehumidification process but also the power to drive the air circulation.

The dehumidification system has to be integrated in the climate conditioning. Prevention of pests and plagues requires a homogeneous greenhouse climate without cold or hot spots. Moreover with a homogeneous climate, quality can be controlled better and crop production is more homogeneous with easier labour management. This indicates that dehumidification has to be a decentralized operation

Various dehumidifying systems for greenhouses have been developed and tested (Boulard *et al.*, 1989; Chasseriaux, 1987; Seginer & Kantz, 1989; Gauthier *et al.*, 1995; Isetti *et al.*, 1997). The main problems of these systems concern high energy consumption due to forced air circulation, large humidity gradients in the greenhouse, a lack of capacity, high air velocities in the greenhouse and large size of the installation causing high light interception. Also, dehumidification in air conditioning systems for commercial and industrial buildings has a high level of energy consumption and needs forced air circulation.

Therefore, a low energy demand dehumidification system was designed eliminating most of these problems. First the simple theoretical principles of the system are described. Due to the complex spatial distributed flow phenomena and thermal effects computational fluid dynamics (CFD) was applied in the design process. A prototype was constructed and tested to check the results of the model calculations.

## **3.2 Theoretical considerations**

### **3.2.1 Dehumidification**

Air can be dehumidified in two principal ways: by hygroscopic absorption or by condensation at an actively cooled surface.

### *3.2.1.1 Absorption of water vapour by a hygroscopic medium*

Due to the very low vapour pressure at the hygroscopic surface water is absorbed at this surface. The driving force for absorption is the vapour pressure difference between the greenhouse air and the air at the hygroscopic surface. The latent heat is released at the absorbing surface. The absorbed water has to be removed in a reconditioning unit (Pritchard *et al.*, 1993). The installation can be designed as a distributed system in the greenhouse with air circulation driven by natural convection.

An important aspect is that the mass transfer coefficient between hygroscopic surface and air is coupled to the heat transfer coefficient at this surface. Therefore, the absorbed latent heat is released immediately to the greenhouse air or has to be removed for later use by active cooling of the surface. So hygroscopic dehumidification can preferably be used in periods with greenhouse energy demand or demands complex installations for active cooling of the absorption surface.

Another more practical aspect is the inherent risk of the installation. The hygroscopic media are highly concentrated salt solutions (bromides, chlorides, *etc*) that have to be pumped between the absorbing surface and the re-conditioner situated outside the greenhouse. The liquids are expensive and may cause severe problems to the environment if a system failure or leakage occurs.

For these reasons, this principle is not applied in this study.

### *3.2.1.2 Condensation of water to cold surfaces*

If air temperature is below the dew point temperature, the vapour pressure will be lower than the actual vapour pressure and the difference will act as driving force for condensation. In the greenhouse, this surface temperature has to be below about 5°C for sufficient condensing capacity. The cold surface can be cooled by a heat pump, for example. The evaporator of the heat pump absorbs the latent heat from condensation and the sensible heat from cooling. At the condenser of the heat pump, this heat and the energy to drive the compressor is released at a higher temperature for heating or for storage. So the principle can be applied in periods with and without greenhouse heat demand but with a need for dehumidification. Heat pump systems are technically well developed and can be connected to cooling and heating systems in an easy way without risks for the environment. Therefore, this principle is applied in the current study.

### *3.2.1.3 Application of the condensation principle*

An important aspect of the system is the energy consumption due to the dehumidification process and the air circulation through the system.

The energy consumption of the dehumidification process is given by the power input of the heat pump that is linked to the amount of transported energy via the coefficient of performance (COP). This COP is given by the type of heat pump and its capacity, and

depends on the operating temperature level and the temperature difference between heat pump evaporator and condenser (Boot *et al.*, 1990). If the transported energy can be decreased, the heat pump power consumption is decreased. In the dehumidifying application, the transported energy is the sum of absorbed latent and sensible heat. For normal greenhouse air at 80% relative humidity ( $H_R$ ) and temperature of 22°C which is cooled to 5°C and 100%  $H_R$ , it can be calculated easily that the absorbed sensible and latent heat are about equal. In this application, the power consumption of a heat pump is about 50% for dehumidification and 50% for cooling. Therefore, the design includes reduction of the effective cooling of the air by applying heat recovery between the inlet greenhouse air and the outlet air from the cold surface.

If fans are applied for air circulation, then electric power demand ranges from 5 to 10 W m<sup>-2</sup> which can even be higher if the dehumidifying unit has high air flow resistance (De Jong *et al.*, 1993). So preventing forced air circulation has great energy saving potentials. Therefore, application of natural air circulation is very attractive.

From the given considerations the dehumidifier should contain a cold section heat exchanger for removal of water vapour by condensation and a heat exchange unit between the entering warm greenhouse air and the cooled dehumidified air to recover the sensible heat. A hot section heat exchanger has to recondition the greenhouse air to the desired temperature.

### 3.2.2 Flow phenomena

As deduced in Section 3.2.1.3, the dehumidifier design with potentially low energy consumption is based on a combination of three heat exchangers: a cold section for condensation, a heat recovery unit between inlet and cold air and a hot section for heating. The air circulation in the system has to be buoyancy driven in balance with the energy dissipation by friction. Due to the demand for high heat and mass transfer rates, this system will have high internal resistance to airflow.

For a first estimation of the effects, it is assumed that a temperature difference is driving the flow in a vertical channel with length  $L$  and hydraulic diameter  $D_h$  both in m. The friction can then be expressed as a pressure difference  $\Delta p$  derived from pipe or channel flow friction and friction of other parts according to:

$$\Delta p = \sum_i 4f \left( \frac{L}{D_h} \right)_i \frac{1}{2} \rho u^2 + \sum_j \left( K_w \frac{1}{2} \rho u^2 \right)_j \quad (3.1)$$

where:  $f$  is the Fanning friction factor for pipe or channel flow;  $K_w$  is the friction loss coefficient of non channel parts;  $\rho$  is the density of the fluid in kg m<sup>-3</sup>; and  $u$  is the local average flow velocity in m s<sup>-1</sup> (Rohsenow *et al.*, 1973). For a channel between two plates,  $D_h$  is  $2D$ , with  $D$  the distance between the plates.

The driving pressure difference  $\Delta p$  in Pa for buoyancy driven air flow between two locations at vertical distance  $L$  is induced by the density difference  $\Delta\rho$  in  $\text{kg m}^{-3}$  over this distance:

$$\Delta p = g \Delta\rho L \quad (3.2)$$

where  $g$  is the acceleration due to gravity in  $\text{m}^2 \text{s}^{-1}$ .

The density difference is due to the water vapour concentration difference and the temperature difference. For the dehumidifying conditions, it can easily be calculated that the concentration effect is small compared to the temperature effect. Therefore, the pressure difference can be expressed in the temperature difference  $\Delta T$  in K as:

$$\Delta p = g\beta \rho L \Delta T \quad (3.3)$$

where  $\beta$  is the gas expansion coefficient in  $\text{K}^{-1}$ .

Equations (3.1), (3.2) and (3.3) can be used for a first estimation design rule for the driving force, the resulting flow, the heat transfer rates due to the given temperature differences and the geometrical parameters.

The flow can be expected to be laminar in the channels of the apparatus. The Fanning friction factor  $f$  is given by:

$$f = 16/\text{Re} \quad (3.4)$$

where  $\text{Re}$  is the Reynolds number. For laminar flow with narrow channels at a small distance  $D$  the viscous friction in the channels will overrule the friction in the other parts, and it can be deduced from Eqns (3.1) to (3.4) that:

$$u = aD^2 \Delta T \quad (3.5)$$

where  $a$  is the proportionality factor containing air properties according to  $a = g\beta/(8\nu)$ ,  $\nu$  being the kinematic viscosity in  $\text{m}^2 \text{s}^{-1}$ . For greenhouse conditions,  $a$  can be calculated at a numerical value of about  $2.4 \cdot 10^2 \text{ K}^{-1} \text{ m}^{-1} \text{ s}^{-1}$ . Of course,  $D$  is a small distance suppressing secondary flow in the channels. While both friction and buoyancy are proportional to  $L$ , it can be read from Eqn (3.5) that the average velocity is expected to be independent of  $L$ . The velocity is sensitive to the smallest channel dimension  $D$ .

For the dehumidifier, the effective heat transfer is the central item. It can be expressed in the heat transfer coefficient  $\alpha$  in  $\text{W m}^{-2} \text{ K}^{-1}$ . In the total apparatus, flow is driven by buoyancy; but, at the heat exchanging surfaces, it can be considered as forced flow heat transfer. Then  $\alpha$  can be found from a typical Nusselt  $\text{Nu}$  against Reynolds  $\text{Re}$  relation for laminar channel flow (Kutateladze, 1963) for air:

$$\text{Nu} = 0.593\text{Re}^{0.5} \quad (3.6)$$

The effective heat transfer depends on the total heat exchanging surface area per meter length of the apparatus  $A^*$  in  $\text{m}^2 \text{ m}^{-1}$ . With  $W$  the width of the apparatus channels and  $D$  the distance,  $A^*$  is:

$$A^* = \frac{2LW}{D} \quad (3.7)$$

From Eqns (3.6) to (3.8), it can be deduced that the effective heat transfer per meter length of the apparatus is:

$$\alpha A^* = b \left\{ \frac{LW}{D^{1/2}} \right\} \Delta T^{1/2} \quad (3.8)$$

where  $b$  is a proportionality factor containing air properties which can be calculated at a numerical value of about  $77 \text{ W m}^{5/2} \text{ K}^{3/2}$ . This estimation of the effect of characteristic parameters demonstrates that length and width of the channels have a linear effect on the heat transfer and this will decrease with the square root of the smallest channel dimension. The heat capacity of the flow in the channel is the limit for the total heat transferred. If some typical dimensions are chosen, such as channel length of 0.5, width of 0.1 and plate distance of 0.02, all in m, and a temperature difference of 20 K, then a specific heat transfer can be expected of about  $120 \text{ W m}^{-1}$ . This is quite reasonable as the basis for dehumidifier design. The expected flow velocity according to Eqn (3.5) is  $0.4 \text{ m s}^{-1}$  and then the value of  $Re$  is about 1000, confirming that the flow is indeed within the laminar region.

However, this provides only the first estimate because of the number of assumptions in the estimation procedure. Moreover, the process from general concept to detailed design includes a great number of parameters for the dehumidifier geometry. Optimization would require an extended experimental program. The macroscopic equations [Eqns (3.1) to (3.3) and (3.6)] lump all local flow or thermal phenomena. Detailed analysis of the local flow phenomena in connection to the heat and mass transfer results in a set of partial equations for the velocity, temperature and mass concentration in the apparatus, linked to the geometry via the boundary conditions. These equations can be written in generalized form as:

$$\frac{\partial \varphi}{\partial t} + \nabla \cdot v \varphi = \nabla \cdot \Gamma_\varphi \nabla \varphi + S_\varphi \quad (3.9)$$

where  $\varphi$  is the concentration of transported quantity (momentum, energy, total mass and mass of a considered component);  $t$  is the time in s;  $v$  is the velocity vector in  $\text{m s}^{-1}$ ;  $\Gamma_\varphi$  is the diffusion coefficient for  $\varphi$  in  $\text{m}^2 \text{ s}^{-1}$ ; and  $S_\varphi$  is the source term for  $\varphi$ . In the continuity equation (total mass balance),  $\varphi = \rho$  in  $\text{kg m}^{-3}$ ; in the momentum equation,  $\varphi = \rho v$  in  $\text{kg s}^{-1} \text{ m}^{-2}$  (three equations for the three velocity components); in the energy equation,  $\varphi = \rho C_p T$  in  $\text{J m}^{-3}$  where  $C_p$  is the specific heat in  $\text{J kg}^{-1} \text{ K}^{-1}$  and  $T$  is the temperature in  $^\circ\text{C}$ ; and in the mass equation  $\varphi = c\rho$  in  $\text{kg m}^{-3}$  or in  $\text{kmol m}^{-3}$ .

This set of coupled partial differential equations cannot be solved analytically but has to be solved numerically with the boundary conditions given by the apparatus geometry.

Computational fluid dynamics (CFD) including a sub-model for transport due to turbulence is developed to do so (Lauder *et al.*, 1974). A commercial CFD software tool, Fluent 5.2 (Fluent, 1998) was applied to calculate the spatial distribution of air flow and temperature. In this way, the interaction between the geometry, the acting temperature differences and the resulting spatial distribution of the flow and temperature was modelled allowing easy variation of the design parameters. The effect of differences in concentration of water vapour on the air circulation was not included in the CFD modelling. This is justified while it is only a small effect as can be read from the well-known Mollier diagram.

### **3.3 Results and discussion**

The design based on the principles described in Section 3.2, is analysed and improved by CFD. To illustrate the design process the first design is discussed resulting in an improved geometry. The dimensions of this geometry are optimised. Finally the CFD calculations are experimentally verified using a prototype.

## 3.3.1 First layout of the dehumidifier

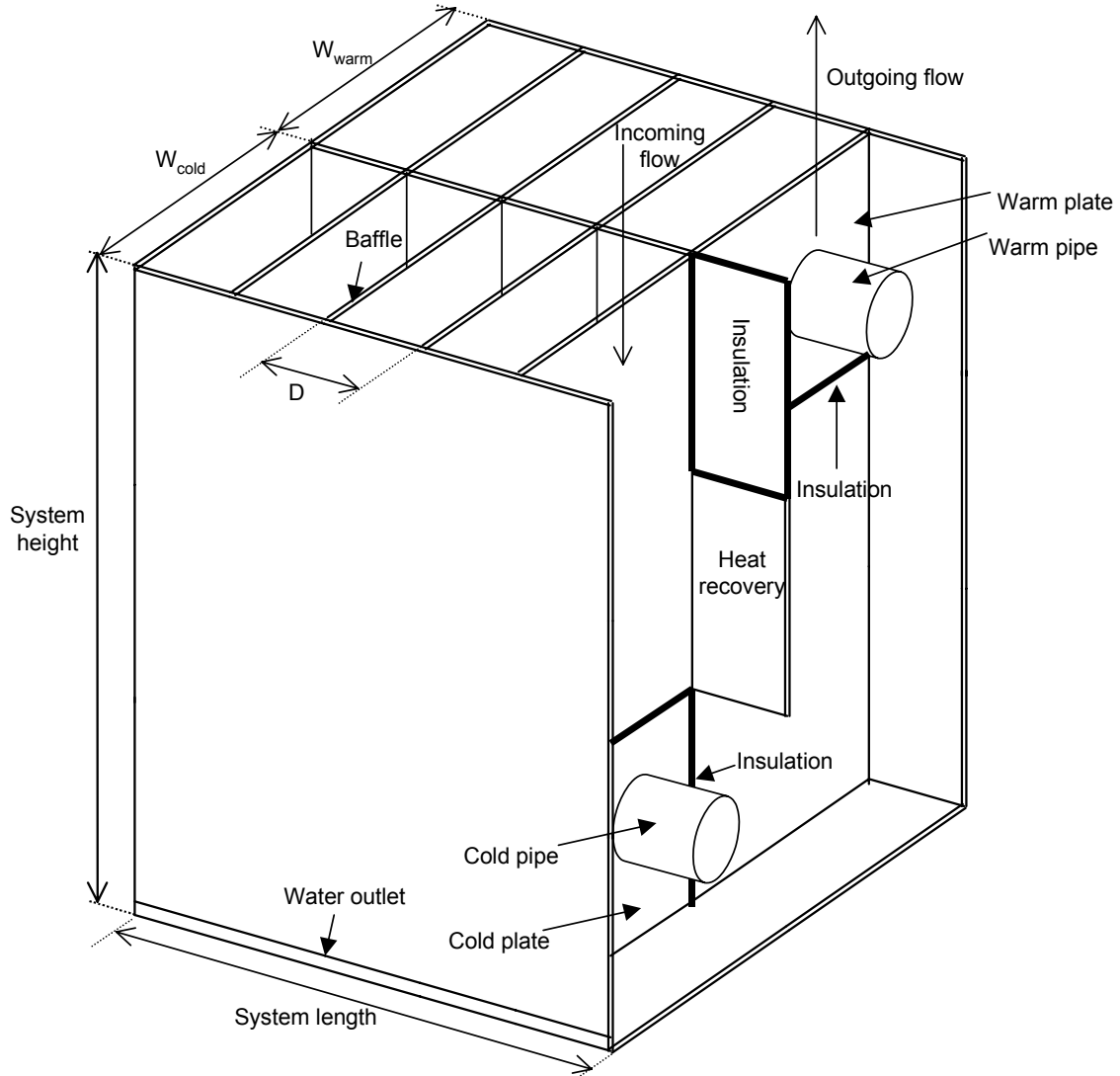


Figure 3.1 First layout of the dehumidifier;  $D$ , distance between plates;  $W_{warm}$ , width of warm section;  $W_{cold}$  width of cold section

In the first layout, the dehumidifier was designed according to the chimney effect. The cold surface was at a low position relative to the inlet and the hot surface at a high position relative to the cold surface. In this way, the vertical distances and the temperature differences between inlet and cold surface and between cold and hot surface produce the driving forces for air circulation according to Eqn (3.3). The layout is given in Figure 3.1. Between the inlet air and cooled air a heat recovery unit is implemented to regain sensible heat. At the various heat exchanging surfaces, baffles improve heat exchange. In this design, circulation is driven by the acting temperature differences and heat is recovered from the entering warm air to the cooled air. The



advantages is that no fan power is needed for air circulation and that mainly latent heat is absorbed from the inlet air demanding low heat pump energy input. Moreover, the system can easily be manufactured in long units, which can be distributed in the greenhouse in the same way as a pipe heating system enabling a homogeneous greenhouse climate.

The performance of this design was studied by calculating the velocity and temperature distribution using CFD. For simplicity reasons condensation of water vapour was not included in the CFD calculations while it was not needed to include the differences in water vapour concentration in the driving force for circulation (Section 3.2.2). Only half of the parallel cross-section between two baffles shown in Figure 3.1 was represented in the model because of the geometrical symmetry.

To evaluate the design, a reference situation was defined. In this situation, the distance between the baffles (thickness 1 mm) was 9 mm, the inlet temperature  $T_g$  is at 20°C, the warm plate was set to a temperature  $T_{warm}$  of 50°C and the cold  $T_{cold}$  to 5°C (typical temperatures using a heat pump). The cold and hot pipes have a diameter of 1 cm. All results were scaled for a length of one metre for the system.

Table 3.1 Conditions for the system based on the first design (Figure 3.1) as a function of the height; the warm and cold plates have dimensions of 5 by 5 by 0.1 cm, the distance between the plates is 1 cm and the ambient temperature  $T_g$  is 20°C

Height system, cm	Mass flow ( $\phi_m$ ), $g\ s^{-1}$	Heat cold section ( $P_{cold}$ ), W	Heat recovery unit ( $P_{he}$ ), W	Heat warm section ( $P_{warm}$ ), W	Temperature recovery unit ( $T_{he}$ ), °C	Temperature outgoing flow ( $T_{out}$ ), °C
12.0	2.6	17.1	12.4	84.2	14.5	46.0
15.0	2.3	15.6	12.2	77.5	14.3	46.7
17.5	2.1	13.9	12.2	72.7	14.1	47.8
20.0	2.0	13.1	11.8	68.7	14.0	47.7

Table 3.2 Conditions for the system based on the first design (Figure 3.1) as a function of the plate distance; the warm and cold plates have dimensions of 5 by 5 by 0.1 cm, the length of the heat recovery unit  $L_{he}$  is 10 cm and the ambient temperature  $T_g$  is 20°C

Plate distance, mm	Mass flow ( $\phi_m$ ), $g\ s^{-1}$	Heat cold section ( $P_{cold}$ ), W	Heat recovery unit ( $P_{he}$ ), W	Heat warm section ( $P_{warm}$ ), W	Temperature recovery unit ( $T_{he}$ ), °C	Temperature outgoing flow ( $T_{out}$ ), °C
7.5	2.0	15.1	11.8	74.7	13.8	49.5
10.0	2.3	15.6	12.2	77.5	14.3	46.7
15.0	2.2	13.6	9.1	62.7	15.0	41.8

The main parameters affecting the chimney effect are distance between hot and cold regions and heat exchanging areas so these parameters were varied. The results for different heights of the dehumidifier are listed in Table 3.1. The mass flow  $\phi_m$ , the heat extracted  $P_{cold}$ , the heat added  $P_{warm}$ , the heat exchanged  $P_{he}$ , the temperature of the heat exchanger  $T_{he}$  and the outgoing air temperature  $T_{out}$  are listed.

The mass flow through the system decreases as the height increases due to friction. This conflicts with the design rule (Eqn (3.5) which predicts no dependence of the channel length. From the simulations, however, it could be observed that a stagnant zone develops at the cold plate as a result of the increasing friction. Another effect, which occurred with increasing height of the system, was that cold air past over the warm plate without flowing through the whole system. Both effects diminish the mass flow. This can not be predicted by the design rule. Although the mass flux decreases, the heat exchanged by the recovery unit  $P_{he}$  changes little, indicating a larger effective heat transfer. This is in agreement with Eqn (3.8). For varying plate distance  $D$ , it can be seen in Table 3.2 that the maximum performance of the system is realised at a distance of 1 cm. The existence of an optimum is in agreement with flow phenomena discussed in Section 3.2.2. For a plate distance larger than 1.5 cm, ambient air passes over the warm plate without circulating through the system, as observed with increasing height of the system.

## 3.3.2 Second layout of the dehumidifier

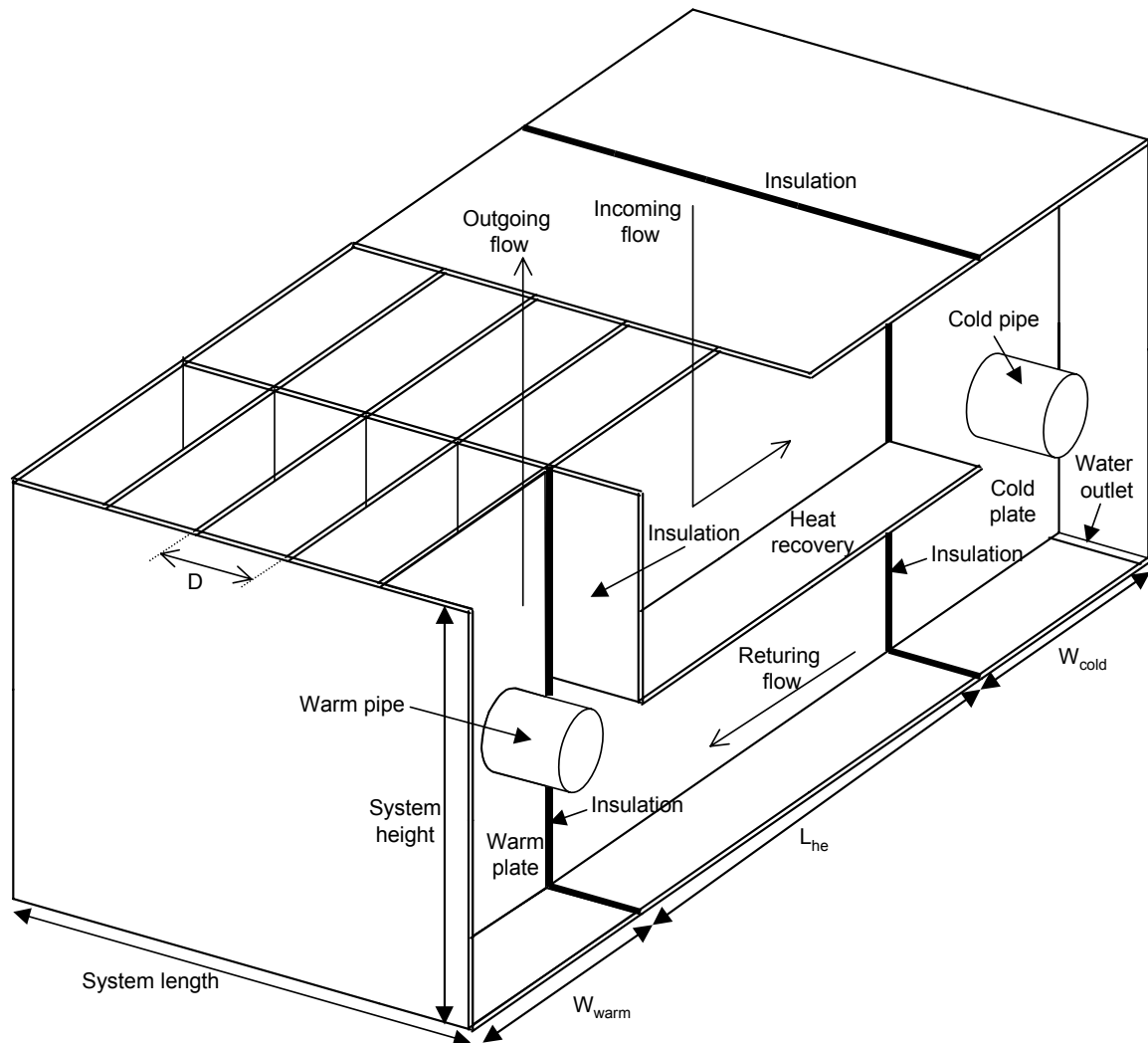


Figure 3.2 Second design of the dehumidifier;  $D$ , distance between plates;  $L_{he}$ , length of heat recovery unit;  $W_{warm}$ , width of warm section;  $W_{cold}$  width of cold section

Based on the results of the first design, a second design was made. Positioning the cold and warm plate at the same height, resulting in a horizontal heat recovery unit (Figure 3.2) can prevent a stagnant zone. CFD calculations confirmed this idea. The dimensions of the system are similar to that for the previous design. The width of the cold  $W_{cold}$  and warm  $W_{warm}$  plate is set to 5 cm. The length of the heat recovery unit  $L_{he}$  is set at 10 cm. The height of the system is 10 cm.

For this design the optimal plate distance  $D$  is 10 mm as can be concluded from Table 3.3. The balance between heat recovery and dehumidifying capacity determines the length of heat recovery unit  $L_{he}$ . For a length of 10 cm, the heat recovery unit removes

75% of the sensible heat removed at the cold plate. Besides this balance, a determination of the optimal dimensions would also include an economic analysis of the installation costs and energy savings. This is beyond the scope of this paper.

The results with the best dimensions for both the designs are summarised in Table 3.4. The second design has a higher heat transfer (>60%) than the first design because there is no stagnating cold layer present in this design.

A visualisation of the temperature profile as calculated by the CFD program is depicted in Figure 3.4.

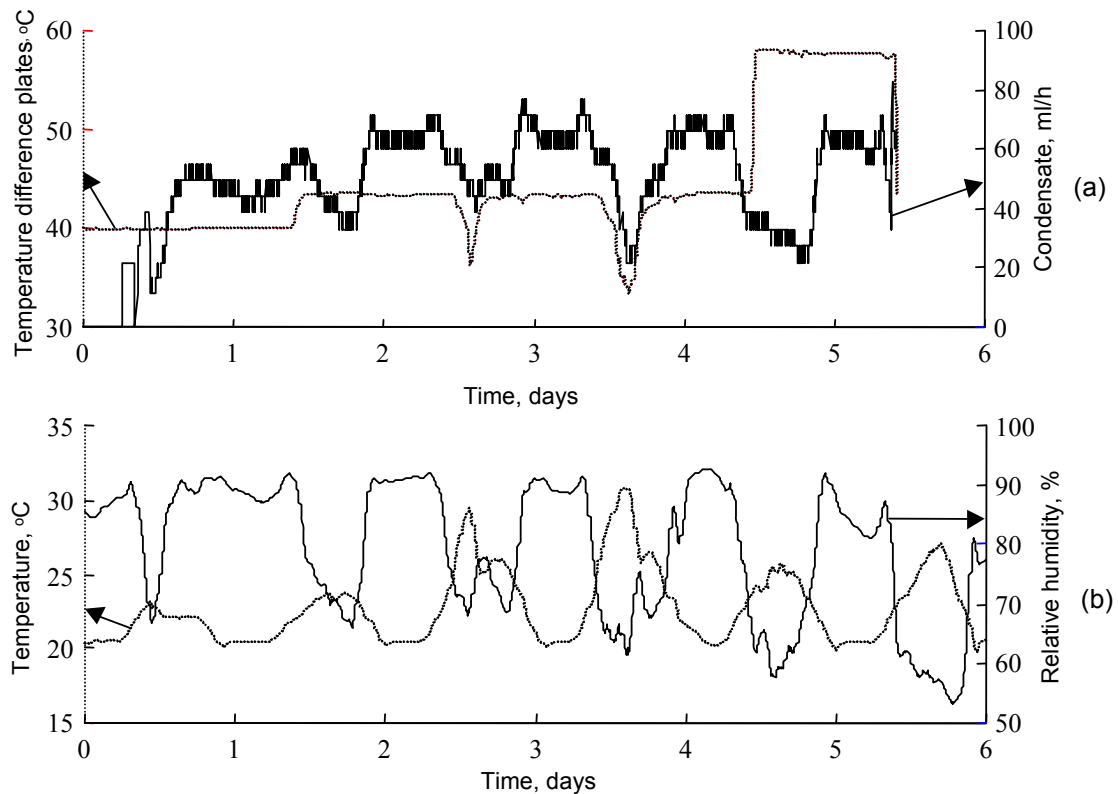


*Figure 3.3. (a) The temperature difference between the warm and cold section together with the condense removal as a function of time; and (b) the temperature and relative humidity in the greenhouse are shown as a function of time*

### **3.3.3 Condensation based on computational fluid dynamics calculations**

If the plate temperature is lower than the dew point of the passing air, condensation occurs. Based on the heat exchange calculated using CFD, the mass transfer can be determined. For simultaneous heat and mass transfer the mass transfer coefficient  $k$  in m/s is related to the heat transfer coefficient  $\alpha$  in  $\text{W m}^{-2} \text{K}^{-1}$  by:

$$k = \frac{\alpha}{(\rho C_p)_{air}} Le^{-2/3} \quad (3.10)$$

where  $C_p$  is the specific heat in J/kg K and the Lewis number  $Le$  is defined by

$$Le = \frac{\lambda_{air}}{(\rho C_p)_{air} \delta} \quad (3.11)$$

where  $\lambda$  is the thermal conductivity in  $W m^{-1} K^{-1}$  and  $\delta$  is the diffusion coefficient of water vapour in air in  $m^2 s^{-1}$ .

**Table 3.3** *Conditions for the system based on the second design (Figure 3.2) as a function of the plate distance; the warm and cold plates have dimensions of 5 by 5 by 0.1 cm, the height of the system is 15 cm and the ambient temperature  $T_g$  is 20 °C*

Plate distance, <i>mm</i>	Mass flow ( $\phi_m$ ), <i>g s<sup>-1</sup></i>	Heat cold section ( $P_{cold}$ ), <i>W</i>	Heat recovery unit ( $P_{he}$ ), <i>W</i>	Heat warm section ( $P_{warm}$ ), <i>W</i>	Temperature recovery unit ( $T_{he}$ ), °C	Temperature outgoing flow ( $T_{out}$ ), °C
7.5	2.9	22.1	19.4	108	13.2	49.6
10.0	3.6	26.4	20.5	123.8	13.4	46.7
15.0	3.8	29.2	14.0	108.8	14.4	41.0

**Table 3.4** *The conditions for design 1 (Figure 3.1) and 2 (Figure 3.2)*

Design	Mass flow ( $\phi_m$ ), <i>g s<sup>-1</sup></i>	Heat cold section ( $P_{cold}$ ), <i>W</i>	Heat recovery unit ( $P_{he}$ ), <i>W</i>	Heat warm section ( $P_{warm}$ ), <i>W</i>	Temperature recovery unit ( $T_{he}$ ), °C	Temperature outgoing flow ( $T_{out}$ ), °C
1 (Figure. 3.1)	2.3	15.6	12.2	77.5	14.3	46.7
2 (Figure 3.2)	3.6	26.4	20.5	123.8	13.4	46.7

**Table 3.5** The heat ( $P_{sens}$  and  $P_{lat}$ ) and condensate ( $\phi_{cond}$ ) removal as a function of the relative humidity (HR) of the incoming flow based on a computational fluid dynamics calculation for the second design (Figure 3.2); heat exchanged by recovery unit ( $P_{he}$ ) is 20.5 W, by cold section ( $P_{cold}$ ) is 26.5 W, the mass flux ( $\phi_m$ ) is  $3.6 \text{ g s}^{-1}$ , the cold section temperature ( $T_{cold}$ ) is  $5^\circ \text{C}$  and the ambient temperature ( $T_g$ ) is  $20^\circ \text{C}$

Relative humidity (HR), %	Sensible heat ( $P_{sens}$ ), W	Latent heat ( $P_{lat}$ ), W	$P_{lat}/P_{sens}$	Dehumidification per hour ( $\phi_{cond}$ ), ml/h	Temperature recovery unit ( $T_{he}$ ), $^\circ \text{C}$
10	46.8	0	0	0	13.4
75	46.1	43.9	0.95	64	14.5
80	45.7	50.1	1.09	73	15.1
85	45.4	56.3	1.24	82	15.6
90	45.0	62.5	1.39	91	16.1
95	44.6	68.7	1.54	100	16.7
100	44.2	74.9	1.69	109	17.2



The heat transfer per meter length of the apparatus  $\alpha A^*$  is defined by the heat removal  $P_{removed}$  per metre length divided by the temperature difference between the incoming air and the plate temperature ( $T_{incoming} - T_{plate}$ ):

$$\alpha A^* = \frac{P_{removed}}{T_{incoming} - T_{plate}} \quad (3.12)$$

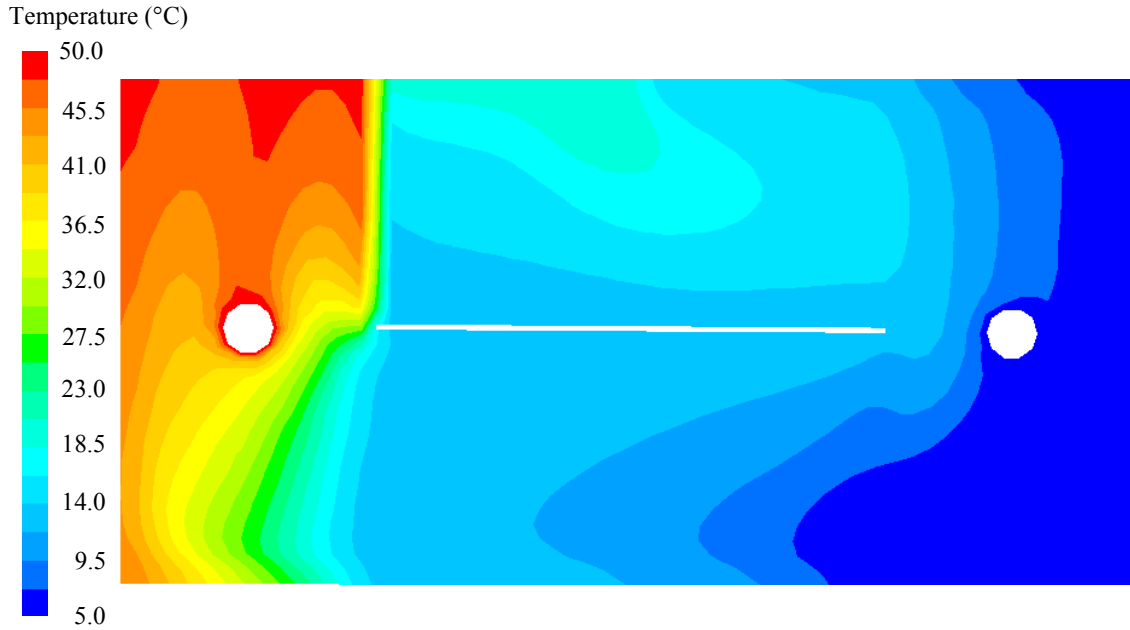


*Figure 3.4 The temperature profile in the system (Figure 3.2) resulting from a computational fluid dynamics calculation*

The temperatures and the heat transfer at the heat recovery unit and the cold plate are determined from the CFD calculations. The temperature of the heat recovery unit changes because latent and sensible heat is transferred on one side of the heat recovery unit while only sensible heat is transferred on the other side. The energy balance for the heat recovery unit is to be solved: (sensible heat + latent heat)<sub>incoming</sub>=(sensible heat)<sub>counter flow</sub>. The latent heat transfer is calculated by

$$P_{lat} = L_v k A^* \rho_{air} (c_{incoming} - c_{plate}) \quad (3.13)$$

where  $c_{incoming}$  and  $c_{plate}$  are the vapour concentrations in  $\text{kg kg}^{-1}$  for the incoming air and at the plate, respectively.

In Table 3.5, the sensible and latent heat removal, the division between the latent and sensible heat removal, the dehumidification and the temperature of the heat recovery unit for ambient air with different a relative humidity are listed. For a relative humidity of 10% no condensation occurs. For air with a higher relative humidity the latent part of total heat removal is about half at 75%RH to almost two-third at 100%RH.

The effect of decreasing buoyancy due to decreasing sensible heat transfer is not taken into account for these calculations because they are small ( $< 4\%$ ).

### 3.3.4 Experiment using a prototype



*Figure 3.5 Photograph of the prototype on a greenhouse floor.*

A one metre long prototype of the dehumidifier based on the second design with optimal dimensions is built (Figure 3.5). Water with fixed temperatures is pumped through the warm and cold section of the prototype. The amount of condensate dripping out is measured as a function of time with a tip bucket rain meter giving an impulse every 10.98 ml. Temperature and relative humidity are monitored every minute during the experiment by a dry and wet bulb thermometer positioned between the full grown cucumber crop at a height of 3 m.

In Figure 3.3 results are depicted for a 5.5 days long period. The top figure (a) shows the temperature differences between the cold and the warm section and the amount of condensate removed in ml/h. The bottom figure (b) shows the temperature and relative humidity. On the first one and half day (0-1.5), the cold and warm water temperatures were set at 9.8°C and 50°C respectively. During the second period (1.5-4.5), the cold water temperature is lowered to 6.4°C. For the third period (4.5-5.5), the warm

temperature is raised to 64°C. For high humidity (around 90%) periods the amount of condensate collected is approximately 50 ml/h in the first period, and 65 ml/h during the other two periods. The average humidity in the greenhouse for the third period is low at night time compared to the other periods, explaining the same level of condensate removal as in the second period where the warm plate temperature is lower. At 2.6 and 3.7 days, a dip in the temperature difference between the cold and warm section occurs caused by a lack of cooling capacity during high greenhouse temperatures.

### **3.3.5 Comparison between experiments and calculations**

The experimental results can be compared to calculations according to Section 3.3.3. For the first period (conditions:  $H_R=90\%$ ;  $T_g=20.5^\circ\text{C}$ ;  $T_{\text{cold}}=9.8^\circ\text{C}$ ;  $T_{\text{warm}}=50^\circ\text{C}$ ), the calculations resulted in a condensate removal of 62 ml/h. This can be compared to the experimental result of 50 ml/h. For the second period, a condensate removal of 85 ml/h was calculated. Also the third period resulted in a condensate removal of about 85 ml/h at a value for  $H_R$  of 85%. These results can be compared to the experimental figure of 65 ml/h. The calculated mass flow through the system and thus the heat transfer is slightly higher than the experimental figures but within the expected accuracy. In the prototype, roughness and water droplets decrease heat and mass transfer which is not incorporated in CFD. However, this will not affect the design process while it will be the same for all discussed designs.

## **3.4 Conclusions**

A concept for a new dehumidifier has been developed based on physical laws. Using computational fluid dynamics (CFD), the design could be analysed and improved. The layout was improved changing various dimensions. As there is no condensation included in the CFD calculations, a model has been created calculating the heat transfer including condensation based on the CFD results. A prototype was built based on the improved design. This one metre long prototype removed 50 ml/h and 65 ml/h for a cold plate temperature of 5.5°C and a hot plate temperature of 50 and 65°C, respectively, under greenhouse conditions. The calculations gave a 25 to 30% higher condensate removal as the experiments.

These preliminary results can be used to estimate the energy efficiency of the system for a whole year when operated by a heat pump. First predictions show that 4 to 7% energy can be saved in a conventional single glass greenhouse. For modern well-insulated greenhouses these savings are expected to be much higher while it prevents ventilation to dehumidify the air. In such greenhouses active dehumidification will be a must. The implementation of the dehumidifier in the climate control system is subject to further research including aspects such as climate distribution.

**Acknowledgements**

This research was financed by the E.E.T. (Ecology, Economy and Technology) research programme funded by the Dutch Ministries of EZ (Economic Affairs), of OCW (Education) and of VROM (Environmental Affairs).

---

# 4

## Determination of greenhouse-specific aspects of ventilation using three-dimensional computational fluid dynamics

---

This chapter was published before as:  
J.B. Campen and G.P.A. Bot (2003). Determination of greenhouse-specific aspects of ventilation using three-dimensional computational fluid dynamics. *Biosystems Engineering* 84(1) pp 69-77  
Doi:10.1016/S1537-5110(02)00221-0

### Abstract

The ventilation of a Spanish ‘parral’ greenhouse was studied using three-dimensional computational fluid dynamics (CFD). The calculations were verified by experimental results from tracer gas measurements. Two types of roof openings have been considered; the rollup window configuration and the flap window configuration.

The calculations resembled experimental data within 15%. Wind speed correlated linearly with ventilation rate for both configurations without the buoyancy effect. This is in agreement with basic theory on ventilation. CFD calculations indicated that ventilation rate for both configurations is largely dependent on wind direction, which was also seen with the experimental data. Ventilation rate varied for the flap window configuration from 0.8 to almost 4 renewals per hour per  $\text{m s}^{-1}$  wind speed.

### Notation

$A_o$	total area of all ventilation openings without windows, $\text{m}^2$
$C_p$	specific heat, $\text{J kg}^{-1} \text{K}^{-1}$
$f_\beta$	factor containing all effects related to the opening angle of the window
$H$	Heat flow, W
$K_o$	hydraulic resistance coefficient
$K_w$	proportionality factor
$P, \Delta P$	Pressure and pressure difference, Pa
Re	Reynolds number
$S, S_\phi$	source term
$T$	temperature, K
$u_l$	local wind speed, $\text{m s}^{-1}$
$u_o$	resulting fluid velocity, $\text{m s}^{-1}$
$u_r$	wind speed at reference height, $\text{m s}^{-1}$
$V$	volume, $\text{m}^3$
$R_V$	ventilation rate, renewals per hour
$v$	velocity, $\text{m s}^{-1}$
$Y$	inertial factor
$\phi_V$	ventilation flux, $\text{m}^3 \text{s}^{-1}$
$\alpha$	permeability, $\text{m}^2$
$\mu$	dynamic viscosity, Pa s
$\phi$	concentration of transported quantity

$\rho$	density, kg m <sup>-3</sup>
$\Gamma_{\phi}$	diffusion coefficient, m <sup>2</sup> s <sup>-1</sup>

#### **4.1 Introduction**

Ventilation is essential for a good climate in a greenhouse and great effort has been made for the determination of ventilation as a function of relevant parameters. A generally applicable greenhouse ventilation model has yet to be found (Bailey, 1999) because ventilation experiments are cumbersome and are complicated by variable environmental factors. Wind direction and speed, solar radiation, outside temperature, *etc.*, vary during the measurement period. This source of inaccuracy causes uncertainty in the derived ventilation models. In addition, ventilation models contain greenhouse specific parameters that cannot be generalised up till now. It is known that greenhouse location and greenhouse size greatly affect ventilation (De Jong, 1990). Moreover there is no standard procedure for the measurement of reference outdoor conditions. This means that ventilation models have to be parameterised for each particular greenhouse. This can be done by proper experiments, a time consuming and expensive operation. If the flow phenomena linked to ventilation can be modelled efficiently for a specific greenhouse and its neighbourhood, then the greenhouse specific ventilation aspects can be easily determined.

Computational fluid dynamics (CFD) calculations open the possibility to do so. Boundary conditions are easily set for calculations. For this reason several studies using CFD have been published. Mistriotis *et al.* (1997a; 1997b) studied Mediterranean-type greenhouses using CFD in a two-dimensional grid and concluded that CFD is a powerful tool for developing improved greenhouse designs for efficient ventilation. Kacira *et al.* (1997; 1998) also evaluated the ventilation of a multi-span, saw tooth greenhouse for various conditions. Boulard *et al.* (1997) measured the ventilation of a twin-span greenhouse experimentally in three dimensions. Experimental results and computational fluid dynamics calculations were in very good agreement. Later, Boulard *et al.* (1999) performed experiments on the airflow and temperature patterns induced by buoyancy forces through roof openings. The natural convection flow simulated by CFD was also in good agreement with the experiments, though no quantification was given. Boulard's calculations were performed with a two-dimensional grid while the effects of plants were not taken into account. Lee and Short (2000) were the first to study the effects of crop on the flow determining the pressure drops and inertial loss factors according to a procedure in the Fluent Manual (Fluent, 1998), they developed a CFD model to determine the relationship between air velocity and pressure drop. Unfortunately they did not report the parameters resulting from their study.



Most published CFD calculations were based on two-dimensional models, thus ignoring the three-dimensional characteristics of flow and temperature distribution in the greenhouse. In particular ventilation resulting from wind has a three-dimensional character. Baptista *et al.* (1999) detected some influence of wind direction on ventilation but no conclusions were drawn due to insufficient data. De Jong (1990) discriminated wind direction for a Venlo-type greenhouse in leeward and windward windows only. He stated this rough discrimination was sufficient for small openings.

The purpose of this work was to: (1) use three-dimensional computational fluid dynamics calculations and experimental results to verify if three-dimensional (3-D) CFD can be used to determine greenhouse-dependent ventilation characteristics; and (2) determine the influence of wind direction and geometry of openings on ventilation rate.

## 4.2 Theoretical considerations

### 4.2.1 Theory on ventilation

The theory concerning ventilation as airflow generated through openings can be used to account for greenhouse specific effects in ventilation models (Bot, 1983). One major aspect in this theory is the driving force for ventilation as a function of relevant factors. The other major aspect is describing the relationship between this generated pressure difference and ventilation flux. From an engineering point of view, there is a need to simply quantify ventilation of a greenhouse system from measurable factors.

#### 4.2.1.1 Driving forces for ventilation

The pressure difference over the opening can be due to the wind field outside the greenhouse and due to the temperature difference over the opening. The temperature effect is also called the buoyancy effect. The buoyancy effect contributes only at low wind speeds of about  $2 \text{ m s}^{-1}$  while, at higher wind speeds the wind effect dominates (Bot, 1983). This paper will be focussed on wind-driven ventilation.

The pressure difference due to the wind effect depends on the kinetic energy of the local wind speed  $u_l$  near the opening based on the Bernoulli principle. However, this local wind speed can be different for various openings and it is difficult to measure. Therefore, the effective pressure difference  $\Delta P$  in Pa over all greenhouse openings relates to the kinetic energy per unit volume of the wind at reference height, according to:

$$\Delta P = K_w \frac{1}{2} \rho u_r^2 \quad (4.1)$$

where:  $\rho$  is the density of air in  $\text{kg m}^{-3}$ ;  $K_w$  is a proportionality factor; and  $u_r$  is the wind speed at reference height in  $\text{m s}^{-1}$ . The proportionality factor  $K_w$  is dependent on all



factors affecting the relationship between wind speed at reference height  $u_r$  and effective pressure difference  $\Delta P$  over all greenhouse openings. Therefore this factor is not generally valid for all greenhouses but is affected by location (obstacles, neighbouring buildings or greenhouses, *etc.*) and greenhouse size and geometry. It is not yet possible to quantify these dependencies.

#### *4.2.1.2 Hydraulic characteristics of the openings*

In fluid flow it is common practice to relate a pressure difference  $\Delta P$  over an opening to the resulting fluid velocity  $u_o$  in  $\text{m s}^{-1}$  according to:

$$\Delta P = K_o \frac{1}{2} \rho u_o^2 \quad (4.2)$$

where, the proportionality factor  $K_o$  is the hydraulic resistance coefficient of the opening. In general, such a coefficient is dependent on the Reynolds number  $Re$ , characterising the flow type. If inertia effects dominate over viscous effects at higher  $Re$  values, this factor can be expected to be independent of the value for  $Re$ . However, it will be dependent on the geometry of the opening. This dependency can be easily found from laboratory flow experiments.

#### *4.2.1.3 Resulting ventilation*

The airflow through the opening is the result of the generated pressure difference by the wind so Eqns (4.1) and (4.2) can be combined resulting in:

$$u_o = (K_w / K_o)^{1/2} u_r \quad (4.3)$$

The ventilation flux  $\phi_V$  in  $\text{m}^3 \text{s}^{-1}$  can be found from the average air velocity in the opening, considering that half of the ventilation opening is used for the inflow and the other half for the outflow:

$$\phi_V = 0.5 A_o (K_w / f_\beta K_o)^{1/2} u_r \quad (4.4)$$

In this relation,  $A_o$  is the total area of all ventilation openings without windows in  $\text{m}^2$ . The factor  $f_\beta$  contains all effects related to the opening angle of the window, which is on the available exchange area and the hydraulic resistance of the opening (Bot, 1983).

The result is that ventilation flux for the whole greenhouse is linearly proportional to wind speed at reference height and the area of ventilation openings. This correlation has been confirmed through many experiments for various greenhouses. However, in the combined proportionality factor  $(K_w / f_\beta K_o)^{1/2}$  the factor  $K_w$ , representing the translation between the wind speed at reference height and the effective pressure difference over all openings of the greenhouse, is dependent on the specific greenhouse at its location. The problem is that this factor cannot be generalised. This means that for each greenhouse factor  $K_w$  has to be calibrated. This is a relatively simple tuning of the ventilation equation and can be achieved by some ventilation measurements. Another possibility

nowadays under investigation is modelling the flow phenomena in and around a particular greenhouse including the geometry, surrounding obstacles and other relevant characteristics of the surroundings using CFD.

#### 4.2.2 Theory on computational fluid dynamics

Computational fluid dynamics (CFD) becomes a widely used tool to determine flow field and temperature distributions in and around geometries. As computers get faster and cheaper and the CFD software becomes user-friendlier, more comprehensive cases can be studied using this technique. A general description of CFD is given by Mistriotis *et al.* (1997b). In a CFD program, a system is modelled by discretising space and time (finite volume method) and by solving the conservation equations for the discretised parts for the relevant quantities considered. The general conservation equation reads (Versteeg *et al.*, 1995):

$$\frac{\partial \rho \varphi}{\partial t} + \text{div}(\rho \varphi \vec{v}) = \text{div}(\Gamma_{\varphi} \text{grad} \varphi) + S_{\varphi} \quad (4.5)$$

where  $\rho$  is the density of the fluid in  $\text{kg m}^{-3}$ ;  $\vec{v}$  is the velocity vector in  $\text{m s}^{-1}$ ,  $\Gamma_{\varphi}$  is the diffusion coefficient in  $\text{m}^2 \text{s}^{-1}$  and  $S_{\varphi}$  is the source term. The symbol  $\varphi$  represents the concentration of the quantity considered. Separate models describing the fluctuating part of the flow account for turbulence.

#### 4.3 Experiments

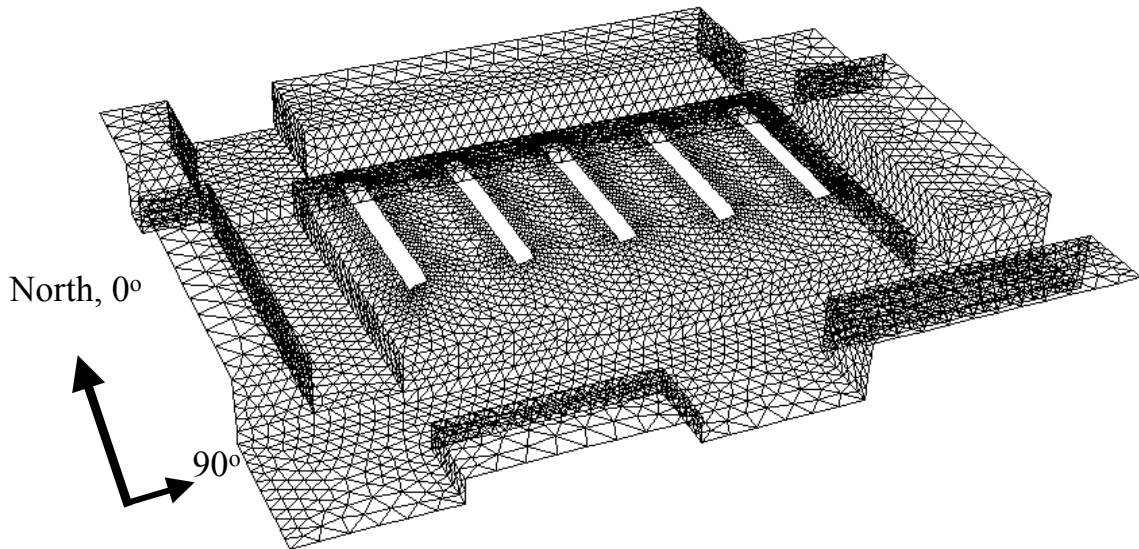


Figure 4.1 The grid on the walls of the test greenhouse with rollup windows including the surroundings

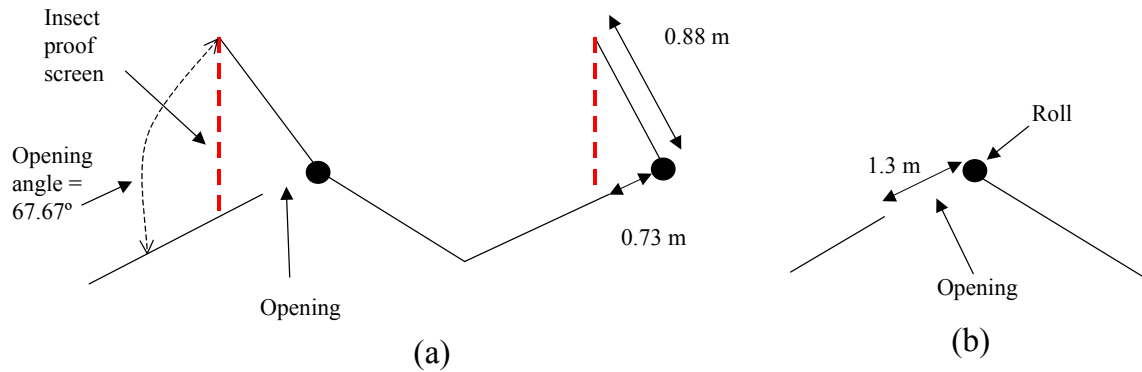


Figure 4.2 Dimensions of the flap window(a) and the rollup windows (b)

#### 4.3.1 Measurements of the natural ventilation of "parral" greenhouses

The verification of the CFD calculations was based on experiments done in an experimental greenhouse at the Experimental Station ‘Las Palmerillas of Cajamar’ at Almería, Spain (Perez Parra *et al.*, 2004). The grid on the walls of this greenhouse and part of its surroundings as used in the CFD model, is given in Figure 4.1. The ventilation rates were determined using the tracer gas method. The five span greenhouse covered with polyethylene film was 38 m long, 23.2 m wide and 4.4 m high with the gutter at 3.6 m. Two types of top ventilation were studied, one with flap windows and the other with rollup windows in the same greenhouse. The flap length was 10.16 m and the width 0.88 m. Ventilation openings were 8.36 m long, and 0.73 m wide. Rollup windows were 14.2 m long and 1.3 m wide. Details of both window types are depicted in Figure 4.2. In both cases there were five windows on the roof. The experimental greenhouse was surrounded by other greenhouses. As the greenhouses were located on a slope, the horizontal ground level of the experimental greenhouse was elevated 1.15 m above the greenhouses to the south. To the north the ground elevation was 1 m. The greenhouses to the east and west were built on the same height. These details were considered in the CFD model. No crop was grown in the greenhouse during the experiments.

The experiments were conducted by closing the windows and filling the greenhouse with tracer gas in period from February till March. The windows were opened and the decay of the tracer gas concentration was measured. As the measurements were done during daytime, buoyancy effects on the ventilation have to be considered especially for low wind speeds. The decay of tracer gas was determined starting at a concentration (60 ppm -15 ppm) less than the initial concentration (100 ppm) thus minimising the additional buoyancy effect caused by the increased air temperature due to the filling of the greenhouse with closed vents. During part of the measurements for the flap window configuration, a 34% porosity anti-insect screen was mounted in the window. This

screen introduced a flow resistance for the passing airflow. In the flap window configuration the screen was mounted along the edges of the windows (Figure 4.2). The screen was hanging vertically on the opening when the flap was fully open. The specifications of the insect screen Econet FL (Miguel, 1998) measured were; porosity of  $0.34 \pm 0.03 \text{ m}^2 \text{ m}^{-2}$ , permeability  $\alpha$  of  $6.51 \times 10^{-9} \text{ m}^2$ ; inertial factor  $Y$  of 0.457 and thickness of 0.25 mm.

The wind speed and direction are measured at 10 m above ground level of the experimental greenhouse.

### 4.3.2 The CFD model

A CFD model of the experimental greenhouse was constructed by means of the commercially available CFD-program Fluent v.5.2 (Fluent, 1998). In all directions, 10 m of the surroundings of the greenhouse was included in the model. The model was 15 m high. Considering more of the surroundings in the model did not alter the solution by more than 2%. The top plane of the model was modelled as a frictionless wall. The geometry of the surrounding greenhouses was simplified to a cubical shape.

The ventilation rate  $R_V$  in renewals per hour was calculated by a thermal model, only considering heat exchange by ventilation:

$$R_V = \frac{H_{input}}{(\bar{T}_{greenhouse} - T_{outside}) C_{p,air} \rho_{air} V_{greenhouse}} \frac{3600}{V_{greenhouse}} \quad (4.6)$$

where  $H_{input}$  is the heat released in the greenhouse in W;  $\bar{T}_{greenhouse}$  is the average temperature of the greenhouse air in °C;  $T_{outside}$  is the outside temperature in °C;  $C_{p,air}$  is the specific heat of air in  $\text{J kg}^{-1} \text{K}^{-1}$ ;  $\rho_{air}$  is the density of air in  $\text{kg m}^{-3}$ ; and  $V_{greenhouse}$  is the volume of the greenhouse in  $\text{m}^3$ . Since only ventilation heat exchange is assumed, the walls of the greenhouse are set as perfect insulators and radiative heat transfer is also not included. If only ventilation due to the wind is studied, the gravity is considered zero. The heat input  $H_{input}$  for this situation can be set to any value not influencing the ventilation rate, in this case  $100 \text{ W m}^{-3}$ . If the buoyancy effect is included the heat input was set to a value equal to the heat supplied by solar radiation and gravity is reset. The air was considered as an ideal gas.

The screen was implemented as a porous jump in the CFD model. An additional source term was added to the standard fluid flow equations. The source term was composed of two parts, a viscous loss term (Darcy) and an inertial loss term (Miguel, 1998):

$$S = \frac{\mu}{\alpha} \vec{v} + \rho \left( \frac{Y}{\alpha^{1/2}} \right) |\vec{v}| \vec{v} \quad (4.7)$$

where  $\mu$  is the dynamic viscosity in Pa s;  $\alpha$  is the permeability in  $\text{m}^2$ ; and  $Y$  is the inertial resistance factor.

The turbulence model used for all calculations is the k- $\epsilon$  model developed by Launder and Spalding (1974). Crop is not considered in the model since no crop was grown during the experiments.

## 4.4 Results

### 4.4.1 Flap windows

Table 4.1 The ventilation rate for the model with flap windows with the same boundary conditions for different number of grid cells

Number of cells	Ventilation rate $R_V, h^{-1}$
119442	17.9
129420	21.4
173305	21.7

The experimental results with the flap window geometry without insect proof screen were first investigated using CFD. Two situations are discriminated; windows windward (wind coming from the west) and windows leeward (wind coming from the east). For wind coming directly from the West at a speed of  $6 \text{ m s}^{-1}$  several grids made for the model were compared. The results are listed in Table 4.1. There was a substantial increase in calculated ventilation rate between the first and second grid indicating grid dependency. The relatively small ventilation rate increase between the second and third grid indicates that the grid dependency on the solution has become minimal. A grid with 129420 cells was used because it consumes the least computational time with a reasonable accuracy.

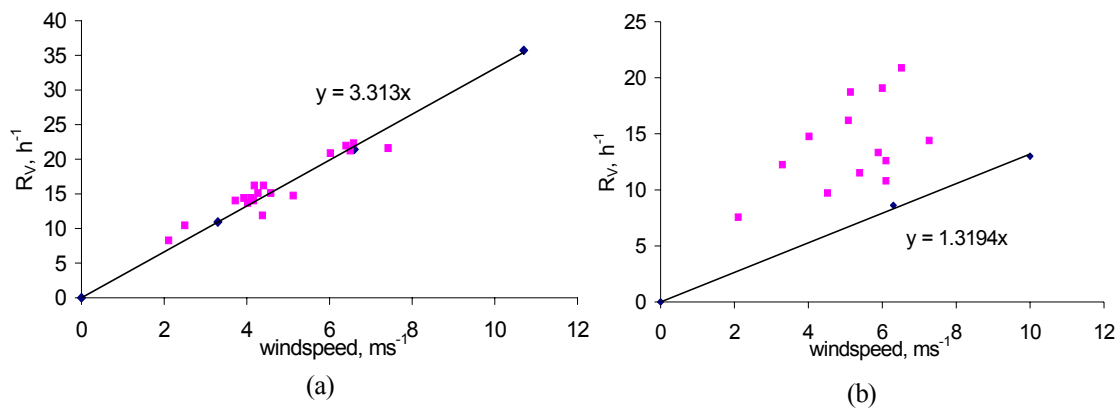


Figure 4.3 The ventilation rate as a function of the wind speed for windward (a) and leeward (b) flap windows;  $\blacklozenge$ , CFD calculations;  $\blacksquare$ , experimental data

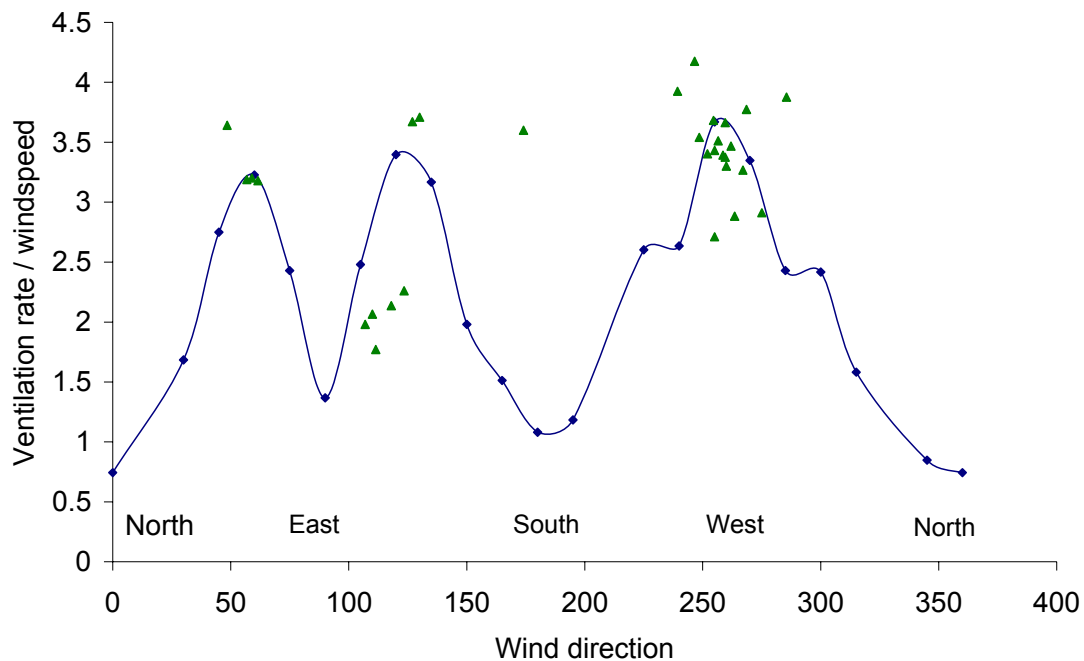


Figure 4.4 Ventilation rate divided by wind speed as a function of wind direction for the flap window configuration; ▲, experimental data; ◆, CFD calculations

The results for the windward (a) and leeward (b) situation are depicted in Figure 4.3. Based on CFD calculations ventilation rate correlated linearly with wind speed since buoyancy effects were not included in these calculations. The combined proportionality factor  $(K_w/f_\beta K_o)^{1/2}$  from Eqn (4.4) is 0.22 and 0.08 for the windward and leeward case respectively.

Wind direction was varied with intervals of  $15^\circ$  all around the greenhouse at the same wind speed to determine the influence of wind direction. The ventilation rate divided by wind speed as a function of the wind direction according to CFD calculations together with the experimental results is given in Figure 4.4.

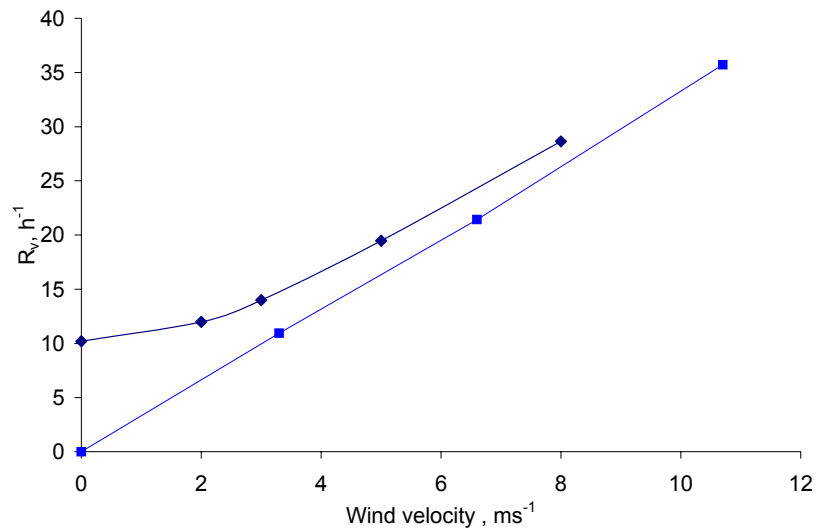


Figure 4.5 The ventilation rate for the windward flap window as a function of wind speed without buoyancy ■ and with 400  $\text{W m}^{-2}$  heat input ◆, both calculated by CFD

The effect of buoyancy was not taken into account for the discussed CFD calculations. The experiments were performed during daytime, hence buoyancy is caused by solar radiation. The effect of buoyancy on the ventilation as a function of the wind speed was determined by imposing 400  $\text{W m}^{-2}$  on the ground, corresponding to 50% of the solar radiation of 800  $\text{W m}^{-2}$  being transferred into sensible heat. The CFD calculations for the windward case with and without solar heat input are depicted in Figure 4.5.

The experimental data on ventilation with insect proof screen attached to the flap windows, showed a reduction of 20% in ventilation. CFD calculations showed a reduction of 30%.

### 4.4.2 Rollup windows

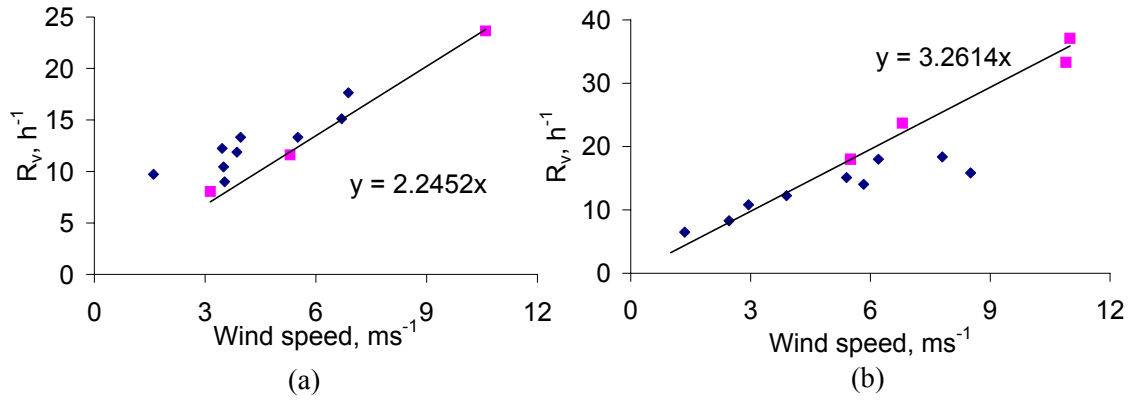


Figure 4.6 The ventilation rate as a function of the wind speed for windward (a) and leeward (b) rollup windows;  $\blacksquare$ , CFD calculations;  $\blacklozenge$ , experimental data

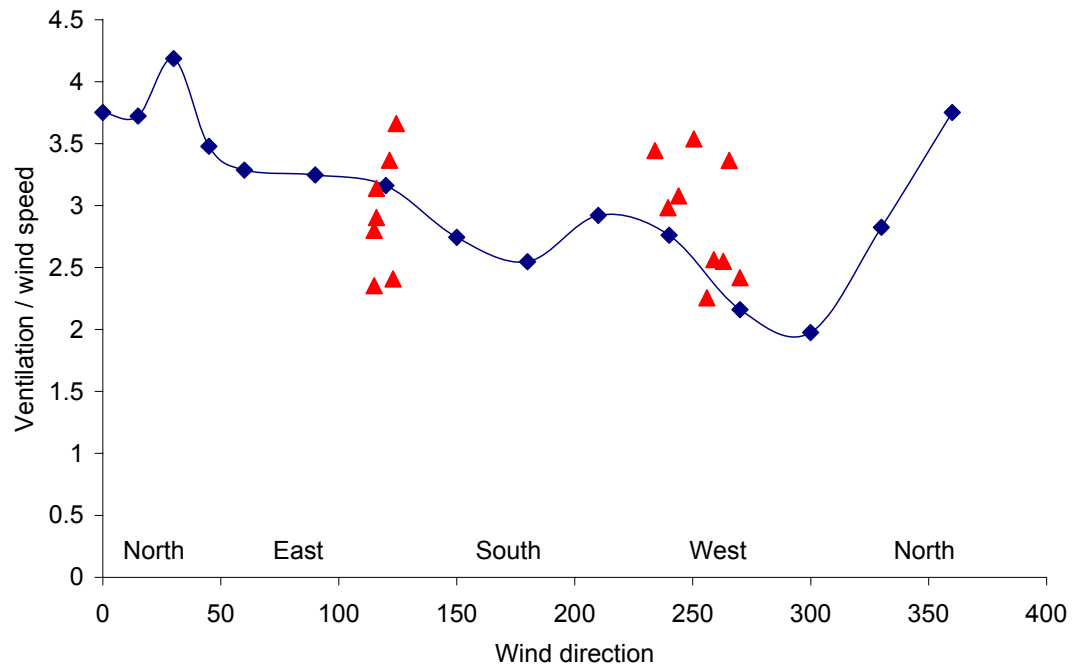


Figure 4.7 Ventilation rate divided by wind speed as a function of wind direction for rollup windows;  $\blacktriangle$ , experimental data;  $\blacklozenge$ , CFD calculations

The optimal grid for this configuration consisted of 111185 cells. The ventilation rate as a function of the wind speed for the rollup window configuration is displayed in Figure 4.6. Based on CFD calculations ventilation rate correlated linearly to the wind speed for this configuration as well. The combined proportionality factor  $(K_w/f_\beta K_o)^{1/2}$  in Eqn (4.4)



is 0.05 and 0.07 for the windward and leeward case respectively. The relationship between wind direction and ventilation rate was also calculated (Figure 4.7).

#### **4.5 Discussion**

The linear relationship between wind speed and ventilation rate for both configurations is in agreement with Eqn (4.4) when buoyancy is not included in the model. For the windward case of the flap windows, the similarities between the experimental and the calculated values are within 15% for a wind speed below  $6 \text{ m s}^{-1}$  (Figure 4.3a). The slightly higher ventilation for the experimental data can be explained by the fact that the buoyancy effect is not included in the CFD calculations. At higher wind speeds, the experimental data shows less ventilation than the calculations with the CFD model. There is reason to doubt the measurement values at high wind speeds since the ventilation rate is high causing the measurements of the decay rate of the tracer gas to become less accurate. There is no evidence that at higher wind speed ventilation is no longer linear. The combined proportionality factor for the windward flap window is in agreement with the results by Papadakis *et al.* (1996), their factor was 0.246 for vertical windows with wind direction parallel to the gutter and ventilators. For the leeward wind the combined proportionality factor is similar to the value 0.09 for a ‘quasi infinite greenhouse’ found by De Jong (1990).

For the leeward case (Figure 4.3b) the similarities between calculated and experimental values seem to be low. The effect of wind direction can explain the above discrepancy. During the experiments with leeward wind, the direction of the wind was not exactly eastward having an offset of around  $25^\circ$  to the south. As shown in Figure 4.4 this offset caused a large increase in ventilation explaining the poor resemblance between experimental measurements and calculations (Figure 4.3b). At eastward wind ( $90^\circ$ ), ventilation rate is at a local minimum, but with wind direction from north or south, ventilation almost doubles. Windward ventilation reaches maximum at  $270^\circ$ . The perpendicular flow from the north and south differed due to the height differences from the ground level in this direction and due to the non-symmetrical surrounding greenhouses. Ventilation rate was five times higher when wind direction was westward ( $255^\circ$ ) compared to northward ( $0^\circ$ ). For the rollup window configuration similar conclusions can be drawn. During the experiments for the windward situation (Figure 4.6a), experimental ventilation rate was 7 to 60% higher than the calculated one. For the windows leeward case (Figure 4.6b), the differences were not so pronounced (around 20%). This discrepancy between the experimental and the calculated results for this configuration is also due to the wind direction (Figure 4.7). During the windward experiments, the wind had an offset of around  $30^\circ$  to the south explaining the higher

ventilation rate shown in Figure 4.6a. The calculated ventilation rate was 40% larger for the leeward wind than for the windward wind.

The ventilation rate for the rollup windows configuration (Figure 4.7) was not symmetrical around  $90^\circ$  and  $270^\circ$  indicating some influence of the surrounding buildings and the elevation to the north and south. There was a local maximum in ventilation rate at this wind direction due to the fact that interception of wind flow was maximal. Ventilation averaged over wind direction was higher for the roll up configuration is due to the fact that the opening surface area of this configuration was three times larger than the flap configuration.

Ventilation rate with buoyancy as shown in Figure 4.5 is increased by 80% due to buoyancy for a wind speed of  $2 \text{ m s}^{-1}$ . This is in agreement with De Jong (De Jong, 1990) who concluded that the ventilation is dominated by wind effect for wind speeds above  $1.5 \text{ m s}^{-1}$ .

The further decrease of ventilation rate due to the insect screen can be explained by the fact that the screen was not precisely vertical during the experiment. It was observed that the wind caused the screen to curve thereby increasing the surface area, which decreases flow resistance.

## 4.6 Conclusions

A three-dimensional computational fluid dynamics (CFD) model was able to determine the greenhouse specific ventilation characteristics. The linear relationship between ventilation rate and wind speed for a distinct wind direction as known from experimental data for various greenhouses and theory was reproduced. The dependency of the slope of this relationship could be calculated in relation to wind direction, greenhouse geometry, and greenhouse surroundings. CFD calculations showed that variations in wind direction of only  $10^\circ$  can increase the ventilation up to 50% in some cases. In order to compare experimental results with CFD calculations, wind direction has to be monitored.

The geometry of the windows largely influenced ventilation rate. Averaged over wind direction the rollup window configuration has higher ventilation rates, due to the larger ventilation openings in the cover.

It is clear from this study that three-dimensional calculations are preferable over the two-dimensional calculations since for the computational assessment of ventilation rate, wind direction plays an important role in ventilation.

## Acknowledgements

This research was financed by the Ecology, Economy and Technology (E.E.T.) research programme funded by the Dutch Ministries of EZ (Economic Affairs), OCW

(Education), VROM (Environmental Affairs), and by the Energy Research Program (ministry of agriculture).



---

# 5

## Dehumidification of Greenhouses at Northern Latitudes

---

This chapter was published before as:  
J.B. Campen G.P.A. Bot and H.F. de Zwart (2003).  
Dehumidification of Greenhouses at Northern Latitudes.  
Biosystems Engineering 86(4) pp 487-493  
doi:10.1016/j.biosystemseng.2003.08.008

## Abstract

Three dehumidifying methods, being condensation on a cold surface, forced ventilation using a heat exchanger, and an absorbing hygroscopic dehumidifier, were compared with ventilation as the conventional way to dehumidify a greenhouse. The calculations were performed using a dynamic physical simulation model with a single- and a double-layer greenhouse under Dutch weather conditions. The comparison was made based on the energy consumption and the costs. The methods with a cold surface or an absorbing hygroscopic material are less attractive than the conventional method, mainly because of the high investment costs. Dehumidification by forced ventilation with a heat exchanger can be competitive. The success of this system depends on the efficiency of the system in terms of energy consumption and the effectiveness of the heat exchanger.

## 5.1 Introduction

Humidity is one of the key factors in greenhouse climate. It usually tends to be high due to crop transpiration. The transpiration of the crop depends on solar radiation, CO<sub>2</sub> concentration, temperature of the greenhouse air and relative humidity in the greenhouse

(Stanghellini, 1987). Crops exposed to high humidity levels have a higher risk of developing fungal diseases and physiological disorders (Hand, 1988; Bakker, 1991; Bakker *et al.*, 1995). In conventional greenhouses with a single layer cover, humidity level is limited by condensation on the relatively cold cover and by ventilation through air leaks. Moreover, ventilators can be opened for water vapour removal.

New greenhouses tend to be better insulated, reducing the total energy use (Sonneveld, 1999). However, condensation on the cover is lower for these greenhouses so additional dehumidification becomes more important. With the conventional method of dehumidification by ventilation the benefits of the better insulation are reduced. For this reason, various alternative dehumidifying systems have been tested. (Seginer *et al.*, 1989) modelled the vapour balance of a single- and double-layer greenhouse and concluded that dehumidifiers such as hygroscopic absorption have an advantage in mild weather conditions, in well-insulated greenhouses. (Jolliet, 1994) concluded from a model that dehumidification could be cost effective for double-glazing.

The present paper compares the available methods for dehumidification. A dynamic simulation model with the input of Dutch climatic conditions performs this comparison. The dehumidifying methods discussed in this paper are: (1) natural ventilation as the reference method; (2) condensation on a cold surface; (3) forced ventilation using a heat exchanger; and (4) absorption by a hygroscopic material. The relevant criteria used to compare these different methods are energy consumption and cost.

## 5.2 Dehumidifying methods

Numerous studies have been done on the dehumidifying methods discussed in this section. The practical implementation was usually limited due to the energy consumption resulting from forced air circulation, large humidity gradients in the greenhouse, lack of capacity, high air velocities in the greenhouse, and large size of the installation causing high light interception. New concepts were developed to solve part of these problems as discussed in chapter two and three.

### 5.2.1 Dehumidification by natural ventilation

By opening the windows, moist greenhouse air is replaced by relatively dry outside air. This is common practice to dehumidify a greenhouse. This method does not consume any energy when excess heat is available in the greenhouse and ventilation is needed to reduce the greenhouse temperature. Though, when the need for ventilation to reduce the temperature is less than the ventilation needed to remove moisture from the air, dehumidification consumes energy. The warm greenhouse air is replaced by cold dry outside air, lowering the temperature in the greenhouse. The sensible heat loss in W per square meter of greenhouse is given by:

$$P_{sens} = C_p \rho_{air} V_{vent} (T_i - T_o) \quad (5.1)$$

where  $\rho_{air} C_p$  is the volumetric specific heat of air in  $\text{J m}^{-3} \text{K}^{-1}$ ;  $V_{vent}$  is the air exchange through the window in  $\text{m}^3 \text{s}^{-1} \text{m}^{-2}$ ; and  $T_i$  and  $T_o$  are the temperatures of the air inside the greenhouse and outside in  $^{\circ}\text{C}$ .

Beside sensible heat also latent heat is removed:

$$P_{latent} = L_v V_{vent} (c_i - c_o) \quad (5.2)$$

where  $L_v$  is the heat of evaporation in  $\text{J kg}^{-1}$ ;  $c_i$  and  $c_o$  are the concentrations of vapour in the air inside and outside the greenhouse in  $\text{kg m}^{-3}$ .

The air exchange  $V_{dehumid}$  in  $\text{m}^3 \text{s}^{-1} \text{m}^{-2}$  needed to maintain the concentration set point  $c_i$  in the greenhouse is calculated by

$$V_{dehumid} = \frac{\phi_{trans} - \phi_{cond}}{c_i - c_o} \quad (5.3)$$

where  $\phi_{trans}$  and  $\phi_{cond}$  are the mass vapour fluxes by transpiration, condensation and ventilation in  $\text{kg s}^{-1} \text{m}^{-2}$ . The actual air exchange is the highest ventilation needed for either temperature control or humidity control.

### 5.2.2 Condensation on a cold surface

Chasseriaux (1987) tried to dehumidify a double layer plastic greenhouse of around  $3000 \text{ m}^2$  with roses. The equipment was able to remove around 5 litres of water per hour

with 2.5 kW electric power to drive the installation. This was not sufficient to improve the greenhouse climate. The climate was not affected by a similar heat pump used in a 7.5 times small greenhouse by Boulard (1989) during the night either. Condensation on the cover was reduced though.

The study with cold finned pipes in the greenhouse discussed in chapter two showed that the fraction of latent heat removal over the total heat removal  $F_{latent}$  is less than 50%, dependent on the relative humidity in the greenhouse. Hence, the total heat removal from the greenhouse is more than twice the amount needed for dehumidification. By using a heat pump the latent heat and the sensible heat gathered at the cold surface can be returned to the greenhouse together with the power needed to operate the heat pump. For a temperature difference between the cold surface and the greenhouse air of 10 K, the fraction  $F_{latent}$  can be deduced from Figure 2.8:

$$F_{latent} = 8.0 \times 10^{-3} H_R - 0.36 \quad (5.4)$$

where  $H_R$  is the relative humidity in %.

The total amount of heat transferred by the heat pump divided by the energy consumed by the heat pump, is defined as the coefficient of performance  $\eta$ . This coefficient is set to 4 in the calculations. A co-generator produces the power supplied to the heat pump with an efficiency of 40% and a thermal efficiency of 50% which is also supplied to the greenhouse. The total heat supplied to the greenhouse consists of the latent heat transferred to sensible heat, and 90 % of the energy consumed by the co-generator to power the heat pump:

$$H_{system} = \phi_{vapour} L_v \left( 1 + \frac{2.25}{\eta F_{latent}} \right) \quad (5.5)$$

where  $\phi_{vapour}$  is the vapour flux in  $\text{kg s}^{-1} \text{m}^{-2}$ . The 10% heat loss in the co-generator is included in the costs resulting from the gas consumption.

### 5.2.3 Forced ventilation in conjunction with a heat exchanger

Mechanical ventilation is applied to exchange dry outside air with moist greenhouse air, exchanging heat between the two airflows. Albright and Behler (1984) tested an air-liquid-air heat exchanger for greenhouse humidity control. They concluded that around one-third of the enthalpy could be recovered from the ventilation air. De Hallaux & Gauthier (1998) studied this system and concluded that the use of heat exchangers would lower the energy consumption in direct proportion to the efficiency of the exchanger. The energy savings did not justify the costs of the equipment though. In a more recent study Rousse (2000) studied a heat recovery unit in Canada. The heat recovery unit had an efficiency of around 80%. The ventilation flux of  $0.9 \text{ change h}^{-1}$  was not enough to dehumidify the greenhouse. The coefficient of performance defined



by dividing the recovered heat by the power consumed by the fan, ranged between 1.4 and 4.8 in their study. In a study with smaller sized heat exchangers that were placed in the gutter of the greenhouse, it was possible to retrieve between 60 and 70% of the sensible heat (Speetjens, 2001).

In the present study, dehumidification by forced ventilation was applied when the relative humidity  $H_R$  in the greenhouse exceeded 85% and the vapour concentrations inside and outside the greenhouse differed by more than  $3 \text{ g m}^{-3}$ . The second criterion was set to avoid the need of large ventilation rates for dehumidification. A proportional integration routine calculates the necessary forced ventilation in time. For the presented calculations the heat recovery was assumed ideal, meaning the temperature of the air entering the greenhouse was set equal to the temperature inside the greenhouse. Since condensation is likely to occur in the outgoing airflow, this assumption is justified.

#### 5.2.4 Hygroscopic dehumidification

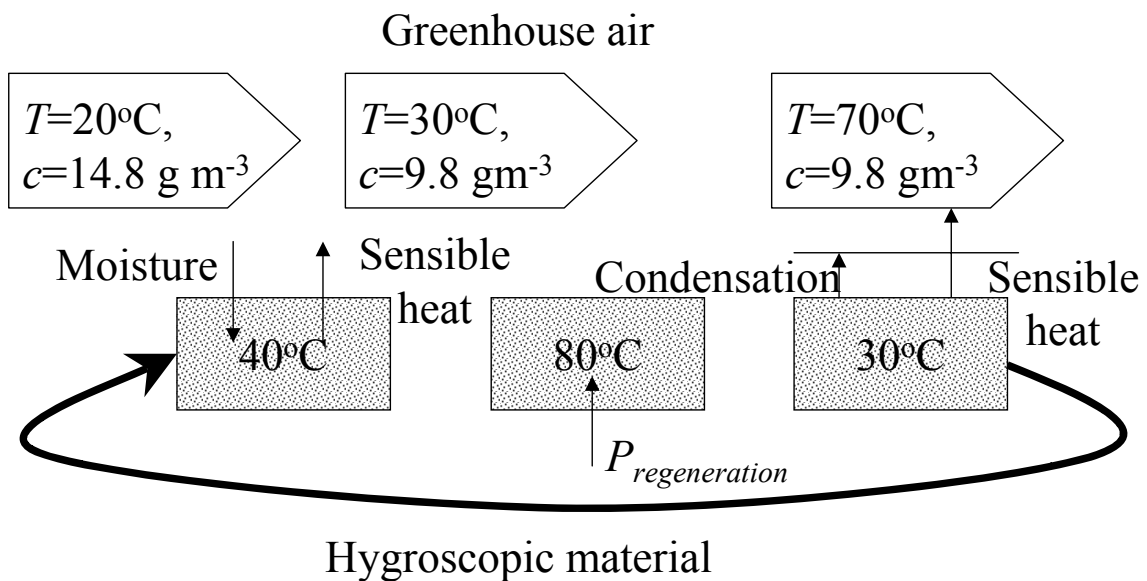


Figure 5.1 The dehumidifying process with a hygroscopic material;  $T$ , temperature of the greenhouse air during dehumidifying process;  $P_{regeneration}$ , the energy needed to regenerate the hygroscopic material

The research on the application of hygroscopic dehumidification in greenhouses is minimal because the installation is too complex and the use of chemicals is not favourable in greenhouses. The process for dehumidifying with a hygroscopic material is displayed in Figure 5.1. Moist greenhouse air is in contact with the hygroscopic material releasing the latent heat of vaporisation as water vapour is absorbed. The hygroscopic material has to be regenerated at a higher temperature level. A maximum of 90% of the energy supplied to the material for regeneration  $P_{regeneration}$  can be returned to

the greenhouse air with a sophisticated system involving several heat exchange processes including condensation of the vapour produced in the regeneration process.

In the presented calculations, the heat released when air passes the hygroscopic material is returned to the greenhouse and the excess moisture is removed from the greenhouse air. This situation is similar to the dehumidifying process with the cold surface, except for the additional heat input by the heat pump. Hygroscopic dehumidification in greenhouses is only useful when the heat released during absorption is needed to heat the greenhouse.

### **5.3 Methodology**

Calculations were performed with KASPRO, a dynamic physical simulation model developed by De Zwart (1996). This model serves to study the effects of climate control on the mass and heat flows in a greenhouse based on weather data. Based on the climatic set points, the model regulates the heating system, the CO<sub>2</sub> supply, etc. The heat and mass fluxes related to the dehumidifying methods described in the previous paragraph are added to the model for this study.

Table 5.1 The greenhouse area under glass in 2000 in The Netherlands (LEI, 2001; PBG, 2000)

Crop	Area, ha	Production, M€
Tomato	1134	300
Sweet Pepper	1155	300
Rose	932	450
Cucumber	663	160

The dehumidifying methods are studied using four crops, which are economically the most important for the Dutch greenhouse industry (Table 5.1).

For the cost evaluation the prize of one cubic metre of natural gas is set at 0.14 €. A cubic meter of natural gas contains 31.65 MJ of energy of which 95% can be used to heat the greenhouse without condensation of water in the flue gasses. All data is presented for one square metre of greenhouse.

Table 5.2 The climatic set points, planting dates, and dates crop is removed for the different crops

Crop	Day time air temp., °C	Night time air temp., °C	Minimum pipe temp., °C	Planting date	Date crop is removed
Tomato	19	18	45	11 Dec	20 Nov
Sweet pepper	22	20	45 (15 Sep- 15 Mar)	25 Nov	7 Nov
Rose	19	18	45	Multi year crop	Multi year crop
Cucumber	21	20	5	14 Dec, 15 May, 1Aug	5 Nov, 14 May, 31 July

Table 5.3 The vapour balance during one year in  $\text{kg m}^{-2} \text{y}^{-1}$  in the greenhouse for various crops for a single and a (double) layer greenhouse.

Crop	Vapour flux, $\text{kg m}^{-2} \text{y}^{-1}$			
	Transpiration	Ventilation	Condensation	Dehumidification
Tomato	693 (718)	484 (561)	125 (43)	84 (114)
Sweet pepper	591 (598)	344 (424)	161 (52)	86 (122)
Rose (ilum.)	696 (699)	405 (470)	175 (68)	116 (161)
Cucumber	545 (553)	306 (356)	135 (49)	104 (148)

All calculations were based on a Venlo-type greenhouse with a single and a two-layer glass cover. The crop specific conditions are presented in Table 5.2. Thermal screens were used in wintertime. Rose was illuminated in the period from the first of September till the first of May with  $40 \text{ W m}^{-2}$  when the solar radiation was less than  $125 \text{ W m}^{-2}$ . Four hours a night the light was switched off. The minimum greenhouse temperature was set to  $5^\circ\text{C}$  when no crop was present. The greenhouse climate for the different crops was set to the conditions normally used by Dutch growers (Swinkels *et al.*, 2000). The relative humidity was set to 85%. In order to maintain sufficient air circulation in the greenhouse, growers set a minimum pipe temperature. This minimum temperature was linearly decreased to 5 degrees as solar radiation increases from  $100 \text{ W m}^{-2}$  to  $300 \text{ W m}^{-2}$ . For sweet pepper the minimum temperature is set to  $5^\circ\text{C}$  between 15 March and 15 September. Heat storage was included in the calculation with a capacity of  $80 \text{ m}^3 \text{ ha}^{-1}$ . The heat is stored during daytime, supplying the  $\text{CO}_2$  to the greenhouse. During night-time the heat is used to warm the greenhouse.

The weather conditions are defined in a selective year (Breuer *et al.*, 1989). This year has been set as a national standard year for energy calculations for Dutch greenhouses. The hourly averaged values of outside temperature, relative humidity, global radiation, etc., are in this database. The month of the year that has a similar average value as the average value of the period between 1971 and 1980 is selected as a month in the selective year. For example, the month January of the year 1971 is set as the first month of the selective year. For the calculations with a time step of two minutes, the hourly weather data were interpolated.

## 5.4 Results and discussion

### 5.4.1 Dehumidification needed

The moisture balance in the greenhouse is calculated to get a general impression of the amount of dehumidification needed. The incoming vapour flux is generated by the transpiration of the crop. The outgoing fluxes are ventilation, condensation on surfaces, and dehumidification. The ventilation is partially through leakage and mainly to regulate the temperature in the greenhouse. Condensation occurs mainly on the cover of the greenhouse. The excess vapour not removed by ventilation and condensation needs to be removed by dehumidification. The excess vapour to be removed per  $\text{m}^2$  greenhouse area over the year for both a single and a double layer greenhouse, as determined by the simulation model, are presented in Table 5.3.

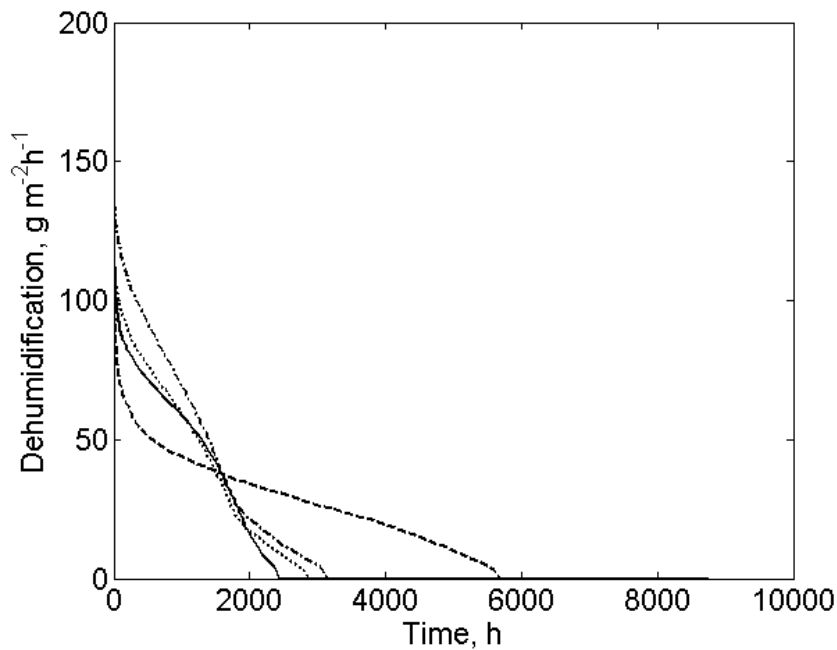


Figure 5.2 Dehumidification needed in  $\text{g m}^{-2}\text{h}^{-1}$  as a function of the number of hours per year for a single layer greenhouse: —, tomato; ..., sweet pepper (red); ---, rose (illuminated); -.-, cucumber

The average leaf area index of cucumber is less because it was planted three times a year explaining the lower transpiration. Tomato grows faster than sweet pepper explaining the difference in transpiration. The major part of the vapour left the greenhouse by ventilation in warm periods, when excess heat is available and the crop transpires relatively more. The air temperature for tomato was set lower than the other crops, explaining why this crop dehumidifies more by ventilation. The condensation on the cover was less for the double layer greenhouse, as expected.

In Figure 5.2 a histogram displays the dehumidification needed over the year. Rose has most dehumidifying hours due to the illumination resulting in more transpiration during cold and dark periods. The highest dehumidification at a certain point in time is needed for cucumber.

Table 5.4 The number of hours, the maximum dehumidification, and the average dehumidification needed in the period with and without additional heating for a single and (double) layer greenhouse

Crop	With additional heating			Without additional heating		
	Time, h	Max., $\text{g m}^{-2} \text{h}^{-1}$	Average, $\text{g m}^{-2} \text{h}^{-1}$	Time, h	Max., $\text{g m}^{-2} \text{h}^{-1}$	Average, $\text{g m}^{-2} \text{h}^{-1}$
Tomato	1070 (1135)	145 (144)	14 (34)	1044 (1279)	161 (163)	8 (8)
Sweet pepper	2142 (2663)	147 (140)	15 (26)	148 (338)	124 (138)	2 (3)
Rose	3349 (4015)	128 (135)	16 (24)	1536 (1827)	139 (136)	10 (12)
Cucumber	2120 (2950)	165 (166)	15 (22)	371 (403)	117 (124)	3 (4)

The conventional dehumidification by ventilation is costly when additional heating is needed. The number of hours dehumidification is needed, the average dehumidification, and the maximum dehumidification in the period with and without additional heating are given in Table 5.4.

For cucumber and sweet pepper the time without additional heating is less than for the other crops because the minimum temperature of the heating system was set to 5°C, hence the temperature of the heating system has to be increased, whereas the heating system for the other crops is already set at a high temperature. For tomato, dehumidification time with additional heating is less than the other crops because the temperature was set lower.

#### 5.4.2 Dehumidification by natural ventilation

Table 5.5 Heat supplied by heating system in terms of gas and sensible heat loss during ventilation needed for dehumidification for a single and (double) layer greenhouse for dehumidification by natural ventilation

Crop	Energy input, $\text{GJ m}^{-2}$	Sensible heat loss, $\text{MJ m}^{-2}$
Tomato	1.56 (1.34)	74 (102)
Sweet pepper	1.48 (1.21)	142 (191)
Rose	1.04 (0.94)	212 (276)
Cucumber	1.44 (1.18)	156 (223)

The total heat supplied to the greenhouse by the boiler in terms of gas and the sensible heat loss resulting from ventilation for dehumidification is given in Table 5.5.

The energy costs for illuminating rose was not included in the total energy amount. The total year round energy use was in good agreement with the data by PBG (2000). The amount of sensible heat loss, as a fraction of the total energy, is lower for the tomato crop because it had a lower greenhouse temperature except for rose because the energy for illumination is not included. This table clearly shows that the advantages of a double layer greenhouse in terms of lower energy use are partially lost due to the increasing ventilation for dehumidification.

### 5.4.3 Condensation on a cold surface

*Table 5.6 The energy from the heating system, from the co-generator; the latent heat transformed into sensible heat by the system; the maximum power of the heat pump; and the money saved on energy compared to the conventional method for a single and (double) layer greenhouse for dehumidification by a cold surface*

	<i>Energy input, GJ m<sup>-2</sup></i>	<i>Co- generator, MJ m<sup>-2</sup></i>	<i>Latent heat, MJ m<sup>-2</sup></i>	<i>Max. power, W m<sup>-2</sup></i>	<i>Saving, € m<sup>-2</sup></i>
Tomato	1.45 (1.21)	133 (166)	70 (88)	22 (23)	-0.09 (-0.18)
Sweet pepper	1.16 (0.83)	207 (262)	111 (140)	29 (31)	0.48 (0.49)
Rose	0.53 (0.43)	248 (316)	131 (168)	20 (22)	1.15 (0.84)
Cucumber	1.00 (0.61)	247 (340)	133 (183)	31 (33)	0.84 (1.02)

The first two columns of Table 5.6 show the amount of energy supplied to the greenhouse in terms of gas. The third column is the heat released at the cold surface when water vapour condenses. This heat is returned to the greenhouse through the heat pump.

For this method of dehumidification the total amount of heat supplied to the greenhouse is higher than with the conventional method (Table 5.5) for tomato. This is a result of the minimum temperature of the heating system providing heat when no heat is needed for tomato. The air temperature of tomato is lower than the other crops increasing this effect.

Heat pump costs are around 0.50 € W<sup>-1</sup>. If finned pipes are used as cold surface, the rest of the installation costs around € 25 m<sup>-2</sup>. In total this installation will cost around € 35 m<sup>-2</sup>. So the pay back time is more than 30 years with the current price of energy.

## 5.4.4 Forced ventilation using a heat exchanger

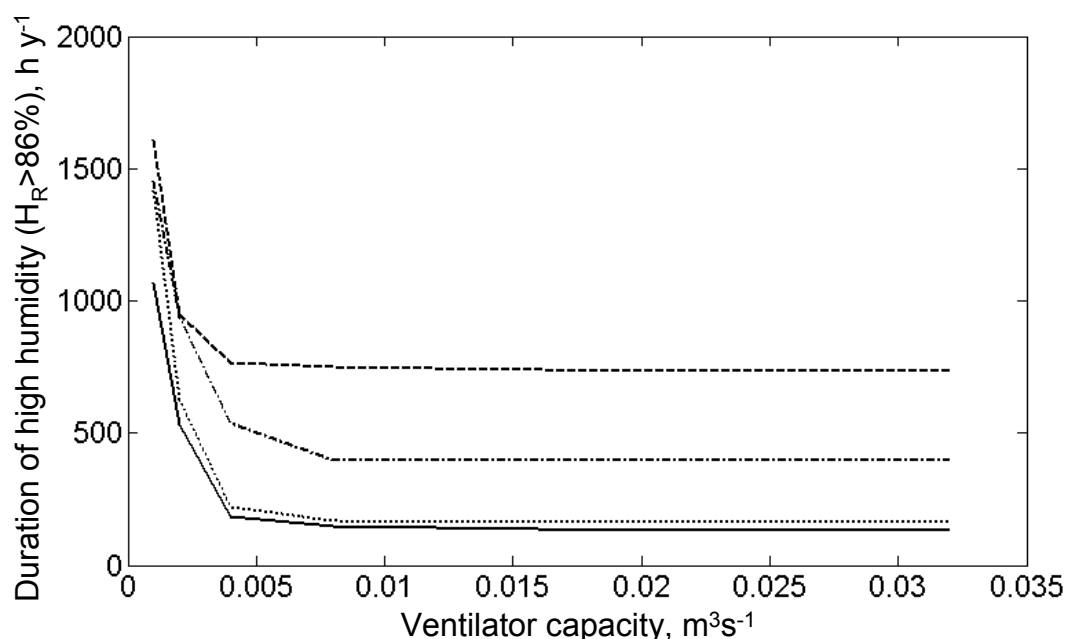


Figure 5.3 The annual period when the relative humidity in the greenhouse  $H_R$  is above 86% as a function of the capacity of the ventilator: —, tomato; ..., sweet pepper (red); ---, rose (illuminated); -.-, cucumber

The yearly number of hours the relative humidity  $H_R$  exceeds 86% as a function of the capacity of the ventilator is shown in Figure 5.3. Due to the illumination, rose tends to have a high humidity for a longer period. A ventilator capacity of  $0.01 \text{ m}^3 \text{ s}^{-1}$  is sufficient for all crops.

The period the relative humidity exceeds the set point is not zero since the system is only used when the difference in the vapour concentration in the greenhouse and outside was more than  $3 \text{ g m}^{-3}$ .

The energy needed to operate the ventilators is not considered because the experimental study by Speetjens (2001) showed that the energy consumption by the ventilators is less than 1% of the energy saved. In the experiments by Rouse et al. (2000) the energy consumption was around 20% to 40% of the energy saved. They used a central dehumidifying unit and a less optimal heat exchange system explaining this large discrepancy.



Table 5.7 The energy from the heating system; the amount of heat exchanged; and the saving by the system for a single and (double) layer greenhouse for dehumidification by forced ventilation in conjunction of a heat exchanger

Crop	Energy input, $GJ m^{-2}$	Heat exchanged, $MJ m^{-2}$	Saving, $€ m^{-2}$
tomato	1.49 (1.24)	108 (145)	0.31 (0.44)
Sweet pepper	1.34 (1.00)	117 (167)	0.62 (0.93)
Rose	0.93 (0.77)	190 (278)	0.49 (0.75)
Cucumber	1.25 (0.88)	142 (208)	0.84 (1.33)

In Table 5.7 the energy use, the amount of heat exchanged, and the savings by the system compared to dehumidification by ventilation (Table 5.5) are given. The installation may cost between 3 and 13 € m<sup>-2</sup> if the return time on investment is 10 years.

#### 5.4.5 Hygroscopic dehumidification

Table 5.8 The energy from heating system; heat transferred from latent heat to sensible heat; released heat in the greenhouse when no heat was needed; and the saving for a single and (double) layer greenhouse for dehumidification using a hygroscopic material

Crop	Energy input, $GJ m^{-2}$	Heat supplied, $MJ m^{-2}$	Surplus heat, $MJ m^{-2}$	Saving, $€ m^{-2}$
Tomato	1.46 (1.22)	92 (116)	83 (111)	0.44 (0.53)
Sweet pepper	1.23 (0.88)	132 (173)	87 (138)	1.50 (1.41)
Rose	0.82 (0.65)	167 (234)	113 (186)	0.97 (1.28)
Cucumber	1.10 (0.71)	151 (211)	97 (147)	1.50 (2.08)

In Table 5.8 the heat released by the hygroscopic material is given together with the portion released when no heat was needed in the greenhouse.

The heat loss needed for regeneration of the hygroscopic material and the energy needed to circulate the air are not included in these calculations. The air treatment has to be done centrally because hygroscopic materials are toxic and dangerous for the greenhouse environment. An air distribution system is needed increasing the complexity of the system making it less attractive for application. In all, the installation is very costly. With a pay back time of 10 years the system may cost between 4 and 21 € m<sup>-2</sup> which is not enough to install this system. But especially the extra environmental risk of the hygroscopic system is a disadvantage.

## 5.5 Conclusions

Three dehumidifying systems have been investigated in this study. The savings on energy in terms of Euros compared the conventional method of dehumidification by natural ventilation, have been calculated for these systems. For tomato the savings are less than for the other crops due to the lower air temperature. Dehumidification with a cold surface by applying a heat pump is not cost-effective when the heat pump is not used for heating as well. For heating with a heat pump, a heat source has to be available, for example an aquifer. This will increase the cost of the total system. Dehumidification with a hygroscopic material has the advantage that latent heat is directly transformed into sensible heat. However, the heat needed for regeneration of the material, the environmental risks and the complexity of the system make it less suitable for a practical application.

The most promising method for dehumidification is forced ventilation with heat exchange. A low cost and efficient system has to be developed in order to make it a success. In greenhouses with a higher insulation the system saves even more energy than in the normal single glass greenhouse.

## Acknowledgements

This research was financed by the E.E.T. (Ecology, Economy and Technology) research programme funded by the Dutch Ministries of EZ (Economic Affairs), of OCW (Education) and of VROM (Environmental Affairs).

---

# 6

## Mechanically controlled moisture removal from greenhouses

---

This chapter was published before as:  
J.B. Campen F.L.K. Kempkes and G.P.A. Bot (2009).  
Mechanically controlled moisture removal from greenhouses.  
Biosystems Engineering 102 pp 424-432  
doi:10.1016/j.biosystemseng.2009.01.001

### **Abstract**

The object of this study was to design and test a system capable of dehumidifying air in a greenhouse when a thermal screen is in use. Dehumidification is required to reduce the risk of fungal diseases and prevent physiological disorders. The most common procedure used to remove moisture from a greenhouse fitted with a thermal screen is to open slightly the thermal screen. This causes an exchange between the relatively dry air above the screen and the humid air below the screen. However, this procedure is difficult to control and it can cause horizontal temperature differences in the greenhouse, which negatively effect crop production. In the dehumidification system proposed here, outside air is exchanged at low level with greenhouse air. This ventilation with cool dry outside air is mechanically controlled using an air distribution system. The dry air is injected near the greenhouse floor thereby forcing humid air to pass through the thermal screen. The excess air in the greenhouse then flows out through leaks in the cover.

The airflow required by the system throughout the year, being dependent on the evaporation of the crop and the outside conditions, was determined using a greenhouse-climate simulation model. The model was validated using climate data from the commercial greenhouse where the system was installed. The dimensions of the system were calculated from the results of the model and a control strategy was suggested. The model calculations showed that using outside air for vapour removal is more energy-efficient than using air from above the thermal screen. The distribution of climate in the greenhouse using the conventional and proposed methods of vapour removal was investigated using computational fluid dynamics (CFD). The system was tested in a commercial greenhouse and compared to a conventional system at the same location. The performance of the system, as determined by the dynamic simulation model, proved to be efficient and the climate proved to be more homogenous, as was predicted by the CFD calculations.

### **6.1 Introduction**

For greenhouse horticulture, climate control is crucial to obtain both a high quality product and a high yield (Bakker *et al.*, 1995; De Pascale *et al.*, 2005). High quality is required to meet the demands of the needs of consumers, and high yield is required for economic production. In modern greenhouses climate is controlled applying heating, ventilation, fogging, CO<sub>2</sub> enrichment and occasionally even cooling (Särkkä *et al.*, 2006). In most cases temperature and humidity are controlled by heating and ventilation. Controlling humidity is more difficult than controlling temperature since it is not only dependent on vapour exchange from ventilation, but also on transpiration of

the crop and condensation on the cover. Transpiration of the crop depends on solar radiation, CO<sub>2</sub> concentration, temperature of the greenhouse air and relative humidity in the greenhouse (Stanghellini, 1987). The amount of condensation on the cover depends on the temperature of the greenhouse cover as described in chapter two. Modern greenhouses have low ventilation through leakage and usually are equipped with thermal screens to reduce heat losses. Thermal screens are widely used in greenhouses because they can be opened during daytime maximising solar radiation for crop production and increasing insulation during the night. Screens also reduce the amount of condensation on the greenhouse cover and reduce the air exchange between the greenhouse and the surroundings. Therefore, controlling humidity is even more crucial since crops exposed to high humidity levels have a greater risk of developing fungal diseases and physiological disorders (Bakker, 1991; Dieleman, 2008).

Greenhouse air can be dehumidified in various ways as described in chapter five. During periods of heat demand, the most economic method of dehumidification is ventilation combined with heating because it has relatively low operating costs. Energy could be saved by applying heat recovery, and with rising energy prices this will soon could be economically viable. Growers usually control humidity under thermal screens by slightly opening the screens when the humidity exceeds a specific limit. As a result, air below the screen is exchanged with air above the screen, which has lower temperature, and because of condensation on the cover and air exchange with the surroundings, a lower vapour content. This method successfully dehumidifies the greenhouse but the control operates within a small range of the openings, so it is not very accurate. Moreover, the large distance between the small screen openings causes horizontal temperature differences, which has negative effects on crop growth.

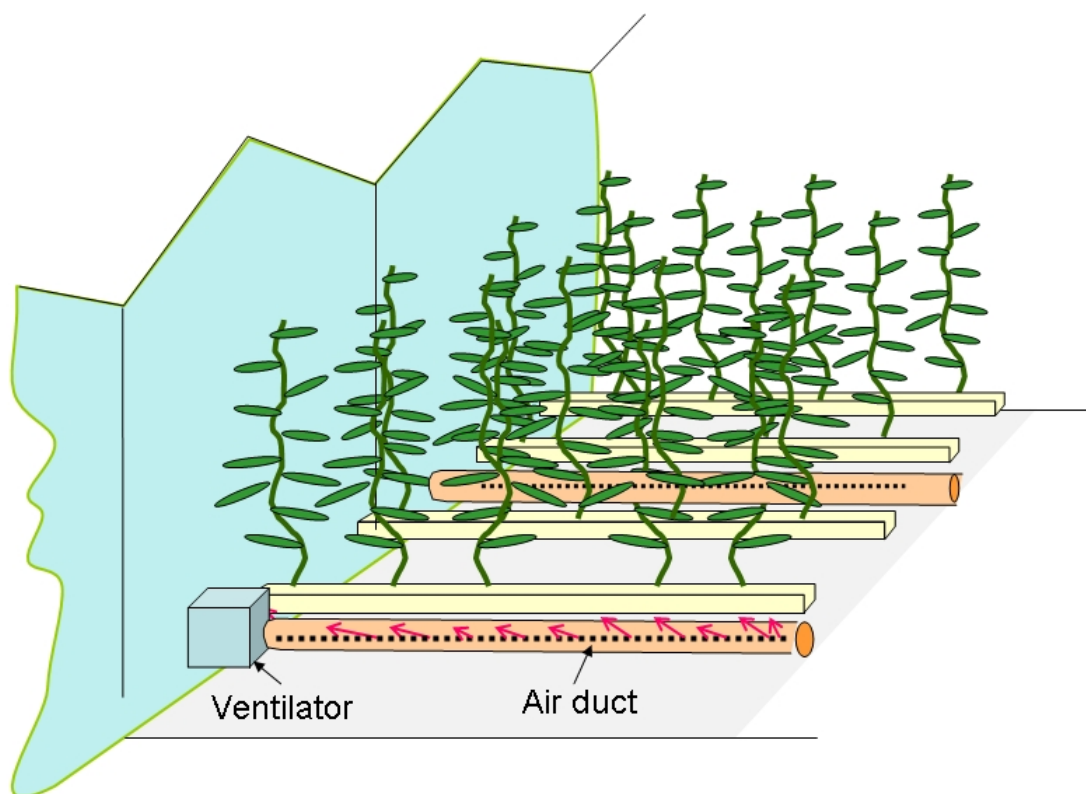


*Figure 6.1 A schematic representation of the system where the ventilator is located at the side wall of the greenhouse allowing outside air to be drawn in and distributed by the air duct.*

To solve this problem an alternative system for the humidity control has been developed by blowing of dry air under the thermal screen. The system is shown in Figure 6.1. The design includes air ducts to distribute outside air from ventilators mounted in the sidewall of the greenhouse. Alternatively, the air could be drawn from above the screen. The system can be installed easily in existing greenhouses. This paper describes the design process and testing of the system.

## **6.2 Materials and methods**

The design of the system was based on theoretical calculations consisting of dynamic simulation and computational fluid dynamics (CFD) calculations. The design was installed and tested at a commercial growing site where the climate is monitored and compared to a reference greenhouse using the conventional method of dehumidification.

### **6.2.1 Theoretical calculations**

To design the controlled forced-ventilation dehumidification system the dynamic behaviour and the spatial distribution of the system in interaction with the greenhouse

climate were calculated by dynamic and CFD simulations respectively. Using dynamic simulation the demand for air refreshment capacity for accurate control of water vapour content can be determined throughout the year. Using spatial distribution simulation, the air distribution requirements can be determined.

#### 6.2.1.1 Dynamic simulation

The greenhouse climate and the energy consumption can be calculated using physical models (Bot, 1983; De Zwart, 1996), representing the heat and mass exchange processes. For the present study the extensively calibrated and validated dynamic physical simulation model KASPRO was used (Van Henten *et al.*, 2006; Elings *et al.*, 2006; De Zwart, 1996). This model was extended to include the effect of climate control on the heat and mass flows in a greenhouse with given weather data. With the chosen climatic set points during the year used as the model inputs, the model continuously regulates the heating system, the CO<sub>2</sub> supply, and other variables. The state variables in the model such as air temperature, heating pipe temperature, air vapour concentration, carbon dioxide concentration, etc. were recalculated every two minutes. Crop production was evaluated with a linked sub-model for crop growth (Gijzen, 1992). The model calculations were performed for a production cycle of greenhouse vegetables for a one-year period.

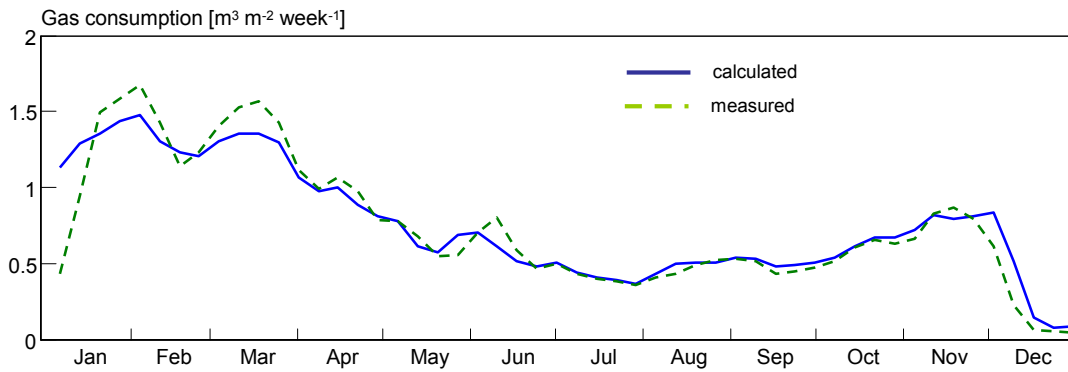
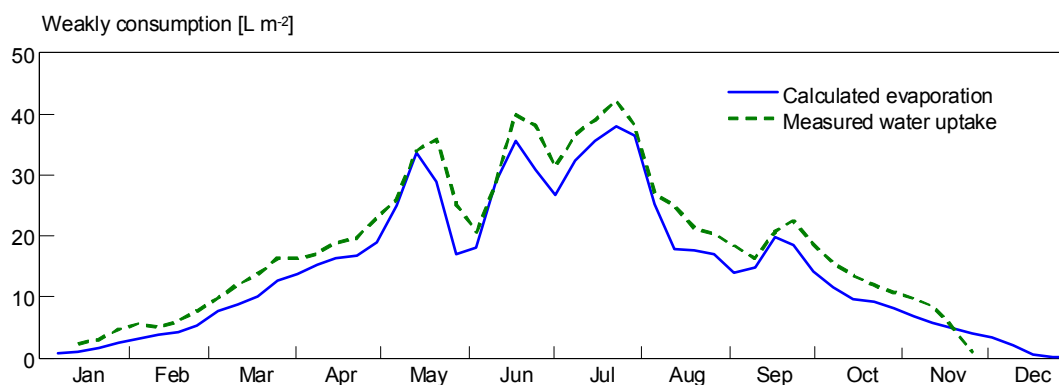


Figure 6.2 Weekly gas consumption per area of greenhouse as calculated by the model and measured in the commercial greenhouse



*Figure 6.3 Weekly water consumption per area of greenhouse as calculated by the model and measured in the commercial greenhouse*

The model was validated for the greenhouse where the proposed dehumidification system was installed and tested by calculating the greenhouse climate based on the system specifications and the outdoor measured climatic data at the site for the year 2006. The comparison was based on energy (natural gas) and water consumption over the year since these data were available and relevant for this study. Validation based on state variables, such as greenhouse air temperature, does not make sense since these state variables are controlled by the system. The results of the energy and water consumption calculations in comparison to measured data are presented in Figure 6.2 and Figure 6.3. The calculated and measured data agreed reasonably although not exactly. This was because the grower constantly adjusted the set points in the climate control computer depending on the weather conditions and his observations of the status of the crop. These set-point variations were not included in the model calculations since they were not recorded. The overall gas consumption for the year 2006 was  $38.8 \text{ m}^3 \text{ m}^{-2}$  whilst it was calculated to be  $39.1 \text{ m}^3 \text{ m}^{-2}$ , so total energy consumption during the year 2006 was calculated accurately. The measured total water at  $800 \text{ l m}^{-2}$  consumption was substantially higher than calculated ( $642 \text{ l m}^{-2}$ ). This was caused by losses in the system and the drainage of recycled water not being separately measured by the grower. The conclusion of the validation was that KASPRO could be used without further calibration to design the dehumidification system.

The design was modelled by dynamically simulating the airflow required for both the case where outside air is used, and where air from above the screen is used. When the thermal screen was used, the airflow was adjusted aiming at keeping the relative humidity below 85%. Heat and vapour fluxes resulting from the airflow were included in the model.



*6.2.1.2 CFD simulations*

The problem with slightly opening the thermal screen to remove the humid air is that it causes local effects from cold air. Here, we are trying to reduce these effects by using the proposed system. Therefore, for these cases the spatial distribution of greenhouse climate (temperature, humidity, velocity of the greenhouse air) were calculated using three dimensional CFD (Versteeg *et al.*, 1995). The commercial CFD software code Fluent 5.3 (Fluent, 1998) was used. The greenhouse was modelled as a rectangular box of 80 by 36 by 6 m with the thermal screen is mounted 1 m below the cover, corresponding to the dimensions of a quarter of the greenhouse where the system was tested. The thermal screen was modelled as a porous medium with the characteristics measured by Miguel (1998). Two sides of the model were assumed symmetrical. The cover was simplified to a flat plate because the cover geometry does not affect the results for the spatial distribution below the thermal screen. This reduced the complexity of the CFD grid meshing. The temperature of the outside air was set to 10°C with convective heat transfer coefficient to the cover of 10 W m<sup>-2</sup> K<sup>-1</sup>. To calculate the radiative heat transfer the sky temperature was set at 0°C with emission coefficient of the cover of 0.86. The greenhouse floor was set to a specific temperature resulting in the average air temperature in the greenhouse below the thermal screen to be 20°C. The vapour concentration at the cover was equal to the saturated vapour concentration of air at the average cover temperature of 10°C. As a result the cover acted as a sink for water vapour. The computational grid consisted of 260,000 cubical cells, and turbulence was modelled using the standard k-e model.

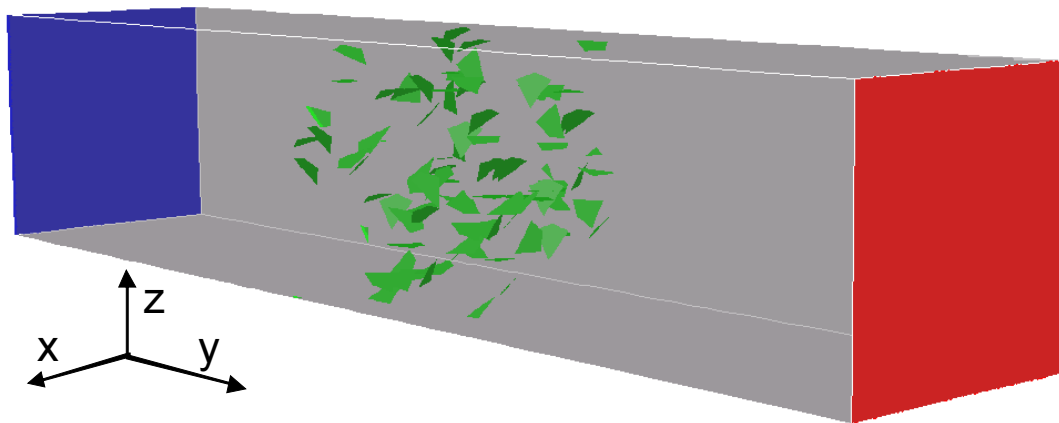


*Figure 6.4 Leaf arrangement in the CFD tomato crop model used to determine the pressure difference over the crop as a function of the average air velocity in the y direction*

The resistance of the crop was taken into account as a porous medium, which is modelled in the greenhouse CFD model by the addition of a momentum source term

determined by the Darcy-Forcheimer equation. This momentum sink created a pressure drop that was related to the fluid velocity in the porous medium (Fluent, 1998; Miguel, 1998; Boulard *et al.*, 2002) by

$$S = -\left(\left(\frac{\mu}{K}\right)v + \rho\left(\frac{C_F}{K^{0.5}}\right)v^2\right) \quad (6.1)$$

where  $\mu$  is the dynamic viscosity of the fluid,  $K$  the permeability of the porous medium,  $\rho$  the density of the fluid, and  $C_F$  the non-linear momentum loss coefficient. This source term is determined by separately detailed modelling the flow through one cubic metre of the crop with geometry, leaf size and number of leaves corresponding to an actual tomato crop as depicted in Figure 6.4. The grid consisted of 100,000 cells and the flow was considered laminar with the maximum Reynolds number being around 3,000. The volume occupied by the crop was 0.6 by 0.6 by 0.6 m with a leaf area of  $1.6 \text{ m}^2 \text{ m}^{-3}$ . The relationship between the velocity and pressure was determined in the x and y direction as shown in Figure 6.4 since the dominant direction of airflow in the greenhouse is horizontal. From these relationships the permeability  $K$  was estimated to be  $2.4 \cdot 10^3 \text{ m}^2$  and the non-linear momentum loss coefficient  $C_F$  was  $5.8 \cdot 10^{-2}$ . The resistance of the crop described by this relationship is 20% lower at air velocities in the range  $0.05$  to  $0.30 \text{ m s}^{-1}$  than measured for a tomato crop by Kacira *et al.* (2004). However, this is acceptable considering the variations in the structures of tomato plants. The transpiration of the crop was included as a source of water vapour in the porous medium. The transpiration was based on the period when the thermal screens were used, so during night time, it was set to  $11.1 \cdot 10^{-6} \text{ kg m}^{-2} \text{ s}^{-1}$ , which is equivalent to  $40 \text{ g m}^2 \text{ h}^{-1}$  (Stanghellini, 1987). The gravitation direction was slightly tilted by 1%, to account for the fact that the gutters were at a small angle to enable rainwater to run off.

The situation where the thermal screen is slightly opened to dehumidify the greenhouse air was modelled with 100 mm wide openings in the screen at every 5 m corresponding to the openings in the test greenhouse when dehumidification is required. The forced ventilation system was modelled by 30 air inlets distributed evenly over the greenhouse floor. Air flowed out the greenhouse through four narrow (200 mm) openings distributed evenly over the 10m length of the cover of the greenhouse. This represented small openings in the greenhouse cover where the air leaked out. Since these openings are small and the pressure in the greenhouse was higher than outside, no air entered the greenhouse at these openings.

6.2.2 Experimental setup

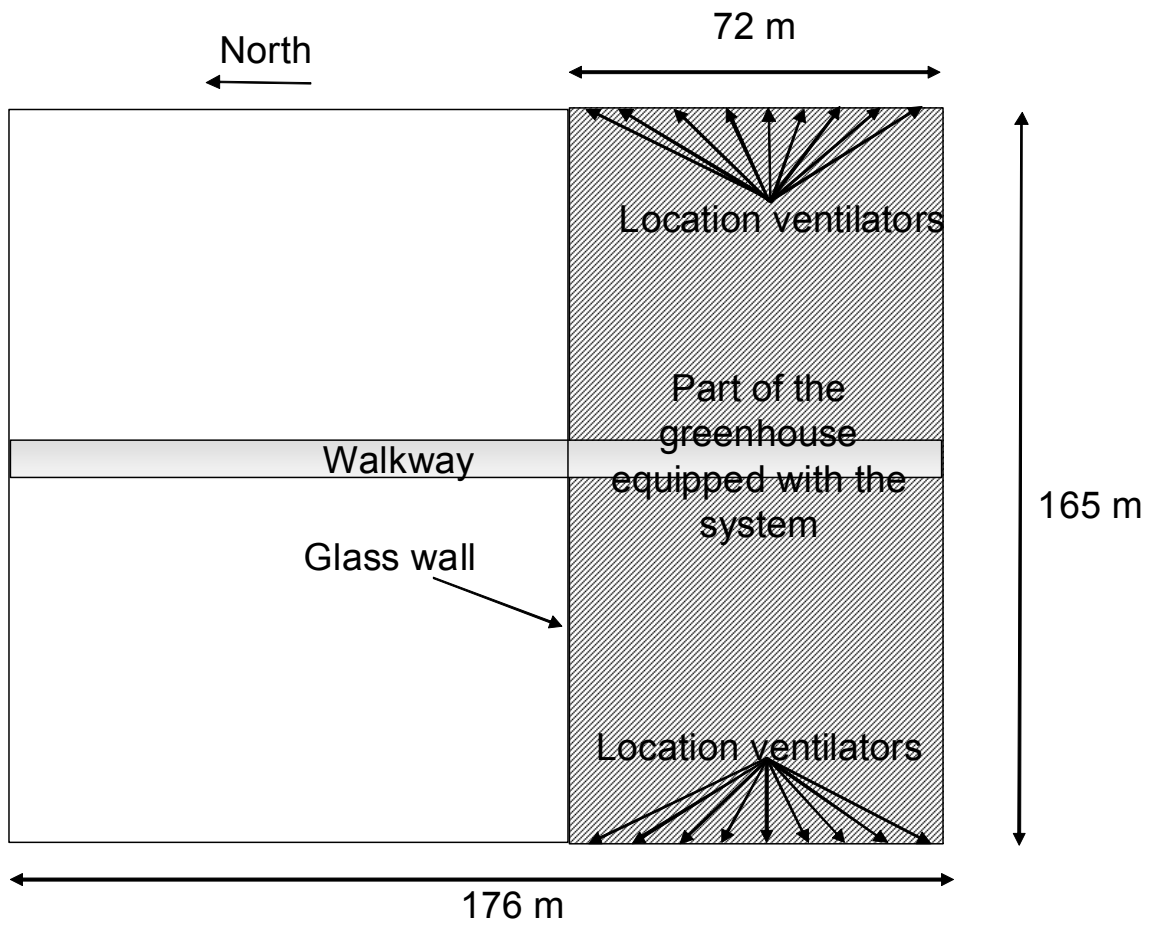


Figure 6.5 Outline of the greenhouse where the experiment was carried out with the locations where the ventilators are installed



*Figure 6.6* Picture of one of the ventilators installed in the side wall of the greenhouse

The system was tested in a commercial greenhouse with a test section of 1.2 ha and a reference section of 1.7 ha (Figure 6.5). The test section of the greenhouse was located at the south side with gutter height of 6 m, which is 1.00 m higher than that of the reference section. The test section and reference section were separated by a glass wall. The test and reference sections were each divided by the central path into 2 compartments, each compartment having individual climate control. The air temperature and relative humidity were recorded in a ventilated box located in the centre of these compartments. Eighteen custom made fans (Holland Heater, custom made, The Netherlands) were mounted at equal distances in the side wall of the test section, as shown in Figure 6.5 and 6.6, each with maximum capacity of  $3,000 \text{ m}^3 \text{ h}^{-1}$  of air. Valves closed off the ventilators when the system was not in operation as can be seen in Figure 6.6. The ventilators were frequency controlled based on the relative humidity in the greenhouse. When the relative humidity exceeded 86%, the ventilators were switched on at 10 Hz and operated at maximum frequency (30 Hz) when the relative humidity exceeded 92%. The air was distributed by plastic ducts from the sidewalls to the central path, having diameter of 446 mm and length of 80 m, with 25 mm diameter holes evenly distributed over the duct every 800 mm (Figure 6.7). The dimensions of the air duct were designed to distribute the air homogeneously,

independent of the speed of the fans. The discharge from the air ducts was calculated using a simple physical model (Yeaple, 1995) where the pressure along the duct was calculated from the dynamic and static pressures. The pressure distribution was calculated iteratively with a fixed inlet pressure until convergence was reached. The coefficient of discharge of the outlets was set to the typical value of 0.66 and the flow resistance along the duct was considered. The air was directed from the ducts towards the heating system so the crop was not directly affected by the cold air. The greenhouse was equipped with a thermal screen (Ludvig Svensson, LS 10 Ultra Plus., Sweden) which was used when the outside temperature was 8 K below the minimum greenhouse temperature. In addition to the measurements in the ventilated boxes, taken for the purposes of climate control, climate in the test and reference sections of the greenhouse was measured using a grid of 36 wireless sensors (Sownet, Model HT100, The Netherlands) located just above the crop that registered local temperature and relative humidity every two minutes. The location of these sensors is shown in Figure 6.8. The sensors were ventilated and shielded to minimise the effect of solar and infrared radiation. The experiments began on the 30th January 2008 and continued until the end of March 2008.



*Figure 6.7* Picture of the air duct installed in the greenhouse



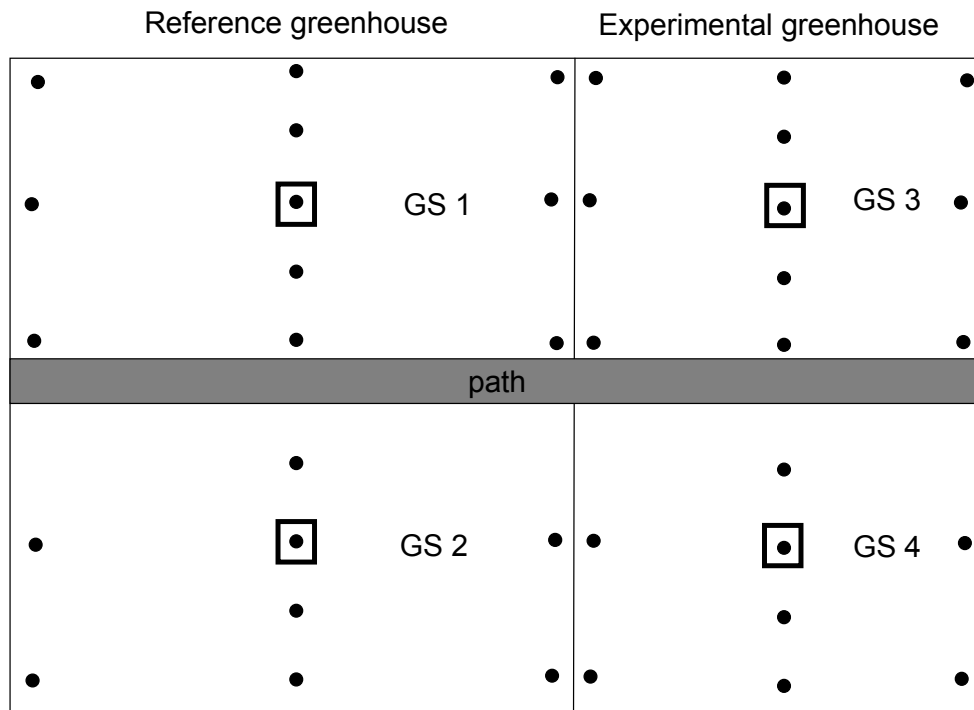


Figure 6.8 Distribution of the ventilated wireless sensors (•) for local temperature and RH measurement together with the location of the control measuring boxes (□). Greenhouse dimensions are not to scale.

### 6.3 Results and discussion

The results from the dynamic simulation model and the climate distribution CFD calculations are described below and are compared with the results of the experiments in the commercial greenhouse.

### 6.3.1 Theoretical analysis

#### 6.3.1.1 Dynamic simulation model KASPRO

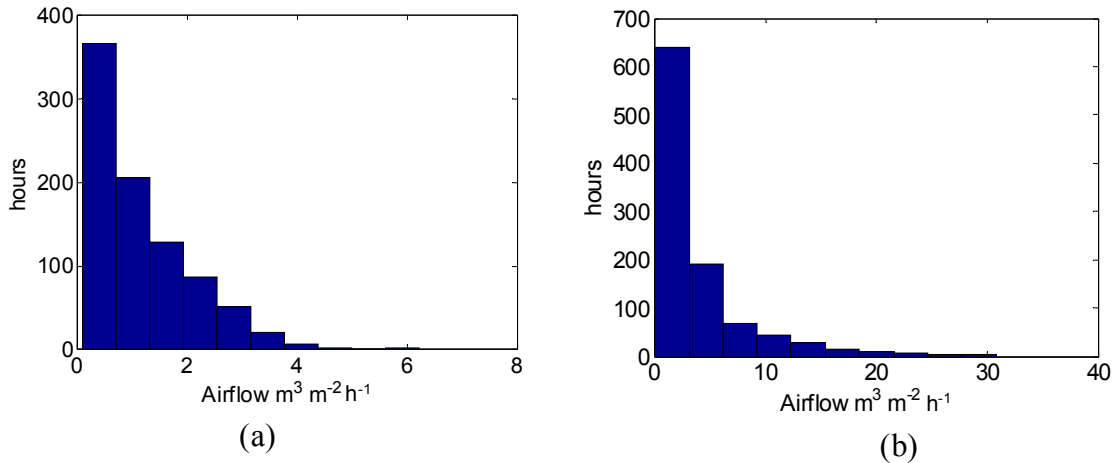


Figure 6.9 Histogram of the hours per year a specific amount of ventilation is needed in order to maintain a relative humidity around 85% for ventilation with outside air (a) and air above the screen (b)

Air blown into the greenhouse under the thermal screen can either come from above the screen, which is analogous to the situation where the screen is slightly opened, or from outside the greenhouse. Because of the different air temperature and humidity conditions above the screen and outside the greenhouse, the air refreshment capacity will be different for each case. For both cases the number of hours at a given level of ventilation that is needed to control relative humidity at 85% was calculated from a year long dynamic simulation using KASPRO. The results are shown in Figure 6.9. The maximum ventilation needed for the case when air from above the screen is used, was  $30 \text{ m}^3 \text{ m}^{-2} \text{ h}^{-1}$ . For the case when outside air is used, the maximum level of ventilation was only  $6 \text{ m}^3 \text{ m}^{-2} \text{ h}^{-1}$ . The air above the thermal screen is relatively dry compared to the air below the screen since water vapour is removed from this air by condensation on the cover. Although the vapour content of outside air is even lower, the outside air temperature is lower than the air temperature above the screen and this increases heat demand. Low-level ventilation using outside air is slightly more energy efficient than using air from above the screen. When outside air is used,  $12.1 \text{ MJ y}^{-1}$  is required to compensate for the heat losses caused by ventilation for the vapour removal. When air from above the screen is used,  $12.9 \text{ MJ y}^{-1}$  was required. Of course, the latter amount of energy would also be lost when the conventional method for vapour removal, slightly opening the thermal screen, is used. In that case, the warm greenhouse air is replaced by the cold relatively dry air from above the screen, but as stated earlier, this method is

much less controllable. The reduced ventilation required when outside air is used also considerably reduces the consumption of electricity by the ventilators. The yearly use of electricity by the ventilators when outside air is used was estimated to be less than  $0.03 \text{ kWh m}^{-2}$ .

The system has to be designed to operate when the thermal screens are in use and crop transpiration is high, as during spring and autumn. The dynamic pattern of vapour removal demand is shown in Figure 6.10 as weekly averaged values

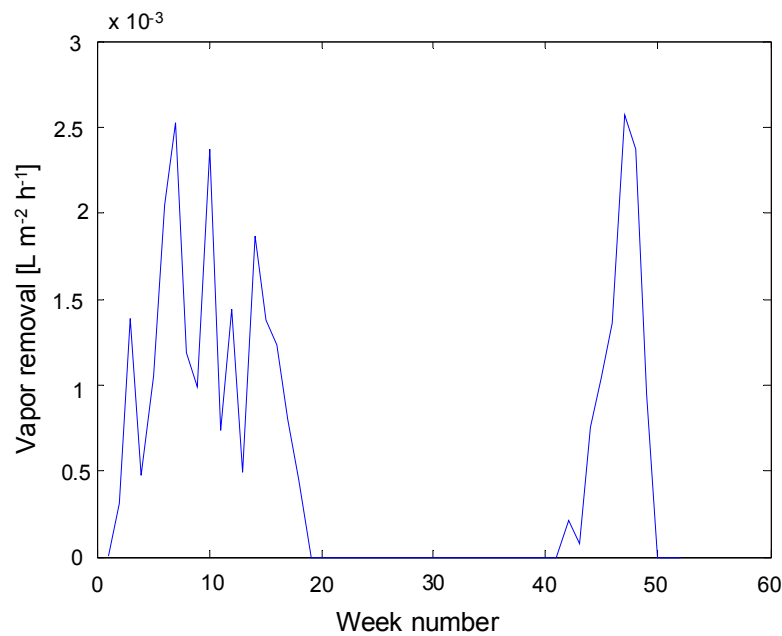


Figure 6.10 Vapour removal by the system as a function of the week of the year.

### 6.3.1.2 CFD simulations

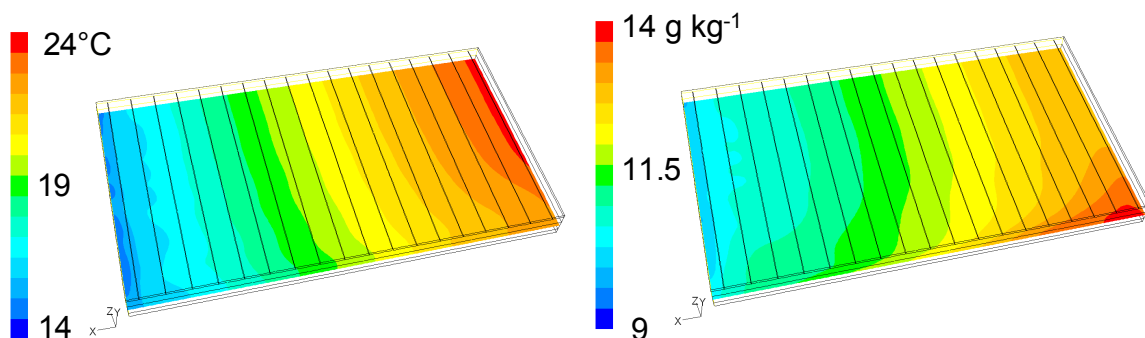
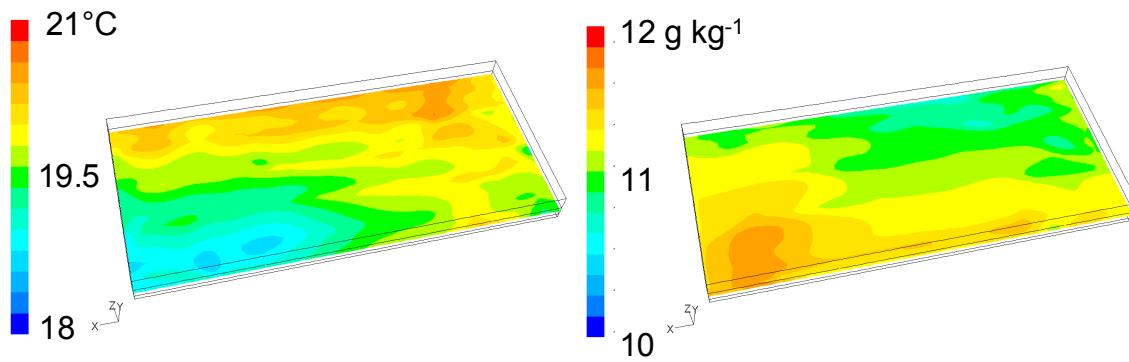


Figure 6.11 Temperature (left) and absolute humidity distribution(right) at a height of 2 meter with the thermal screen opened by 2.5%



The climate distribution for the system with conventional method for dehumidification when a thermal screen is applied was calculated by CFD. The results of the predictions of greenhouse climate (temperature and relative humidity) when the screen is opened (2.5% of the total surface area) are shown in Figure 6.11. The screen separates the cold air above the screen from the warm greenhouse air. The openings in the screen, located at the lines in the figure above the temperature profile, cause the cold air to pass the screen its lowest point and the warm air to rise near the walkway within the greenhouse. This airflow causes temperature differences of almost 10 K in the greenhouse. Because of this temperature drop, instead of decreasing relative humidity as required, the openings increase relative humidity.



*Figure 6.12 Temperature (left) and absolute humidity (right) distribution at a height of 2 meter when outside air is used for dehumidification*

Where humidity control is carried out by forced ventilation, the temperature and relative humidity differences are less than 3 K as can be seen in Figure 6.12. Also the differences in absolute humidity are 2.5 times less. Variations in climate remain due to the cold thermal screen and the warm greenhouse floor, which initiates airflow between these surfaces.

### 6.3.2 Experimental results

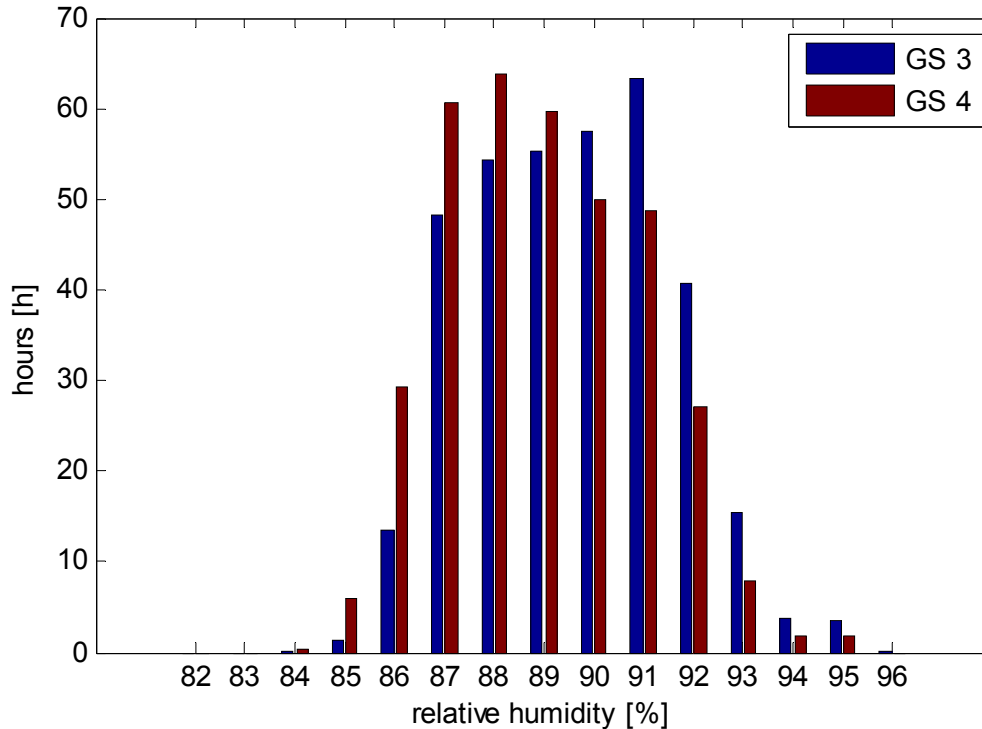


*Figure 6.13 Histogram of the number of hours as a function of the relative humidity in the period 30th January - 1st April 2008 when the system was in operation and the thermal screens were closed for the two compartments (GS 3 and 4) in the experimental greenhouse*

The relative humidity in the greenhouse during operation of the system when the thermal screens were closed is shown in Figure 6.13 for both compartments in the test section GS 3 and 4 (see Figure 6.8). From 30th January until 1st April 2008 the system operated for 222 hours when the energy screens were closed. From Figure 6.13 it can be concluded that the system was capable of maintaining the relative humidity within the range of 87 and 92% for the majority of time. If the system were not limited to operate below 30Hz by the grower, the relative humidity would probably not have exceeded 92%. The relative humidity in GS 3 tended to be higher than in GS 4. The ventilators of GS 4 were located at the west side of the greenhouse, which tended to be exposed to wind since that was the dominant wind direction. As a result, these ventilators tend to transfer more air when the system was in operation. A comparison with the reference greenhouse in terms of RH is not sensible since the grower allowed the relative humidity to be higher in this section. The screen was opened to a maximum of 2.5% when the relative humidity was in the range 89%- 92%. As a result, the relative

humidity in the reference greenhouse was in the range 90%- 98%. Figure 6.14 shows the average horizontal temperature distribution for the whole greenhouse just above the crop when the thermal screen was open 2.5% in the reference greenhouse. The circles show the locations where the sensors are located which are used to make the figure. Due to technical problems, the data for some sensors was lost so no distribution is shown at these locations in Figure 6.14. In the reference greenhouse, the difference between the maximum temperature and minimum temperature is almost 3 K. As was seen in the CFD calculations, the cold air from above the screen dropped along the sidewall and flowed towards the central path, it being the highest point of the greenhouse as could be seen in the CFD calculations. In the experimental greenhouse section the temperature variations are less than 1.5 K with the dehumidifying system operational. The variations are less than given by the CFD calculations since this graph of the measurements shows averaged values whereas the CFD calculations show a steady state situation. The relative improvement of dehumidification with the proposed system over that with the conventional method, in terms of reduction of temperature difference is comparable. Figure 6.15 shows the absolute humidity in the horizontal plane of the whole greenhouse. The absolute humidity in the reference greenhouse varies by  $1 \text{ g kg}^{-1}$  and in the experimental section by  $0.3 \text{ g kg}^{-1}$  which is also in line with the CFD results.

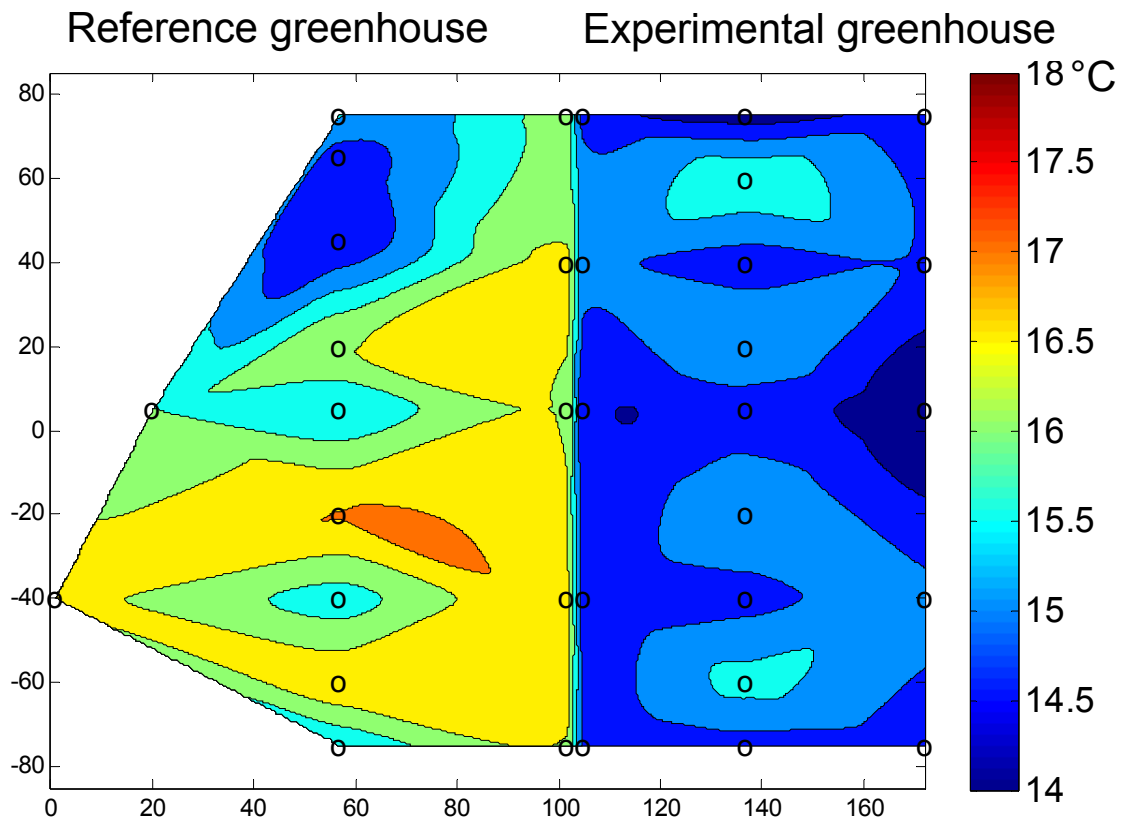


Figure 6.14 Average temperature distribution over the whole greenhouse for one day during the period the thermal screen was opened by 2.5% in the reference greenhouse

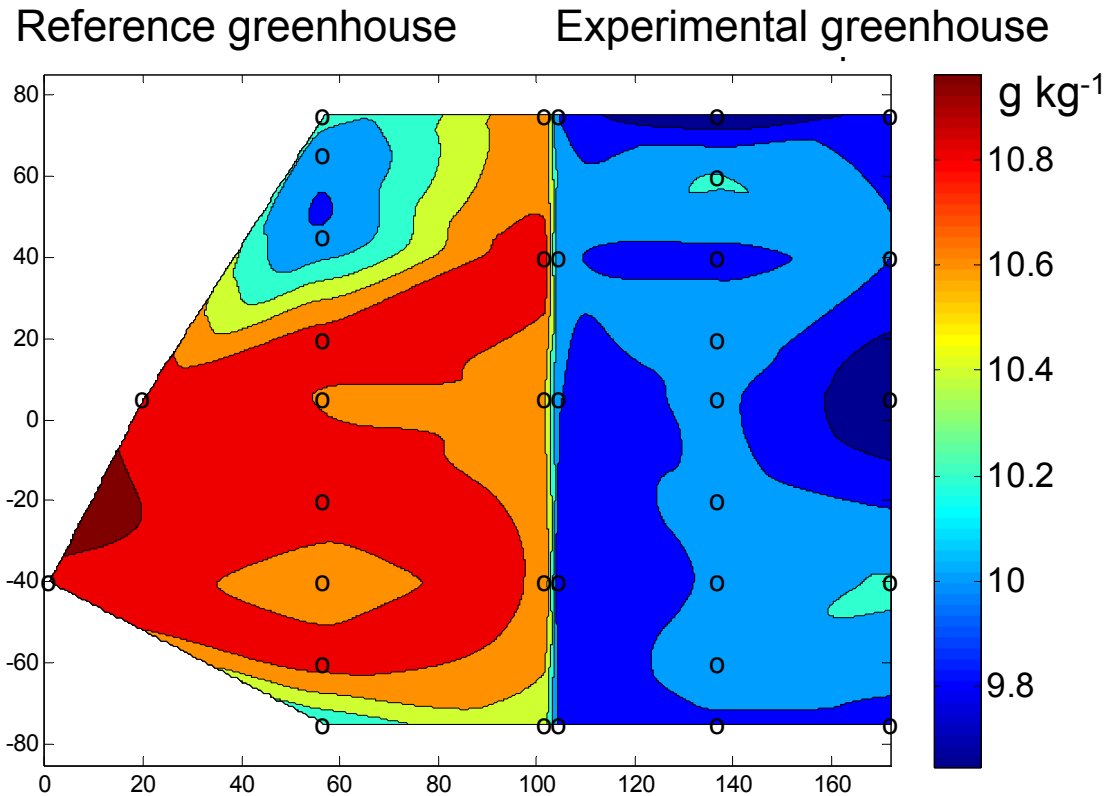


Figure 6.15 Average absolute humidity distribution in  $\text{g kg}^{-1}$  over the whole greenhouse for one day during the period the thermal screen was opened by 2.5% in the reference greenhouse

### 6.3.3 Practical implications

A study under Dutch tomato growers revealed that more extensive use of thermal screens can increase energy savings by 7.5% (Ruijs *et al.*, 2006). In our view, the developed system will encourage more growers to apply thermal screens because they will know that they can control the climate in the greenhouse more accurately. Furthermore, growers will keep their thermal screens closed for longer periods without increasing the risks of high humidity, thereby saving energy.

### 6.4 Conclusions

A design process for a system to dehumidify a greenhouse when the thermal screen is closed has been developed. The capacity of the system, determined using the dynamic simulation model KASPRO, has been validated using climatic data from an experimental greenhouse where the system was tested. Calculations showed that the system required a maximum capacity of  $6 \text{ m}^3 \text{ h}^{-1} \text{ m}^{-2}$  when outside air was used to maintain the relative humidity within given limits. Using outside air for vapour removal compares favourably with using the air from above the thermal screen since less airflow

is required and heating losses are lower. CFD simulations show that slightly opening the thermal screen for vapour removal causes horizontal temperature and humidity differences. This problem could be resolved using the proposed system since local temperature and humidity differences were shown by CFD calculations to reduce. Experiments showed that, although the full capacity of the system was not used during the experiment, the capacity of the designed system was sufficient. When the designed system is used, the climate under the thermal screen is more homogenous with average temperature differences on a daily base being less than 1 K. The system can easily be implemented in existing greenhouses using an air duct and a ventilator mounted in the greenhouse sidewall.

By controlling the dehumidification process more effectively, humidity limits can be set more strictly and energy can be saved. It is likely that the use of the developed system will encourage more growers to use thermal screens, and encourage them to keep their screens closed for longer periods, thus providing energy savings.

### **Acknowledgements**

This research was financed by the Dutch Ministry of Agriculture, Nature and Food Quality and the Product Board for Horticulture.

---

# 7

## Discussion and conclusions

---

## 7.1 Humidity control

Dehumidification is an essential part of greenhouse climate control. High humidity is a cause of diseases which ultimately reduce the quantity and quality of production. The risk of diseases affecting the crop increases when crops are wet. As the humidity is higher, the chance of condensation on the crop increases, decreasing the product quality and production. In theory condensation should not occur when the relative humidity is below 100% and the plant temperature is equal to the air temperature. However, the plant temperature in practice tends to differ from the air temperature. Parallel studies supported the statements on this subject made in the introduction. It was found that the temperature in the top of the canopy is lower due to radiation to the cover which had a lower temperature than the greenhouse air. (Marcelis *et al.*, 2008). Condensation is likely to occur on this part of the canopy when the humidity is high. It was also found that due to their thermal capacity, the more heavy organs of the canopy like the fruits and the stem tend to remain colder during periods when the greenhouse temperature is increasing (Campen *et al.*, 2005), normally around sunrise.

Besides temperature differences between the air and the crop, air temperature varies throughout the greenhouse. The air temperature distribution results from numerous factors like ventilation, heating, transpiration of the crop, solar radiation *etc.* (Campen, 2006c; Campen *et al.*, 2007b; Campen *et al.*, 2007a). The absolute humidity tends to be rather evenly distributed (Campen *et al.*, 2008). As a result, the relative humidity distribution depends mainly on the temperature distribution. The above mentioned studies confirm that locations where the temperature is low ultimately results in high relative humidity, increasing the chance of condensation on the crop as was stated in the introduction. For this reason the temperature distribution in a greenhouse should be homogeneous especially when the relative humidity is high. Temperature differences can be kept to a minimum provided the climate control is well organized, but they will persist due to the setup of the greenhouse and physical laws (Campen *et al.*, 2007b; Campen, 2004). The heating system is installed near the floor of the greenhouse so it will not reduce light conditions at crop level. Dominant heat losses from the greenhouse are near the cover (roof and gables) of the greenhouse through convection and ventilation. The warm air near the heating system rises in the greenhouse and the cold air near the cover drops; resulting in air circulation (with horizontal and vertical components) causing temperature differences, which in turn determine the maximum acceptable humidity level. Moreover, temperature differences should be kept to a minimum so humidity can be high saving energy as shown in Table 1.1.

Humidity is conventionally controlled by using the heating system set to a specific minimum temperature. This increases the greenhouse temperature and lowers the



relative humidity, also simulating the air circulation in the greenhouse. Alternatively, the windows are opened slightly so the wind or buoyancy effects also initiate air exchange reducing humidity. When thermal screens are used, they are slightly opened to exchange greenhouse air with air above the screen reducing humidity (Campen, 2006a; Campen, 2006b). These actions increase the climatic heterogeneity as discussed in chapter six, but also increase the temperature of the heating system due to the additional heat losses. On the other hand, these actions also stimulate the transpiration of the crop by warming the crop and decreasing the humidity. These strategies increase energy consumption.

Increasing humidity decreases transpiration, which in turn lowers the need for dehumidification. However transpiration is required for the physiological processes in the plant (Bakker, 1993). On a short term basis, transpiration can be minimal by increasing the humidity in the greenhouse, but on a long term basis, transpiration is necessary for the calcium uptake of the plant (Dieleman, 2008). Moreover, evaporation is needed to dry the crop when it is wetted *e.g.* from a wound in the stem or due to water strayed over the crop.

## 7.2 Dehumidifying methods

The classical way to dehumidify greenhouse air is by ventilation. The process of ventilation was studied by means of computational fluid dynamics in chapter four. This study showed that ventilation is not a well controlled process. It depends on the geometry of the windows, the surroundings, temperature differences, wind direction and wind speed *etc.* and contains greenhouse specific aspects, so will be different for different greenhouses. The fact that this process is difficult to control results in dehumidification often exceeding the needs, and results in a higher energy consumption. Calculations also showed ventilation increases the heterogeneity of the climate which can be the source of humidity problems.

Condensation on a cold surface seems like a logical way to dehumidify a greenhouse since the heat of evaporation is transferred during this process and can be re-used to heat the greenhouse. From this point of view, the systems described in chapter two and three were developed. From these studies it was concluded that the sensible heat transferred during this process is equal or more than equal to the latent heat transferred, even when heat recovery is applied as described in chapter three. This conclusion was also made by other researchers (Chou *et al.*, 2004). As a result, the heat that needs to be removed from the cold surface in order to maintain the desired temperature (below dew point temperature) is relatively large. Therefore, more cooling capacity is needed than for the condensation process only, increasing the energy consumption of the heat pump

removing this heat. Since this method is applied during periods of heating, the sensible heat extracted from the greenhouse has to be supplied to the greenhouse. The heat produced by condensation and the energy input of the heat pump can be only partially used directly for heating the greenhouse. The excess heat can be stored but this will increase the overall costs of the system making it not economically feasible as was concluded in chapter five.

Dehumidification with a hygroscopic material has the advantage that latent heat is directly transformed into sensible heat. This heat can be used to heat the greenhouse. However, the heat required for regeneration of the material, the environmental risks of the applied hygroscopic materials and the complexity of the system make it less suitable for practical application. For these reasons this method of dehumidification is not considered practical for humidity control as was concluded in chapter 5.

The alternative methods of dehumidification have to be compared to the conventional method, natural ventilation. Dehumidification by ventilation is the best option from an economical and energy consuming point of view, as was concluded in chapter five. However, as concluded above, ventilation by natural convection cannot be accurately controlled and it leads to a non-uniform climate distribution, as shown in chapters four and six. Opening thermal screens or windows to dehumidify often results in climatic differences throughout the greenhouse. In this case the airflow is dependent on the temperature differences and wind influences which makes it difficult to control. These drawbacks can be resolved if the ventilation is realised by mechanical fans in combination with an air distribution system, controlling the local air exchange (Campen, 2008). An extra improvement is made by heat recovery: the outgoing warm, humid air should exchange heat with the incoming cold, dry air. This is to be even more preferred as the greenhouses are more insulated, as indicated in the introduction of this thesis. The principle of controlled ventilation without heat recovery was put into practice at a commercial grower (Campen *et al.*, 2008). The investment and operational costs of a mechanically controlled dehumidification were compensated by energy savings resulting from a well controlled environment. The amount of airflow was minimized to maintain an accurate specific humidity, whereas the humidity level with the conventional method is set lower to compensate for differences in the greenhouse. Air circulation in the greenhouse is lower with this system compared to conventional ventilation. Additional air movement may be necessary for some crops with a dense leaf area, in order to compensate for the fact that the microclimate is less affected. In some cases the system can be designed to release the air in this dense part of the crop, compensating for the lack of local air circulation. Moreover, the size and dimensions of

the dehumidifying system depend on the crop as was indicated in chapter four. Cucumber for example has a higher level of transpiration than sweet pepper. Also the relative humidity and temperature settings vary, thus the system has to be optimized to the crop being grown.

The principle of controlled ventilation with heat recovery was included in the comparison of dehumidifying methods in chapter 5. It was concluded that when accurate humidity control is combined with heat recovery, the energy saved is in the range of 7% to 25% deduced from Table 5.7. Recently this system was implemented by a commercial grower (Van Staalduinen, 2009).

### **7.3 Future perspectives**

The insulation of greenhouses has been enhanced over the years. This tendency is driven by the increase of energy costs. Thermal screens are commonly used to insulate the greenhouse for crops that favour higher light intensities. Thermal screens can be applied when the solar radiation is low and can be removed to allow the maximum amount of light to enter. Greenhouses facilitating crops grown with a moderate light level are often equipped with an insulating cover.

Improved insulation increases humidity since the amount of condensation on the cover and screens is reduced and leakage ventilation is also reduced as indicated in chapter five. For this reason humidity control is more essential and necessary in modern greenhouses. Thermal screens can be applied for a longer duration when the humidity can be controlled by the presented mechanical ventilation system, thereby saving energy.

It is expected that insulation of greenhouses will further improve by the introduction of new materials combining high light transmission with a high insulation value (Swinkels *et al.*, 2001). Then dehumidification will be crucial to utilize the energy saving potentials. This can be realized by the controlled dehumidification presented here, through mechanical ventilation in combination with heat recovery.

A recent development to use the excess heat available in the summer period to heat the greenhouse in the winter period is by storing it in an aquifer (Bot *et al.*, 2005). The principle was applied in the “Kas als energiebron” which was realized in practice and tested extensively (De Zwart, 2007). The stored energy is utilized using a heat pump. The cold water produced by the heat pump in the winter is then used for summer cooling and can also be used in principle for dehumidification.

In chapter five it was concluded that dehumidification by condensation when heating is needed is not favourable since the sensible heat removed during the process has to be supplied by the heating system again, thereby increasing the energy consumption of the

heat pump. Alternatively, the cold water can be used for dehumidification during a warm period when cooling is required. Then too, latent heat is subtracted and stored in the aquifer at the desired temperature level. When the cold aquifer water is used for dehumidification during periods when the greenhouse temperature is moderate and heating is not needed, the water will still be fairly cold when it is returned to the warm well of the aquifer. This is unfavourable from an energy point of view since warm water is to be used in the winter to supply the heat for the heat pump. The water in this well should be of a high temperature to minimize the pumping costs and the aquifer capacity, which is directly linked to its investment cost. For this reason regenerating the aquifer during periods of high temperature in the greenhouse is more economical and sustainable. Dehumidification by controlled mechanical ventilation in combination with heat recovery is preferred for these systems.

#### **7.4 Computational fluid dynamics**

CFD has proved to be a useful tool for the various studies described in this thesis. In chapter two CFD was also used to determine the dimensions of the finned pipes system installed near the cover of the greenhouse to dehumidify the air by condensation. In the next chapter CFD was used as a design tool to determine the dimensions of the heat recovering dehumidifying system with free convection based circulation. The outcome of the CFD calculations proved to be correct compared to measurements on a prototype. Following the success of these two design process studies, CFD was used to describe the ventilation rate of a Spanish greenhouse. In this study a three dimensional grid was applied, which at that time was a novelty in greenhouse studies. The calculations could be verified by tracer gas measurements in the actual greenhouse. It was concluded that the wind direction has a large influence on the ventilation of the greenhouse. Through experimental measurements, this conclusion can not be hold since the wind direction and velocity are constantly changing. This study also proved that three dimensional calculations are needed to simulate the airflow through a greenhouse when wind dominates the ventilation. CFD was also used in the sixth chapter of this thesis to visualize the temperature distribution in the greenhouse when a thermal screen is used, which is slightly opened to remove moisture. The CFD model was improved by taking into account the influence of the crop resistance to the airflow. This was achieved by separately modelling the flow through a section of the crop (0.6 by 0.6 by 0.6 m) in great detail, by which the resistance could be determined. This approach had never been used before and proved correct when the modelling results were compared to experimental results.

## **7.5 Overall conclusion**

The overall conclusion of this thesis is that dehumidification using air exchange between outside air and greenhouse air is most efficient, from an economical point of view. The method is already being used conventionally to dehumidify greenhouses by opening the vents and thermal screens. However, this method is difficult to control and the resulting climate distribution is not homogeneous. These problems can be resolved however, by mechanically controlling the air exchange with fans. The incoming air can be evenly distributed throughout the greenhouse and be exactly controlled so that the vapour influx from evaporation is in balance with the outgoing vapour flux. This method can be further optimized by applying heat recovery, warming the incoming cold air with the outgoing warm, humid greenhouse air, thereby saving energy. For better insulated greenhouses, the use of this technique will be essential since the relative losses by ventilation for dehumidification are higher compared to those in traditional greenhouses, as stated in the introduction. A homogeneous climate allows the humidity to be higher thereby reducing the transpiration and decreasing the need for dehumidification.



---

## References

---

- Albright L D; Behler M L** (1984). An air-liquid heat exchanger for greenhouse humidity control. *Transactions of the ASAE*, **27**(5), 1524-1530
- Bailey B J** (1999). Constraints, limitations and achievements in greenhouse natural ventilation. *Acta Hort.*, **534**, 21-30
- Bakker J C** (1991). Analysis of humidity effects on growth and production of glasshouse fruit vegetables. PhD Thesis, Agricultural University, Wageningen
- Bakker J C** (ed) (1993). *Luchtvochtigheid*. Van de Sande, Naaldwijk
- Bakker J C; Bot G P A; Challa H; Van de Braak N J** (1995). *Greenhouse climate control*. Wageningen Pers, Wageningen
- Baptista F J; Bailey B J; Randall J M; Meneses J F** (1999). Greenhouse Ventilation Rate: Theory and Measurement with Tracer Gas Techniques. *Journal of Agricultural Engineering Research*, **72**(4), 363-374
- Becker M** (1986). *Heat Transfer*, London
- Boot H; Nies J; Verschoor H J E; De Wit J B** (1990). *Handboek Industriële Warmtepompen (Handbook for Industrial Heat Pumps)*. Kluwer Bedrijfsinformatie Deventer
- Bot G P A** (1983). *Greenhouse climate: from physical processes to a dynamic model*. PhD Thesis, Agricultural University of Wageningen, Wageningen
- Bot G P A; Van de Braak N; Challa H; Hemming S; Rieswijk T H; Van Straten G; Verlodt I** (2005). The solar greenhouse: state of the art in energy saving and sustainable energy supply. *Acta Horticulturae*, **691**, 501-508
- Boulard T; Baille A; Lagier J; Mermier M; Vanderschmitt E** (1989). Water vapour transfer in a plastic house equipped with a dehumidification heat pump. *Journal of Agricultural Engineering Research*, **44**, 191-204
- Boulard T; Haxaire R; Lamrani M A; Roy J C; Jaffrin A** (1999). Characterization and Modelling of the Air Fluxes induced by Natural Ventilation in a Greenhouse. *Journal of Agricultural Engineering Research*, **74**(2), 135-144
- Boulard T; Papadakis G; Kittas C; Mermier M** (1997). Air flow and associated sensible heat exchanges in a naturally ventilated greenhouse. *Agricultural and Forest Meteorology*, **88**(1-4), 111-119
- Boulard T; Wang S** (2002). Experimental and numerical studies on the heterogeneity of crop transpiration in a plastic tunnel. *Computers and Electronics in Agriculture*, **34**, 173-190
- Breuer J J G; Van de Braak N J** (1989). Reference year for Dutch greenhouses. *Acta Horticulturae*, **248**, 101-108



- 
- Campen J B** (2004). Betere temperatuurverdeling door regelbare gevelverwarming. Agrotechnology & Food Innovations, Report 132, Wageningen
- Campen J B** (2006a). Effect van maatregelen ter voorkoming van temperatuurverschillen in de kas bij gebruik van energieschermen met open bandjes. Plant Research International, Nota 411, Wageningen
- Campen J B** (2006b). Gecontroleerde vochtafvoer bij schermen. Plant Research International, Rapport 121, Wageningen
- Campen J B** (2006c). Ventilation of small multispan greenhouse in relation to the window openings calculated with CFD. Acta Horticulturae, **718**, 351-356
- Campen J B** (2008). Vapour removal from the greenhouse using forced ventilation when applying a thermal screen. Acta Horticulturae, **801**, 863-868
- Campen J B; Bontsema J; Ruijs M** (2007a). Relatie tussen toenemende kashoogte en het energieverbruik in de glastuinbouw. Wageningen UR Glastuinbouw, Rapport 144, Wageningen
- Campen J B; De Gelder A** (2007b). Horizontale variatie. Plant Research International, Rapport 131, Wageningen
- Campen J B; Kempkes F L K** (2008). Praktijkproef mechanische vochtafvoer. Wageningen UR, Rapport 212, Wageningen
- Campen J B; Kempkes F L K; Houter B; Rijpsma E C** (2005). Planttemperatuur als stuurparameter in kasklimaatregelingen : deelverslag: ontwikkeling plant temperatuursensor. Agrotechnology & Food Innovations, Rapport 415, Wageningen
- Chasseriaux G** (1987). Heat pumps for reducing humidity in plastics greenhouses. *Plasticulture*, **73**, 29-40
- Chou S K; Chua K J; Ho J C; Ooi C L** (2004). On the study of an energy-efficient greenhouse for heating, cooling and dehumidification applications. *Applied Energy*, **77**(4), 355-373
- De Hallaux D; Gauthier L** (1998). Energy consumption due to dehumidification of greenhouses under Northern latitudes. *Journal of Agricultural Engineering Research*, **69**(35-42),
- De Jong T** (1990). Natural ventilation of large multi-span greenhouses. PhD Thesis, Agricultural University of Wageningen, The Netherlands
- De Jong T; Van de Braak N J; Bot G P A** (1993). A wet plate heat exchanger for conditioning closed greenhouses. *Journal of Agricultural Engineering Research*, **56**, 25-37
- De Pascale S; Maggio A** (2005). Sustainable protected cultivation at a mediterranean climate. *Acta Hort. (ISHS)*, **691**, 29-42

- De Zwart H F** (1996). Analyzing energy-saving options in greenhouse cultivation using a simulation model. PhD Thesis, Agricultural University of Wageningen, The Netherlands
- De Zwart H F** (2007). Overall Energy Analysis of (semi) closed greenhouses. *Acta Horticulturae*, **801**, 811-817
- De Zwart H F; Bot G P A** (1997). Energy saving prospective of combined heat and power in horticulture in the Netherlands: a simulation study. *Netherlands Journal of Agricultural Science*, **45**, 97-107
- Dieleman J A** (2008). Effecten van luchtvochtigheid op groei en ontwikkeling van tomaat [effects of humidity on growth and development of tomato]. Wageningen UR Horticulture, Nota 519, Wageningen
- Fluent** (1998). User's guide, Lebanon, United Kingdom
- Gijzen** (1992). Simulation of photosynthesis and dry matter production of greenhouse crops. CABO-DLO, Simulation Report No. 28, Wageningen
- Hand D W** (1988). Effects of atmospheric humidity on greenhouse crops. *acta Horti. (ISHS)*, **229**, 143-158
- Jolliet O** (1994). Hortitrans, a model for predicting and optimising humidity and transpiration in greenhouses. *Journal of Agricultural Engineering Research*, **57**, 23-37
- Kacira M; Sase S; Okushima L** (2004). Optimization of vent configuration by evaluating greenhouse and plant canopy ventilation rates under wind-induced ventilation. *Transactions of the ASAE*, **47(6)**, 2059-2067
- Kacira M; Short T H; Stowell R R** (1997). A fluid dynamics evaluation of naturally ventilated gutter-connected greenhouses. ASAE paper, **97-4059**,
- Kacira M; Short T H; Stowell R R** (1998). A CFD Evaluation of naturally ventilated, multi-span, sawtooth greenhouses. *Transactions of ASAE*, **41(3)**, 833-836
- Kittas C; Bartzanas T** (2007). Greenhouse microclimate and dehumidification effectiveness under different ventilator configurations. *Building and Environment*, **42(10)**, 3774-3784
- Köhl J; Visser P H B d; Wubben J** (2007). Risico's op schimmelaantasting in vruchtgroenten:lituurstudie [risks for fungal diseases in vegetables: literature survey]. Wageningen UR Glastuinbouw, Nota 467, Wageningen
- Kutateladze S S** (1963). *Fundamentals of Heat Transfer*. Edward Arnold, London
- Launder B E; Spalding D B** (1974). The numerical computation of turbulent flows. *Computer Methods in Applied Mechanics and Engineering*, **3(2)**, 269-289
- Lee I B; Short T H** (2000). Two-dimensional numerical simulation of natural ventilation in a multi-span greenhouse. *Transaction of ASAE*, **43(3)**, 745-753

- 
- LEI** (2001). Land- en Tuinbouwcijfers 2001 [Agricultural production figures 2001]. Den Haag
- Marcelis L; Benninga J; Hofland-Zijlstra J; K€ærner O; Os E v; Slootweg C; Westra E** (2008). Botrytis bestrijden en energie besparen bij gerbera, Gewasbeschermingsmanifestatie 22 mei 2008. Wageningen UR, Wageningen
- Miguel A A F** (1998). Transport phenomena through porous screens and openings : from theory to greenhouse practice. PhD Thesis, Wageningen University, Wageningen
- Mistriotis A; Arcidiacono C; Picuno P; Bot G P A; Scarascia-Mugnozza G** (1997a). Computational analysis of ventilation in greenhouses at zero- and low-wind-speeds. *Agricultural and Forest Meteorology*, **88**(1-4), 121-135
- Mistriotis A; Bot G P A; Picuno P; Scarascia-Mugnozza G** (1997b). Analysis of the efficiency of greenhouse ventilation using computational fluid dynamics. *Agricultural and Forest Meteorology*, **85**(3-4), 217-228
- Norton T; Sun D-W; Grant J; Fallon R; Dodd V** (2007). Applications of computational fluid dynamics (CFD) in the modelling and design of ventilation systems in the agricultural industry: A review. *Bioresource Technology*, **98**(12), 2386-2414
- Papadakis G; Mermier M; Meneses J F; Boulard T** (1996). Measurement and Analysis of Air Exchange Rates in a Greenhouse with Continuous Roof and Side Openings. *Journal of Agricultural Engineering Research*, **63**(3), 219-227
- PBG** (2000). Kwantitatieve informatie voor de glastuinbouw 2000-2001 [Quantitative information for cultivation under glass 2000-2001]. Naaldwijk
- Perez Parra J; Baeza E; Montero J I; Bailey B J** (2004). Natural Ventilation of Parral Greenhouses. *Biosystems Engineering*, **87**(3), 355-366
- Pritchard C; Currie J** (1993). Absorption-dehumidification - a unit operation for heat recovery from dryers. Elsevier, Barking (UK).
- Rohsenow W M; Hartnett J P** (1973). *Handbook of Heat Transfer*. McGraw-Hill Inc., New York
- Rousse D R; Martin D Y; Thériault R; Léveillé F; Boily R** (2000). Heat recovery in greenhouses: a practical solution. *Applied Thermal Engineering*, **20**, 687-706
- Ruijs M N A; Dieleman J A; Esmeijer M; Kempkes F L K; Reijnders C** (2006). Intensiveren schermgebruik [Intensifying thermal screen use]. LEI, Rapport 3.06.05, Den Haag
- Särkkä L E; Hovi-Pekkanen T; Huttunen J** (2006). Greenhouse cooling in summer in Finland - preliminary results of climate control and plant response. *Acta Hort. (ISHS)*, **719**, 439-445

## References

---

- Seginer I; Kantz D** (1989). Night-time use of dehumidifiers in greenhouses: an analysis. *Journal of Agricultural Engineering Research*, **44**, 141-158
- Sonneveld P J** (1999). Nieuwe kasbedekkingsmaterialen besparen energie. [Novel greenhouse cover materials save energy.]. *Groente en fruit*, 99
- Speetjens S L** (2001). Warmteterugwinning uit ventilatielucht [Heat recovery from ventilation]. IMAG, Wageningen
- Stanghellini C** (1987). Transpiration of greenhouse crops : an aid to climate management. PhD Thesis, Agricultural University of Wageningen, The Netherlands
- Swinkels G L A M; Huijs J P G; De Zwart H F** (2000). Standaard teelten [Standard cultivation]. IMAG, Wageningen
- Swinkels G L A M; Sonneveld P J; Bot G P A** (2001). Improvement of Greenhouse Insulation with Restricted Transmission Loss through Zigzag Covering Material. *Journal of Agricultural Engineering Research*, **79**(1), 91-97
- TNO** (1996). TNO rapport 96-CON-R1584. Delt
- Van Staalduinen J** (2009). Bij de flowdeck kas doen water en regainers het werk. *Onder Glas*, 5
- Vermeulen P C M** (2008). Kwantitatieve Informatie voor de Glastuinbouw 2008. Wageningen UR, 185, Wageningen
- Versteeg H K; Malalasekera W** (1995). An introduction to computational fluid dynamics : the finite volume method. Longman, Harlow
- Weast R C** (1981). *CRC Handbook of Chemistry and Physics*, Boca Raton, FL, USA
- Yeaple F D** (1995). *Fluid Power Design Handbook*. CRC Press

## Summary

Dehumidification is an essential part of greenhouse climate control. High humidity is a cause of diseases which ultimately reduce the quantity and quality of production. The risk of diseases affecting the crop increases when crops are wet. The relative humidity surrounding the crop differs since the air temperature in the greenhouse is not homogenous. This heterogeneity should be minimised by a proper greenhouse climate management so the relative humidity can be higher which saves energy. Part of the temperature differences cannot be resolved as a result of physical laws. Therefore, humidity control is needed. Humidity control increases energy consumption during heating periods. The work presented describes energy-saving measures to dehumidify a greenhouse where also the practical and economical feasibility are considered.

Three methods of dehumidification can be applied in greenhouses: ventilation with outside air, condensation on a cold surface, and using a hygroscopic material.

In chapter two, an experimental dehumidifying system for greenhouses was designed and tested based on the method of condensation. The system used finned pipes fixed under the gutter of the greenhouse. The pipes were cooled below the dew point of the greenhouse air by cold water. The humid air passed the pipe and fins by natural convection and condensation occurred reducing the humidity in the greenhouse. The performance of the system in relation to its location and dimensions were studied by computational fluid dynamics calculations (CFD). The total heat transferred and condense removed were monitored as a function of the greenhouse conditions during the experiment. The system removes 40 grams of condensate per hour per square metre of greenhouse floor from the humid air which is sufficient during periods when heating has to be applied and ventilation is minimised. The main conclusion of this chapter is that the heat transferred at the cold surface by condensation is less than one third of the total heat removed by the system at a relative humidity of 80%.

In response to the findings of the second chapter, a condensation system was designed combined with heat recovery to increase the relative amount of heat transfer by condensation. Important constraints for the design were low energy consumption and homogeneous greenhouse climate. Low energy demand was achieved by natural air circulation through the system and by recovering sensible heat. A homogeneous climate can be realised by decentralised local dehumidification in the greenhouse. Computational fluid dynamics was used in the design process. A vertical geometry was chosen first in a double chimney approach to exploit the vertical distance between inlet

and cold surface and that between cold and hot surface for natural convection air circulation. However, CFD calculations indicated stagnating flow in this vertically oriented system. Orienting the system horizontally greatly enhanced the systems performance.

A separate model for condensation has been created to complement the CFD program that did not include condensation. A prototype of the designed dehumidifier was built and tested. Calculations and experiments were in fair agreement and demonstrated the potential for practical application.

In the fourth chapter, the method of ventilation was explored through three-dimensional computational fluid dynamics calculations on a Spanish ‘parral’ greenhouse. The calculations were verified by experimental results from tracer gas measurements. Two types of roof openings have been considered; the rollup window configuration and the flap window configuration.

The calculations resembled experimental data within 15%. Wind speed correlated linearly with ventilation rate for both configurations without the buoyancy effect. This is in agreement with basic theory on ventilation. CFD calculations indicated that ventilation rate for both configurations is largely dependent on wind direction, which was also seen with the experimental data. Ventilation rate varied for the flap window configuration from 0.8 to almost 4 renewals per hour per  $\text{m s}^{-1}$  wind speed.

The calculations showed that the process of ventilation is difficult to control since it is dependent on various parameters like, greenhouse characteristics, surroundings, wind direction, wind speed, and temperature differences.

In the fifth chapter, three dehumidifying methods, being condensation on a cold surface, forced ventilation using a heat exchanger, and an absorbing hygroscopic dehumidifier, were compared with natural ventilation as the conventional way to dehumidify a greenhouse. The calculations were performed using a dynamic physical simulation model with a single- and a double-layer greenhouse under Dutch weather conditions. The comparison was made based on the energy consumption and the costs. The methods with a cold surface or an absorbing hygroscopic material are less attractive than the conventional method, mainly because of the high investment costs. Dehumidification by forced ventilation with a heat exchanger can be competitive.

In chapter six a system was designed and tested capable of dehumidifying greenhouse air by ventilation when heating is applied. The ventilation with outside air is mechanically controlled. Moreover, an air distribution system improves greenhouse

climate homogeneity. The excess humid air leaves to greenhouse through leaks in the cover.

The amount of air necessary to maintain a desired humidity level was determined using a greenhouse climate simulation model. The dimensions of the system were calculated from the results of the model and a control strategy was suggested. The distribution of the climate in the greenhouse using the conventional and proposed method of vapour removal was investigated using computational fluid dynamics (CFD). The system was tested in a commercial greenhouse and compared to a conventional system at the same location. The performance of the system, as determined by the dynamic simulation model, proved to be efficient and the climate proved to be more homogenous, as was predicted by the CFD calculations.

Through a thorough analysis of the various methods to dehumidify a greenhouse, the most energy-friendly, economical, and practical method was determined. This method being dehumidification using air exchange between outside air and greenhouse air, has been enhanced by mechanically controlling and distributing the airflow. The method is further optimized by applying heat recovery, warming the incoming cold air with the outgoing warm, humid greenhouse air, thereby saving energy. For better insulated greenhouses, the use of this technique will be essential since the relative losses by ventilation for dehumidification are higher compared to those in traditional greenhouses. A homogeneous climate allows the humidity to be higher thereby reducing the transpiration and decreasing the need for dehumidification in turn also saving energy.

The result is an energy-friendly, economical, and practical method to dehumidify greenhouses. The designed system has been implemented at commercial growers already. The implementation has great potential as optimal climate control and energy-saving will be more and more indispensable in future for cost-effective high quality production.





## Samenvatting

Ontvochtiging van kassen is een essentieel onderdeel van de klimaatregeling. Een hoge luchtvochtigheid vergroot de kans op ziektes en zorgt daarmee voor een verlaging van de kwaliteit en kwantiteit van de productie. De relatieve luchtvochtigheid rond een plant varieert omdat de temperatuurverdeling over de kas niet homogeen is. Deze heterogeniteit moet worden beperkt door een goede klimaatregeling waardoor de relatieve luchtvochtigheid hoger kan worden ingesteld wat zorgt voor energiebesparing. Temperatuurverschillen zijn niet geheel te voorkomen door de natuurkundige wetten. Om deze reden blijft vocht controle in kassen noodzakelijk. Ontvochtiging zorgt voor een hoger energiegebruik in de periodes dat de kassen verwarmd moeten worden. Dit proefschrift beschrijft energiebesparende methodes om kassen te ontvochtigen waarbij de praktische en economische factoren ook worden beschouwd.

Er zijn drie methodes om kassen te ontvochtigen: door ventilatie met buitenlucht, door condensatie op een koud oppervlak of door gebruik te maken van een hygroscoopisch materiaal.

Hoofdstuk twee beschrijft het ontwerp en testen van een experimenteel ontvochtigingsysteem gebaseerd op basis van de methode van condensatie. Het systeem bestaat uit gevinde buizen welke onder de goot van de kas zijn geplaatst. De buizen worden gekoeld onder het dauwpunt van de kaslucht middels koud water. De vochtige kaslucht stroomt langs de buizen door natuurlijke convectie waarbij de condensatie plaatsvindt. De invloed van de locatie en afmetingen van de buizen en de vinnen op het functioneren van het systeem is onderzocht met computational fluid dynamics (CFD). In het experiment is de totale warmteoverdracht en de hoeveelheid condens gemeten in relatie tot de kas omstandigheden. Het systeem voert 40 gram vocht af per uur per vierkante meter kas oppervlak wat voldoende is gedurende periodes dat de kas wordt verwarmd en de ventilatie minimaal is. Uit het onderzoek werd geconcludeerd dat de warmte die wordt overgedragen door condensatie minder dan een derde is van de totale hoeveelheid warmte die wordt overgedragen bij een relatieve luchtvochtigheid van 80%.

Het systeem beschreven in hoofdstuk twee kan worden verbeterd door warmteterugwinning toe te passen waardoor de relatieve hoeveelheid warmte die wordt overgedragen ten gevolge van condensatie wordt vergroot. Bij het ontwerp van het systeem beschreven in hoofdstuk drie is ook meegenomen dat het systeem zorgt voor een homogene klimaatverdeling en dat het systeem weinig energie gebruikt. Het

energiegebruik van dit systeem is laag omdat de lucht door natuurlijke ventilatie door het systeem stroomt en het feit dat er met warmteterugwinning wordt gewerkt. Voor het eerste ontwerp is gekozen voor een verticale warmtewisselaar waardoor het schoorsteen effect ten gevolge van het temperatuurverschil tussen de omgevingslucht, de koude plaat en de warme plaat zorgt voor de natuurlijke convectie. CFD berekeningen lieten zien dat in een verticale warmtewisselaar de stroming stagneerde. Het horizontaal plaatsen van de warmtewisselaar verbeterde de werking van het systeem enorm.

Voor de condensatie is een apart model gemaakt aangezien het niet mogelijk was condensatie in de CFD berekeningen mee te nemen. Op basis van dit systeem ontwerp is een prototype gebouwd die getest is. De berekeningen en de experimentele resultaten kwamen goed overeen en lieten zien dat het systeem potentie had voor de praktijk.

In het vierde hoofdstuk is de methode van ventilatie verder onderzocht door drie dimensionale computational fluid dynamics berekeningen uit te voeren op basis van een Spaanse “parral” kas. Deze berekeningen konden worden gevalideerd op basis van experimentele resultaten verkregen door tracer gas metingen. Twee verschillende ventilatie openingen in het dek zijn beschouwd: een dek waarbij de ramen worden opgerold en een systeem waarbij de ramen middels een scharnier op de nok worden geopend.

De CFD berekeningen kwamen binnen 15% overeen met de experimenteel bepaalde data. De ventilatie van de kassen verloopt lineair met de windsnelheid indien de invloed van de temperatuurverschillen gering is voor beide systemen. Dit komt overeen met de theorie over ventilatie. De ventilatie is sterk afhankelijk van de windrichting voor beide systemen wat ook duidelijk te zien was uit de experimentele data. De ventilatie varieert van 0.8 tot bijna 4 verversingen per uur per m s<sup>-1</sup> windsnelheid voor het systeem met de scharnieren.

De berekeningen laten zien dat ventilatie moeilijk te controleren is omdat deze afhankelijk is van diverse parameters zoals de afmetingen van de kas, de omgeving, de windrichting, de windsnelheid en temperatuurverschillen.

In het vijfde hoofdstuk zijn drie ontvochtigingsmethodes zijnde condensatie op een koud oppervlak, geforceerde ventilatie met een warmtewisselaar en een hygroscopisch stof, vergeleken ten opzichte van de conventionele manier van ontvochtigen door ventilatie op basis van natuurlijke convectie. De berekeningen zijn uitgevoerd met een dynamisch simulatie model voor een kas met een enkel en dubbel-laags kasdek op basis van Nederlandse weerdata. De vergelijking is gedaan om basis van energiegebruik en overall kosten. De methodes op basis van condensatie en de hygroscopische stof zijn

minder aantrekkelijk dan de conventionele manier van ontvochtigen met name door de hoge investeringskosten. Geforceerde ventilatie met een warmtewisselaar kan concurreren met de conventionele manier van ontvochtigen.

In hoofdstuk zes is een systeem ontworpen en getest waarmee door ventilatie de kas wordt ontvochtigd op het moment dat er verwarming nodig is. De ventilatie met buitenlucht wordt mechanisch gecontroleerd. Daarnaast wordt de lucht gelijkmatig over de kas verdeeld zodat het klimaat homogeen blijft. De vochtige kaslucht verlaat de kas door kleine openingen in het kasdek.

De benodigde hoeveelheid ventilatie om een specifieke luchtvochtigheid te handhaven is bepaald met een dynamisch kasklimaat model. De afmetingen van het systeem en de manier waarop het systeem wordt geregeld zijn bepaald op basis van deze berekeningen. Het klimaat in de kas, indien het vocht wordt afgevoerd op de conventionele manier en door het systeem, is vergeleken met CFD berekeningen. Het systeem is getest bij een commerciële tuinder met een referentiekas waarop de traditionele manier werd ontvochtigd. Het systeem functioneerde, zoals ook volgde uit de berekeningen, goed. Het klimaat was homogener door het systeem in vergelijking tot de traditionele manier van vocht afvoeren.

Ventilatie met buitenlucht blijkt, na een grondige analyse op basis van energiebesparing, economische haalbaarheid en praktische toepasbaarheid, de beste methode om een kas te ontvochtigen. Deze methode kan worden verbeterd door de ventilatie mechanisch te controleren en de lucht gelijkmatig over de kas te verdelen. Verder kan deze methode nog worden verbeterd door warmteterugwinning toe te passen waarbij de binnenkomende koude lucht wordt voorverwarmd door de uitstromende warme en vochtige kaslucht. Het energiegebruik neemt hierdoor af. Voor beter geïsoleerde kassen is warmteterugwinning van groter belang aangezien de relatieve bijdrage van de verliezen ten gevolge van ontvochtiging hier groter zijn. Een homogener kasklimaat zorgt ervoor dat de relatieve luchtvochtigheid hoger kan worden ingesteld waardoor de verdamping en de ontvochtigingsbehoefte afneemt wat ook tot energiebesparing leidt.

Het ontwikkelde systeem ten behoeve van de ontvochtiging van kassen zorgt voor energiebesparing, is betaalbaar en praktisch toepasbaar. Het systeem is reeds geïmplementeerd bij commerciële tuinders. Het systeem zorgt voor een verder optimalisatie van de klimaatbeheersing en vergroot de energiebesparing. Deze aspecten zijn essentieel in de toekomst voor de Nederlandse glastuinbouw.



## **Curriculum Vitae**

Jouke Berend Campen werd op 30 november 1973 geboren te Amersfoort. In 1992 na zijn voltooiing van het Atheneum aan het Corderius College in Amersfoort ging hij Technische Natuurkunde aan de Technische Universiteit in Delft studeren. In 1997 werd deze studie afgerond met warmtetransport als afstudeerrichting. Voor een half jaar is hij in dienst geweest van de universiteit bij Mijnbouw Techniek om de standtijd van een chemische verbrandingsoven te verlengen.

November 1997 kwam hij in dienst bij het IMAG in Wageningen waarbij hij zich in de loop der jaren specialiseerde op het gebied van klimaat in tuinbouwkassen met name op het gebied van vochthuishouding. Door interne reorganisaties is de naamgeving van het instituut waar hij werkzaam was binnen Wageningen Universiteit en Research Centrum regelmatig gewijzigd. Vanaf 1999 werd dit Agrotechnology and Food Innovations waarna het Plant Research International werd om vervolgens Wageningen UR Glastuinbouw te heten.

Jouke is getrouwd met Marianne Campen-Van de Ven en heeft drie zonen (Ruben, Hendrik en Floris).